AN ABSTRACT OF THE THESIS OF

Colin Bruce Elliott for the degree of Doctor of Philosophy in Chemistry presented on November 2 1982

Title: Application of Flow Injection Analysis to Enzymatic Fluorescence Kinetic Methods

Redacted for Privacy

Abstract approved: _____
James D. Ingle Jr.

Studies of the use of NADH as the monitored fluorophore for enzymatic fluorescence kinetic methods are discussed. Interference studies for the detection of NADH and the adaptation and optimization of fluorescence kinetic measurements to four serum assays are also described. A microcomputer-controlled flow injection analysis (FIA) system was designed and built to automate fluorescence kinetic assays. The performance of the FIA-fluorometer for kinetic assays was tested.

Optimization of the fluorometric reaction-rate instrument was made, resulting in a detection limit of 2 nM for NADH. An interference study of fluorometric measurements of NADH in a serum matrix showed serum proteins and bilirubin to be the major interferents.

Assays for ethanol and glucose were adapted to fluorescence kinetic methods which yielded detection limits of 0.3 μM and 0.01 mg/dL (in-cell concentrations), respectively. The analytes of the other two assays

were enzymes, lactate dehydrogenase (LDH) and creatine kinase (CK) which showed detection limits of 0.2 and 1 mU/mL (in-cell activities), respectively. The LDH assay was conducted such that the decrease in fluorescence per unit time was measured, while for the other assays the increase in fluorescence due to the formation of NADH was measured.

To improve the performance of these fluorometric serum assays, a fluorophore called resorufin was utilized, which could be coupled directly to NADH-producing assays. Coupling the resorufin reaction to the CK assay lowered the CK detection limit to 0.09 mU/mL (in-cell).

An FIA system was constructed to provide computer-controlled fluorometric kinetic assays. Operations of the system such as injections, flow rates, timing and data acquisition are controlled by software. Optimization of the system and measurements of the performance of the flow cell were conducted. Stopped-flow and continuous-flow modes of kinetic measurements, made the the FIA-fluorometer were thoroughly studied using the ethanol assay. The stopped-flow mode of measurement gave the lowest detection limit for ethanol (0.4 μM, in-cell) and the greatest throughput (75 runs/hr). The CK assay, was adapted to the FIA system and showed a detection limit of 0.2 mU/mL.

Application of Flow Injection Analysis to Enzymatic Fluorescence Kinetic Methods

by

Colin Bruce Elliott

A THESIS

submitted to

Oregon State University

in partial fulfillment of
the requirements for the
degree of
Doctor of Philosophy

Completed November 2 1982

Commencement June 1983

APPROVED:

Redacted for Privacy

Professor of Chemistry in charge of major

Redacted for Privacy

Chairman of Department of Chemistry

Redacted for Privacy

Dean of Graduate School

Date thesis is presented November 2, 1982

Typed by Mary Ann (Sadie) Airth for Colin Bruce Elliott

TABLE OF CONTENTS

LIST OF FIGURES

LIST OF TABLES

Application of Flow Injection Analysis to Enzymatic Fluorescence Kinetic Methods

INTRODUCTION

In enzymatic fluorescence kinetic methods, the rate of change in the fluorescence signal due to the formation or disappearance of a fluorescent species involved in an enzymatic reaction is measured and related to the initial concentration of the analyte. Experimental conditions can be adjusted such that either the enzyme or its substrate can be the analyte. This technique combines the selectivity and sensitivity of enzymatic reactions and fluorescence monitoring with the fast analysis times of kinetic methods.

Kinetic methods, also referred to as reaction rate methods, have been thoroughly classified and defined by Pardue (1). The technique of rate computation used for the studies presented here is the fixed time method where the change in the reaction monitor signal is recorded during the fixed measurement time. Integrations of the signal are used to calculate the rate by subtracting the integral obtained for the first half of the measurement period from the integral for the second half (2,3).

There are several advantages and limitations of using kinetic methods for analytical purposes as opposed to equilibrium methods (4-10). Since only a portion of the reaction is measured in a kinetic

method, much shorter analysis times are possible, especially for slow reactions. Only the change in the signal level is measured; therefore, differences in the background signal from sample to sample are automatically compensated for. Kinetic methods have certain limitations which include the need for strict control of reaction conditions and lower signal to noise ratios (S/N) than equilibrium methods.

The sensitivity and specificity of fluorescence make it ideal for monitoring kinetic assays. The concentration of species in the reaction mixture which cause scattering, pre-and post-filter effects, photodecomposition and quenching must be minimized in order to utilize the maximum sensitivity of fluorescence monitoring.

Enzymes are large protein molecules which serve as catalysts for a wide variety of biochemical and metabolic reactions. The value of enzymes to analytical chemistry has been their high specificity for a given substrate even in the presence of closely related molecules. Several texts have been written about the analytical applications of enzymes (11-14). Enzymes are quantified by their activity or catalytic rate, which is expressed in terms of units, where one unit is defined as the conversion of 1 μmol of substrate per minute when using the defined experimental conditions.

The initial studies undertaken for this thesis involved the development and investigation of fluorescence kinetic methods for enzymatic assays of human blood serum. Many enzymatic assays for serum components have been developed which utilize absorbance

monitoring of the reduced form of nicotinamide adenine dinucleotide (NADH), a common cofactor used in oxidation reduction reactions (15). Since NADH is an effective fluorophore and since enzymatic assays can be easily adapted to kinetic monitoring (11), enzymatic serum assays are ideal candidates for fluorescence kinetic monitoring.

Four different assays were chosen for studies of enzymatic fluorescence kinetic monitoring, each of which are typically monitored using the absorbance of NADH (15). The first two assays involved the measurement of ethanol and glucose, both of which are enzyme substrates. The other two assays were for the determination of lactate dehydrogenase (LDH) and creatine kinase (CK) which are both enzymes. These four assays differ significantly from one another in terms of complexity and required sensitivity. The application of fluorescence kinetic monitoring to these four assays was therefore a good test of the advantages and limitations of this type of measurement method for enzymatic serum assays.

Interference studies were conducted to determine which species in serum would cause spectral interference of fluorometric measurements of NADH. In addition, studies were made of the use of alternate fluorophores (other than NADH) to eliminate the spectral interferences of serum components.

In order to automate fluorescence kinetic methods, a flow injection analysis (FIA) system was constructed and coupled to the fluorometer. FIA techniques involve the direct injection of samples and reagent aliquots into a carrier stream (within small bore tubing)

in order to conduct analyses. The development of the FIA system involved the selection and construction of the proper components for optimum performance and versatility and for ease of computer control. The major components of the FIA system were interfaced to a KIM microcomputer to automate the operation and timing of the system. The microcomputer also serves to collect and calculate data in addition to controlling the FIA system. Once completed, the FIA-fluorometer system was thoroughly tested to determine the optimum parameters for conducting kinetic assays.

HISTORICAL

Reaction Rate Methods

Reaction rate methods for quantitative analysis have been in use for over a century. The first published data on a quantitative rate method was published by Roberts in 1881 (16) where the amylolytic activity of pancreas extracts was determined. Interest in kinetic measurements grew in the 1920's and 30's as more research was done with catalysts, especially enzymes. The next 2 decades saw more biochemical and clinical applications of reaction rate methods which generally utilized colorimetric monitoring. By the early 1960's kinetic methods had become widely accepted and were being applied to a variety of different applications including measurement of non-catalytic species such as cofactors or metals in solution (17).

Development of rate measurement instrumentation was in response to the need for faster, more convenient and more reproducible kinetic measurements. Automation of the mixing step and fast repetitive analyses were made possible by the development of stopped-flow instrumentation (18). The advent of the centrifugal analyzer was another instrumental development which allowed fast, multiple sample analyses (19).

The introduction of solid-state analog and digital electronics spurred the development of circuitry which could automatically extract rate information from the raw signals obtained from the instrument

(3,20). Systems were also devised in which minicomputers controlled the timing and functions of digital ratemeters (21,22). The characteristics and theoretical performance of kinetic methods, including signal to noise ratios (S/N), have been described and discussed (10, 23-25).

Fluorescence Methods

During the 1930's and 40's fluorescence methods were first used for quantitative analysis of complex molecules such as vitamins (26). Widespread application of fluorescence methods did not begin until the development of more sensitive and stable instrumentation. In 1956, commercial spectrofluorometers (Aminco-Bowman and Farrand) were first marketed after their development by R. L. Bowman and S. Udenfriend (26-28). The development of more sophisticated, specialized and stable fluorescence instrumentation awaited the introduction of stable solid-state analog and digital electronics in the 1960's.

Applications of Fluorometric Kinetic Methods

The first use of fluorometric monitoring for measurement of initial reaction rates was for the study of flavin mononucleotide and its apoenzyme by Theorell and Nygaard in 1954 (29). Fluorescence monitoring has also been applied to measurement of the activity of certain enzymes for both biochemical and clinical purposes (13,30). Fluorescence kinetic methods have also been adapted for measurement

of metal ions in solution (31,32) and for several different organic compounds and vitamins (33-37). A more thorough review of fluorescence kinetic methods has recently been compiled by Ryan and Ingle (10).

NADH Fluorescence Studies

The first spectroscopic methods for measurement of the reduced forms of pyridine nucleotides (NADH and NADPH) were based on their absorbance at 340 nm (38). As the need for greater sensitivity increased, interest grew in the use of fluorometry for measurement of NADH and NADPH. Kaplan et al. developed a method where NAD^+ could be converted into a highly fluorescent species when combined with 6 M NaOH (39). A more complete study was made of this fluorescent species and of the native fluorescence of NADH and NADPH (30). Reference (13) describes the application of fluorescence measurements of NADH and NADPH to a variety of assays and it also discusses many practical aspects such as the effects of pH and temperature on the native fluorescence of NADH.

Fluorescence Measurements in Serum

Although many assays have been developed which utilize fluorescence measurements made in human blood or serum, very little has been published concerning the specific effects of serum on fluorometric techniques. Several references qualitatively describe

the observed effects of high background fluorescence, scattering and pre-and post-filter effects caused by serum (28, 40).

Another problem which can effect fluorescence measurements in serum is photodecomposition of serum proteins which can cause drifts in the background signals during fluorometric measurements (41).

Specific Enzymatic Assays

The following section will briefly discuss the past developments made on the four enzymatic assays studied in this research.

Ethanol Assay

The first enzymatic assay for ethanol was developed by Bonnishsen and Theorell in 1951 (42). In this method ethanol was quantified by an equilibrium method where the NADH produced was measured with absorbance monitoring. The first use of fluorometric monitoring of the enzymatic ethanol assay using NADH was by Ellis and Hill who also automated the technique using a Technicon Autoanalyzer (43) in 1969. Kinetic monitoring of the ethanol assay was first done by Malmstadt and Hadjiioannou where the change in absorbance of NADH at 340 nm was measured per unit time (44). An automated kinetic method for ethanol using a centrifugal analyzer has been reported (45). One example of a fluorometric kinetic method for the measurement of ethanol was reported where an immobilized-enzyme stir bar was used to produce NADH (46).

Glucose Assay

According to Guilbault, more assay procedures have been developed for glucose than for almost any other substance, probably due to its importance in clinical analysis (11). For enzymatic assays of glucose, one of the most common methods is the hexokinase procedure where the production of NADH or NADPH is monitored spectroscopically (47-49). The fluorescence of NADH has been used to monitor the hexokinase method using equilibrium techniques (50,51). Kinetic enzymatic assays using absorbance monitoring have also been developed for the measurement of glucose (52,53). Fluorescence kinetic methods have been adapted to enzymatic assays of glucose where the production of resorufin (54) or a dimer of homovanillic acid (55) were measured per unit time.

LDH Assay

The first methods developed for the assay of LDH activity measured the change in absorbance of NADH per unit time (56). The first use of fluorescence monitoring of LDH using the native fluorescence of NADH was by Brooks and Olken in 1965 (57). They measured the reaction in the direction where NADH was formed, thereby measuring the increase in fluorescence per unit time. More recently the fluorometric assay for LDH using NADH has been applied to a surface fluorescence technique (58).

CK Assay

One of the most popular methods for CK analysis was first developed by Oliver in 1955 which involved coupling the CK reaction to the hexokinase - glucose-6-phosphate dehydrogenase system (59). CK activity was monitored by the change in absorbance of NADPH per unit time. The first fluorometric method for measurement of CK activity utilized the formation of a fluorescent complex between creatine and ninhydrin (60). A fluorometric method for CK analysis using NADPH was developed for measurement of CK isoenzymes using a TLC method (61) and for on-line measurement following HPLC separation (62). The NADH fluorometric method has also been used for CK assays in a surface fluorescence technique which utilizes silicone rubber pads (63). No reference could be found which described the use of the NADH fluorescence method for CK assays of serum by a conventional fluorometric technique.

There are several examples of the automation of the NADH and NADPH absorbance methods for CK analysis using Technicon Autoanalyzers (64,65). The fluorometric method which utilizes the creatine-ninhydrin complex has also been automated (66,67).

Applications of Resorufin Fluorescence Techniques

To improve the sensitivity of fluorometric measurements of NADH, a coupling system was developed where a fluorescent molecule called resorufin was produced by the oxidation of NADH. The first use of the formation of resorufin for fluorometric analysis was by Guilbault

where he measured the activity of several different dehydrogenase-type enzymes by monitoring the rate of increase in resorufin fluorescence (68). This same technique was applied to the analysis of NADH and NADPH in apples (69) and for the kinetic measurement of glucose (54) where phenazine methosulfate (PMS) was used to catalyze the conversion of resazurin to resorufin. More recent applications of this indicator reaction have used an enzyme (diaphorase) to catalyze the reaction (70,71).

Flow Injection Analysis

Introduction

Continuous-flow analysis techniques refer to methods where samples and reagents are introduced into a flowing stream (within tubing) for transport to a detector. Systems based on this design have been used to automate a wide variety of wet-chemistry assays (72). The first automated technique for continuous-flow analysis was developed by Skeggs in 1957 (73) where air segmentation was used to minimize dispersion and sample overlap. Disperson must be minimized, especially for longer reaction times, to prevent excessive dilution of the sample which will lower the signal levels and increase the detection limit. Air segmentation of samples was used almost exclusively for continuous-flow systems throughout the 1960's, due in part to the introduction of the Technicon Autoanalyzer which gained wide acceptance as the standard system for automated analysis (72).

By the mid 1970's interest in nonsegmented flow systems began to grow due to the efforts of two research groups, Ruzicka and Hansen et al. in Denmark (who coined the term "flow injection analysis") and Stewart et al. in the USA. FIA became the general term to describe flow analysis systems which utilize direct injection of samples into a carrier stream without the use of air bubble segmentation.

The recent upsurge of interest in flow analysis can be seen in the amount of articles published in the last 5 years dealing with developments and applications of FIA. Several review articles have been published recently which describe the developments made in FIA methodology and equipment and the advantages of FIA over conventional, segmented-stream techniques (74-76). A good review of the early history (pre 1975) of flow systems in general (both segmented and nonsegmented flow analysis) can be found in Ref. 77.

Theory and Principles of FIA

Under the experimental conditions normally used for flow analysis (flow rate between 10 and 0.5 mL/min, tubing diameters (internal) 2 mm or less), laminar flow and radial diffusion are the main factors affecting dispersion (78). Laminar flow is characterized by a gradient of flow rates across the diameter of the tube, where the center of the stream is moving fastest while very slow or no flow is observed at the tubing walls. Radial diffusion, diffusion of molecules at right angles to the direction of flow, becomes significant when using tubing of less than 1 mm i.d.. It has

been shown (78) that the dispersion of plugs injected in a carrier stream (due primarily to laminar flow) can be controlled through the selection of the length and internal diameter of the tubing containing the carrier stream. Dispersion can also be affected by the configuration of the tubing as shown in Reference 79 which describes how tightly-coiled tubing reduces laminar dispersion by inducing secondary radial flow.

The knowledge of how to control dispersion was the key to the successful development of FIA. No longer was it necessary to control dispersion with air segmentation which eliminated many applications which utilize medium or large dispersion of the injected plugs (76). The elimination of air segmentation allowed for improved precision in sample introduction via direct injection of fixed volumes rather than timed aspiration techniques used in air segmented systems (75). Residence times of the injected plugs were also more reproducible since surging of the carrier stream was eliminated when no bubbles were present, thus flow rates could be controlled more precisely (74).

Recent Innovations in FIA Techniques

In the last 5 years many innovations have improved the performance of FIA systems. Stewart et al. introduced the use of positive displacement pumps to drive the carrier stream, as opposed to peristaltic pumps, in order to improve the precision of the flow rate (80,81). The principle of merging zones was first described by Bergamin et al. (82,83) in 1978 where plugs of both sample and

reagent are injected into the carrier stream. This significantly reduces reagent consumption by matching reagent and sample volumes rather than requiring reagent to be continuously present in the carrier stream.

Computer control is becoming an important part of FIA methodology, as with many other types of analytical instrumentation. One of the first examples of computer interfacing to FIA instrumentation was by Stewart et al. (84). This example used a microcomputer to control injection valves and an autosampler in addition to performing data collection and calculations.

Applications of FIA

A wide variety of chemical systems and detection techniques have been applied to FIA methodology (74-76). The discussion of applications presented here will be restricted to examples of fluorometric, kinetic or enzymatic methods which are pertinent to the research conducted in this thesis.

A majority of FIA applications which utilize some type of spectroscopic detection use absorbance monitoring. Fluorescence monitoring is gaining popularity since it can provide greater sensitivity and faster measurement times than absorbance methods. Several recent articles have reported the use of fluorescence monitoring for FIA applications involving analytes such as vitamins (85), metal ions in solution (86) and proteins (87).

The majority of FIA applications have been equilibrium methods although a few examples of reaction rate methods have been published recently. An interesting technique utilizing the difference in the formation rate of CDTA complexes of Mg and Sr has been adapted to FIA methodology (88). Reference 89 reports the use of a merging zone technique followed by stopped-flow kinetic measurement of glucose using glucose dehydrogenase. An enzymatic kinetic method for ethanol has been developed for FIA where the change in absorbance of NADH per unit time was measured (90).

INSTRUMENTATION

Fluorescence Reaction Rate Instrument

Introduction

The instrument used in this research to measure reaction rates with fluorescence monitoring is a modification of an instrument originally constructed by Wilson (2) and later modified by Ryan (91). The major components used in this instrument include a 200 W Hg-Xe arc lamp excitation source and housing, an excitation monochromator, a thermostated sample cell holder equipped with stir bar motor underneath, an emission filter or monochromator, a photomultiplier tube (PMT) detector and the ratemeter. The excitation beam is divided by a beam splitter and the intensity of the reflected beam is monitored by a vacuum phototube (PT). The photoanodic currents from both the PMT and PT are converted to voltages with operational amplifier (OA) current-to-voltage (I-V) converters. These voltage signals are input to an analog divider which is used to take the ratio of the fluorescence PMT signal to the reference PT signal in order to compensate for source fluctuations. The compensated fluorescence signal voltage from the divider is input into the ratemeter and also to a chart recorder for continuous monitoring.

The original ratemeter designed and built by Wilson (2, 23) was a hardwired ratemeter in which the rate calculation was based upon an integration fixed-time method (20). In this approach the integral of the signal from the first half of the measurement period is subtracted

from the integral of the signal from the second half of the measurement period. This yields an integral which is proportional to the change in signal per unit time. This is accomplished by first digitizing the input voltage with a voltage-to-frequency (V/F) converter and then directing the V/F pulse train to up-down counters. The integration is accomplished by counting the pulses received from the V/F during the selected measurement period. The subtraction is performed by counting down for the first half of the measurement period and counting up during the second half. The resulting BCD output of the counters is proportional to the reaction rate being measured and can be directly output to a BCD printer for readout. The start of the rate measurement routine is triggered with a switch after manually adding the final reagent to the sample cell. A variable-length delay period between triggering and the start of integration can be selected. Both the delay and measurement periods are switch selectable.

Two major modifications were made by Ryan to the reaction rate fluorometric instrument described above (91, 92). First an automatic reagent injector was added in order to better synchronize the time of initiation of the reaction with the start of the measurement period. This was accomplished through the use of a pneumatically-controlled automatic injecting and filling syringe (Hamilton model 77000) which introduces the last reagent into the sample cell to start the reaction. The syringe was modified by the addition of pneumatic valves and switching circuitry to permit the injector to be triggered by a +5 V (logic 1) pulse from the ratemeter (93). Plastic tubing carries the solution from the syringe to the sample cell. The tubing is positioned over the cell by an aluminum arm which can swivel out in order to

provide access to the cell. The automatic injector allows better run to run precision since the initiation and measurement periods are more reproducible.

The second modification made by Ryan was the replacement of the Wilson ratemeter with a ratemeter based on a microcomputer. The use of an inexpensive microcomputer as a ratemeter provides increased capability and flexibility compared to the Wilson ratemeter, but with convenience, speed and less expense. The Ryan ratemeter was designed to utilize software to calculate both rates and signal magnitudes during a reaction. The signal used to monitor the reaction is digitized with a V/F converter and the pulse train is counted for selected time periods in order to perform rate or magnitude calculations. Various delay and measurement times may be selected by entering specific variables into the software. The raw data collected during the reaction is stored by the Ryan ratemeter thus allowing rates or magnitudes to be recalculated after the experiment with different delay or measurement times.

The Ryan ratemeter consists of a KIM-1 single board microcomputer (SBC) plus a printed circuit (PC) board which serves as an interface between the computer and fluorometer. The board contains the V/F converter, counters and gates which allow collection of data by the SBC and also perform the interface between computer and printer. The operation of this system will be described in some detail below since much of the hardware and software were utilized in modifications of the system to be described later.

Before starting the ratemeter program, the operator must input four variables into specific memory locations in the KIM. Hexidecimal values are required for the following variables: MEASNO, the number of

data points to be used in a rate or magnitude calculation; TIME, the number of 0.25 s periods per data point; DELAY, the number of 0.25 s periods in the delay period; and SELECT, where the value 1 selects a rate measurement, the value 4 selects a magnitude measurement (DVM). The total measurement time for each rate or magnitude calculation depends on the values given to MEASNO and TIME. Hence for an 8 s rate measurement where 0.50 s data points are to be collected after a 4 s delay, the operator would input hexidecimal values of $10, $2, $10 and $1 for MEASNO, TIME, DELAY and SELECT, respectively. Here and elsewhere the symbol $ will be used to denote a hexidecimal (hex) number.

After the variables have been loaded in memory, the program can be started. Two I/O (input/output) lines trigger the injection of the final reagent to initiate the reaction. Next the delay period is timed after which the counters are cleared and a gate is opened to direct the V/F pulse train into two cascaded binary counters. The overflow signal from the binary counters (the pulse rate of the V/F converter divided by 256) is input to the computer through an I/O line. A loop in the program checks for level changes at the overflow I/O line and stores 1 count in a byte of KIM memory for each change from high to low. The counting loop is exited when the desired number of quarter second periods (TIME) have passed and the gate to the binary counters is closed. The 8 bits that remain in the two binary counters are transferred to the KIM via eight I/O lines and are stored in a single byte of memory. This value becomes the least significant byte of a 16-bit data point. The upper byte (most significant) was previously stored as the sum of the overflow pulses from the binary counters. If too many

overflow pulses were collected and the upper byte has also overflowed an error message is printed.

The program repeats this process of collecting data points and storing each 2-byte word in sequential memory locations. Once the desired number (MEASNO) of data points has been collected, the program checks to determine if a rate calculation has been requested. If it has, the program will add up the first half of the MEASNO number of data points into a 3-byte word and will subtract this sum from the sum of the second half of the data points collected in memory. The resulting 3-byte number is proportional to the reaction rate. If calculation of the signal magnitude had been requested, all MEASNO data points would be summed into the final 3-byte word. In order to display either rate or magnitude values, the 3-byte hexidecimal number must be converted to BCD format prior to output to the digital printer which accepts only parallel BCD code. This BCD conversion is accomplished with use of both hardware and software as previously described (91, 92).

After printing the result, the entire cycle of collecting data points, calculation of rate and printing is repeated continually until the allocated memory space is full. After memory space is full or the operator has halted the run, the operator can instruct the program to recalculate a rate or magnitude measurement over any part of the reaction for which data was originally collected. This is accomplished by inputting new values for the variables MEASNO, DELAY and SELECT.

Expanded KIM System

The fluorometer and the RYAN ratemeter just described were initially used for studies conducted on enzymatic fluorescence kinetic methods where the capabilities of this system were adequate. Later, the fluorometric ratemeter was used as part of a FIA system designed for fluorescence kinetic measurements. In order to interface the components of the FIA system to the microcomputer and allow convenient control of the system, it was necessary to modify the Ryan ratemeter. The following changes were made to the initial KIM system (KIM-1 SBC, V/F interface board, and printer): expansion of computer memory, addition of more I/O capability, of firmware containing a BASIC interpreter, of a CRT and of an alphanumeric printer. Figure 1 is a block diagram of the modified computer system. The expanded KIM system was developed using several commercial PC boards (94, 95) as well as PC boards designed and built in our laboratory (93, 96). Greg Campi was primarily responsible for the hardware expansion and details can be found in reference 97. The net results of these modifications are briefly described below.

The first change made to the Ryan ratemeter was to plug the KIM-1 SBC into a motherboard (MB). This allows expansion of the system by permitting other boards to be connected via the MB to the KIM buss system. A 16 K RAM board was added to the MB to increase the memory space. In addition to the RAM board, 4K of RAM are available on the MB and with the 1K on the KIM SBC the total RAM memory space is 21K bytes. This insures that memory space will not limit the amount of data that can be stored or the size of programs to be used with the system.

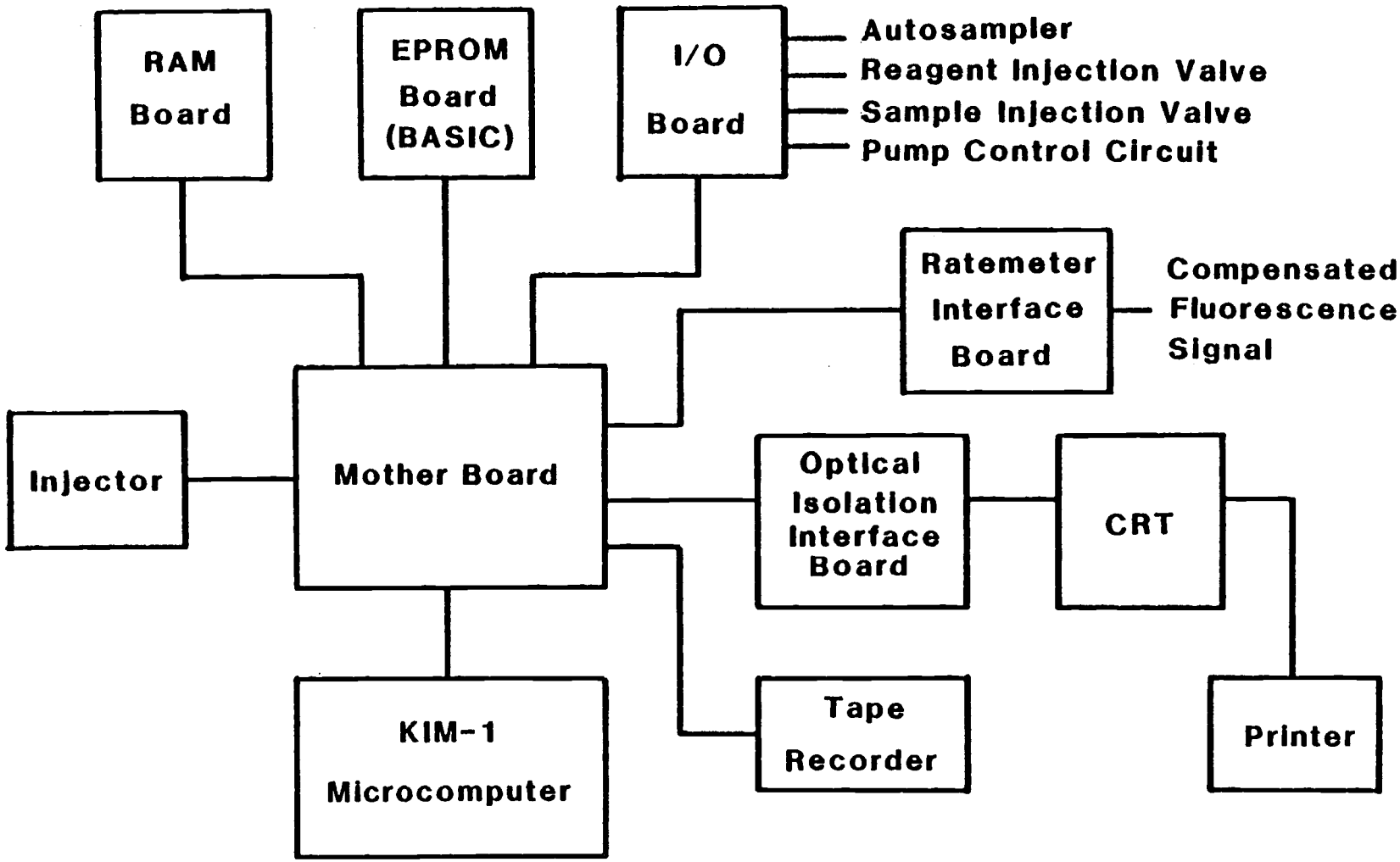

Figure 1. Expanded KIM microcomputer system

A copy of a BASIC interpreter program was loaded into four EPROM chips (8K) via a commercial "Prommer" board. These were then placed on an EPROM board designed to fit in the MB. This addition provides a higher level language for the expanded system thereby allowing more convenient development of complex programs. With BASIC, data can be more easily manipulated since higher level math functions are available.

BASIC provides "bookkeeping" capabilities whereby data or variables can be labeled and stored more conveniently. Instructions and messages in BASIC are in English so the programs are more user compatible than machine language programs. For fast data acquisition and control of peripheral devices, machine language subroutines are still utilized as user routines within the BASIC programs. A detailed description of the software used in the expanded KIM ratemeter will be included later.

The use of higher level languages such as BASIC requires a means of communication between the operator and the computer beyond the capabilities of the KIM hex key pad. A CRT and alphanumeric printer were therefore added to the expanded system for programming, for operator interaction during experiments, and for obtaining a hard copy of program listings or experimental results.

Since the original 15 I/O lines on the KIM SBC are used for the ratemeter, additional I/O lines are required to interact with other devices. An I/O board equipped with two 6522 versatile interface adapters (VIA) was added to the system thereby providing 32 I/O lines. A total of 47 I/O lines are present in the expanded system but for the applications described in this thesis only 31 were utilized.

The expanded KIM system was enclosed in an aluminum box designed and built specifically for this purpose. All the appropriate connectors and cables were mounted on the enclosure to allow connection of the computer to the CRT, tape cassette recorder, power supplies and other external devices (I/O lines). The ratemeter interface board was also installed in the enclosure.

The memory map for the expanded system is presented in Figure 2. A block diagram of the complete fluorescence rate measurement instrument is shown in Figure 3.

This enhanced ratemeter system was first used for discrete analysis using a standard 1 cm square fused silica cell and the automatic injector to add the last reagent. For later studies using the FIA system, a fluorescence flow cell was employed in place of the cuvette. When using the FIA system, the microcomputer controls the pumps, sampler and injection values in addition to performing rate measurements, as shown in Figure 1. This will be discussed in greater detail later in this section.

Software Modifications for the Expanded KIM Ratemeter

The first change made to the Ryan ratemeter program was to modify the data collection subroutine such that more of the increased memory space could be utilized for data storage. This was achieved by using an indirect indexed addressing mode (98) so that memory space greater than 256 bytes could be accessed. The indirect indexed mode allows the program to compute the addresses for the storage of data points. Similar modifications were made to the subroutine used to recalculate

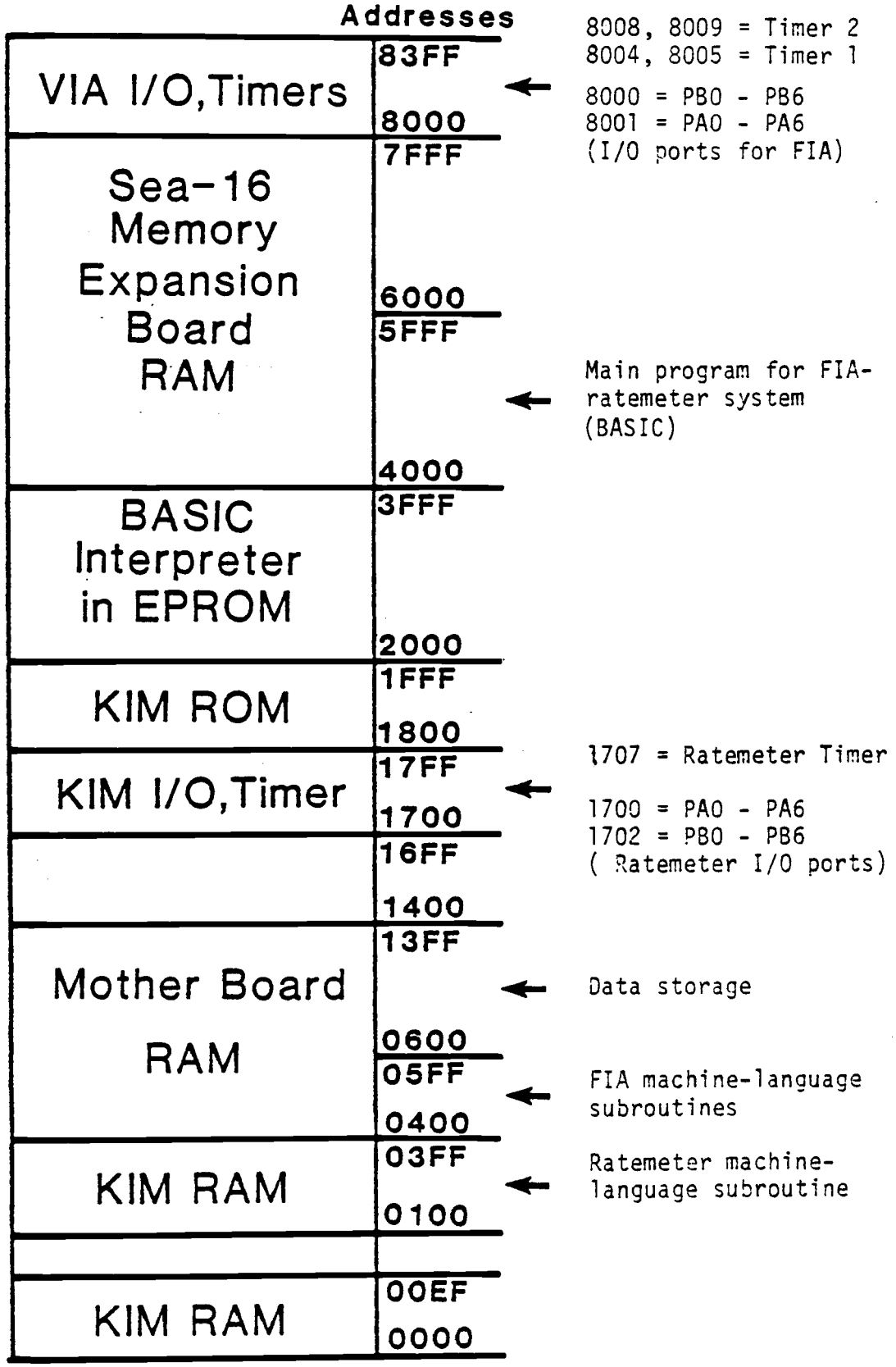

Figure 2. Memory map of the expanded KIM system

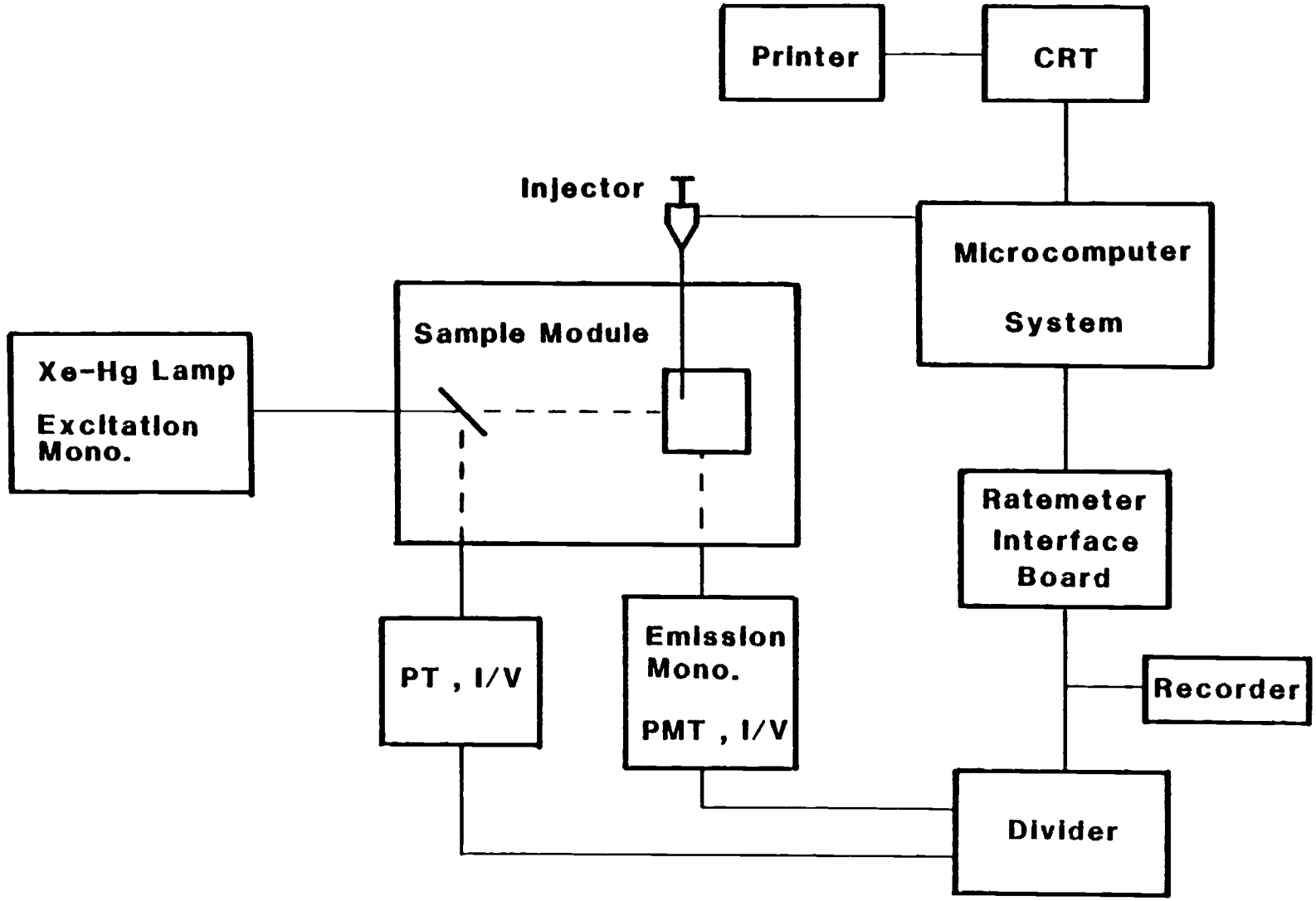

Figure 3. Block diagram of the Fluorescence Ratemeter Instrument

rate or DVM values such that the stored data could be correctly retrieved from memory.

Next, a BASIC program was developed which would utilize the ratemeter software as a subroutine for data collection and rate calculation. To make the ratemeter program compatible with BASIC all but a few variables had to be transferred out of zero page (memory space located between $00DE and $00EE is usable). Most of the memory on zero page is required for the operation of the BASIC interpreter. The "BASIC" ratemeter program was designed to provide the machine language subroutine with the required values of variables such as MEASNO, TIME, DELAY and SELECT. The operator can input the values in units of time since the BASIC program can convert them into the proper form before loading into the ratemeter subroutine. Another important feature of the BASIC ratemeter program is the use of PRINT statements to output the calculated rate or DVM values. This eliminates the need for the BCD printer and the required conversion of hexidecimal values to BCD.

The sequence of events for a typical rate measurement using the BASIC ratemeter program are summarized below. Upon starting the program, the operator is first asked to input the value of the variables TIME, MEASNO, DELAY and SELECT and the number of rate or magnitude values to be calculated. The BASIC program then converts the values into the proper form and loads them into the memory locations for use by the subroutines. Upon input of the last variable, the program waits until instructed by the operator to begin, then jumps to the start of the ratemeter subroutine. As with the Ryan ratemeter the first task of the subroutine is to inject the reagent and following the desired delay time, data collection is begun. When using the FIA

system the ratemeter subroutine is not entered until after the injection of the sample. Details of this are included later in this section.

Following calculation of the rate value the program jumps back to BASIC in order to print the value. If more data are to be collected and additional rates calculated, the program returns to the ratemeter subroutine. This process is repeated until the desired number of rate measurements are made or the operator stops the program. The operator then has the option of using the collected data to recalculate rate or magnitude values or start a new run.

The program listings for both the BASIC program and the machine language subroutine are included in Appendix I.

FIA INSTRUMENTATION

Introduction

This FIA system was designed for maximum versatility and ease of operation for fundamental studies and optimizations of kinetic-based assays. The system utilizes the concept of merging zones in order to minimize the amount of reagent used per analysis (see Figure 4). The samples and the reagent are each injected and carried to the mixing tee by a separate injection loop and pump. Once merged, the combined flow carries the combined plugs through a mixing coil and on to the fluorescence flow cell. After measurement, the combined plug is carried to a waste container. Solutions are drawn into the injection loops by the suction of the house vacuum which is coupled to the loops via side arm flasks to collect the solution not injected. A needle valve between the flask and the injection loops is used to control the flow rate of the withdrawal stream. The introduction of multiple samples and standards was automated by the addition of an autosampler. An automated 3-way valve was used to switch between reagent and rinse solution for the reagent injection loop.

The mode of operation of this system is quite versatile. Normal FIA measurements may be made where the combined plugs are carried through the flow cell and either peak heights or peak areas are measured. For kinetic studies, flow of the carrier stream is stopped while the combined plugs are present in the flow cell. Flow can be stopped by either halting the pumps or by bypassing the carrier stream around the cell using a 4-way valve.

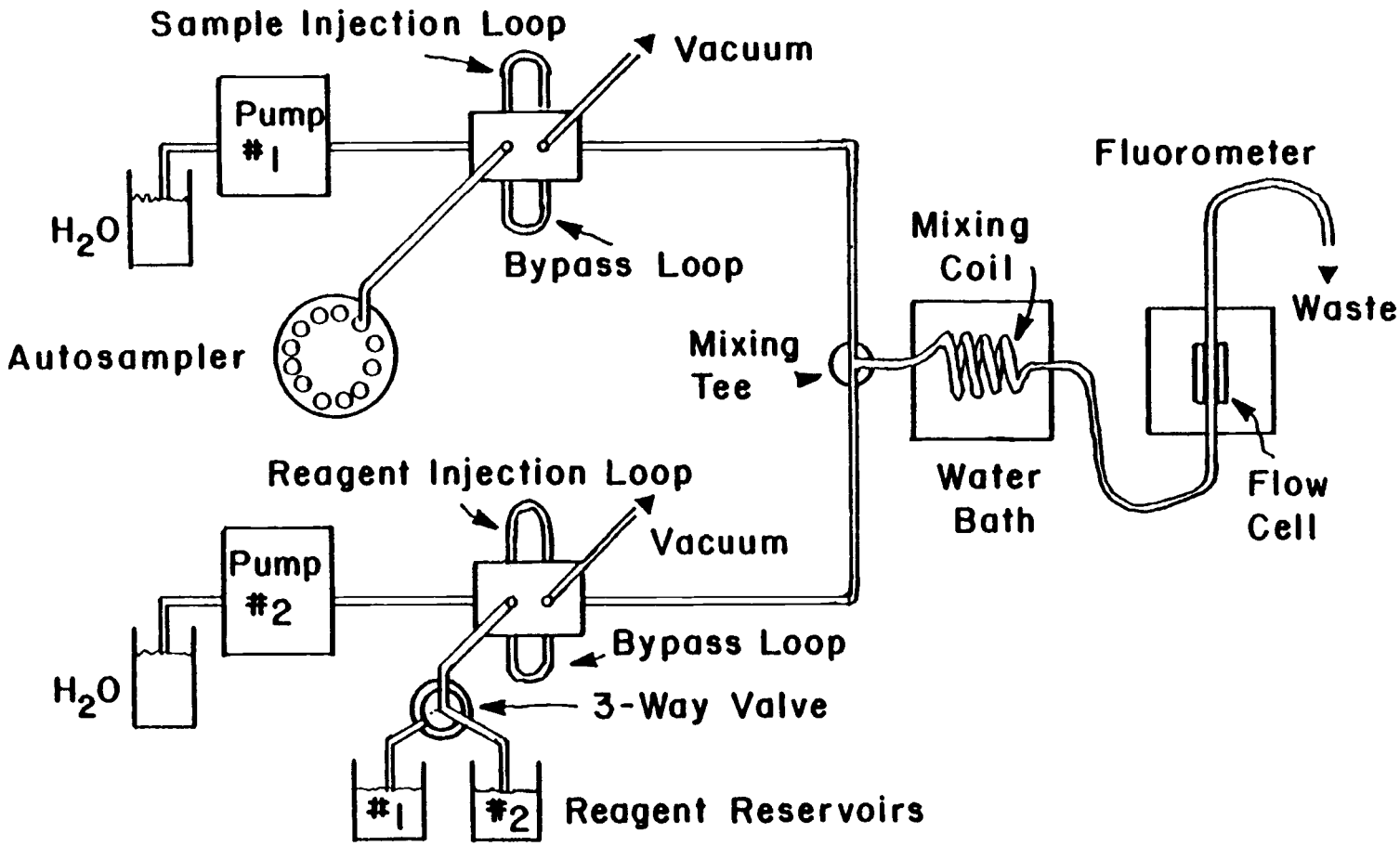

Figure 4. Schematic diagram of the FIA-merging zones system. See Table I for a description of components and Table III for tubing dimensions.

The components used in the system were selected for use because each could be adapted to computer control. The injection loops were purchased with pneumatic activators to allow computer-controlled switching. Both pumps were designed specifically for direct interfacing to permit the computer to select flow rates. The model of autosampler chosen for this system was a unit which could be conveniently modified for computer control. The major components of the system are each described in greater detail below. Table I contains a lists of the components and their sources.

Components

Special consideration was given to the type of pump used in the FIA system. The precision of the flow rate is an important factor for reproducible delivery of samples and reagents to the flow cell. In a merging zone system, the mixing ratio of the sample and reagent depends on the relative flow rates of the two pumps therefore any variation in flow rate could effect the concentration of the injected solutions arriving at the flow cell. The two pumps chosen for this system are positive displacement valveless pumps each driven by a stepping motor. This type of pump provides optimum flow rate precision since a minimum amount of moving parts are needed and it is not susceptible to tube stretching as with peristaltic pumps. Each stepping motor is driven by a variable pulse train provided by an oscillator and digital drive circuits housed in the control box. Since the motor speeds are primarily governed by the frequency of the pulses rather than current or

Table I

List of FIA Components

Component	Source	Comments
Pump and Controller	IVEK Corp. Springfield, VT	Model = Super Lox SO-1, computer controllable, positive displacement valveless pump.
Sample Injection Valve	Dionex Corp. Sunnyvale, CA	Model #30520 slider bar type variable injection loop volume, equipped with pneumatic actuators
4-way Valve	Dionex Corp.	Model #30524 slider bar type equipped with pneumatic actuators
Autosampler	Alpkem Corp. Clackamas, OR	Remanufactured Technicon Sampler III
Fluorescence Flow Cell	Precision Cells Inc. Hicksville, NY	Model #P/N 8830 20 μL capacity, square sample cavity.
Merging Tee	Dionex Corp.	Cat. #24440, compatible with ¼-28 threaded fittings, 0.8 mm i.d.
Autosampler Control Box	Built in house by Dean Marino	Supplies circutry to control the autosampler, also provides the source of +5 V, 300 mA for the logic circuitry for injection valves and autosampler
Solid State AC Relay	Newark Electronics Inc. Chicago, IL	Manufactured by Grayhill, model #70S2-04-B-04-F, for switching AC lines with TTL logic signals
3-Way Solenoid Valve	Skinner Valve Co. New Britian, CT	Model #MBD-002, three-way minature valves switched by 120 V AC

voltage, as with conventional electric motors, the pumps are less subject to variations in flow rate due to changes in fluid viscosity.

The maximum stepper motor rate of 608 RPM limits the flow rate to less than 6 mL/min per pump since the displacement volume per revolution is approximately 10 μL. The displacement volume can be adjusted but the pumps have been factory calibrated such that a specific pulse frequency will correspond to the desired flow rate. The 10 μL displacement volume helps minimize the effects of pulsations since faster RPMS are required to produce reasonable flow rates (1 to 4 mL/min). The time period between pulsations is relatively short (0.3 s between pulses at 2 mL/min) and therefore pulsations average out more completely. Thumb switches on the control boxes allow flow rate selection from 0 to 5.99 mL/min in steps of 0.01 mL/min.

The pump systems as obtained from IVEK (99) were equipped with computer interface boards which allow direct coupling of the control boxes to I/O ports on the KIM system. A 14-pin female connector on the back of each pump control box provides access to the BCD interface which accepts 1.4 to 20 V positive logic signals. For this application only 5 pins out of the possible 12 were utilized since maximum flow rate resolution was not required and it was desired to conserve I/O lines for other purposes. Table II shows the specific connections between the control boxes and the computer. This arrangement provides flow rate control for each pump from 0 to 4.4 mL/min in steps of 0.2 mL/min. The software to convert values in terms of mL/min. into the appropriate hexidecimal number for output to the 5 pins will be described in the section covering FIA software.

Table II

I/O Assignments for Computer Control of Flow Rates

I/O bit on 6522 ($800X)		Corresponding [c] Pin # on Control Box Connector	Respective Flow Rate (mL/min)
Reagent Pump	Sample Pump		
PA7 [a]	PB4 [b]	14	2.0
PA6	PB3	13	1.0
PA5	PB2	3	0.8
PA4	PB1	4	0.4
PA3	PB0	12	0.2

a Port A (PA) = $8001

b Port B (PB) = $8000

c A high (+5 V) or a combination of highs at the respective I/O bit(s) selects the desired flow rate. Remaining bits are held low (0 V).

The two sample injection valves used in this system were both double-stack, slide bar type valves (see Appendix II). These valves are designed to use various lengths and diameters of tubing which can be coupled to the valve with ¼-28 NF thread fittings. The advantage of this design is that a wide range of injection loop volumes may be utilized. Each injection loop was fitted with a bypass loop of approximately 15 μL to allow quick wash out while the injection loop is on line. A variety of injection loops were made in our laboratory using various lengths of 0.5 and 1.5 mm i.d. teflon tubing. The volume per cm of length is 1.96 μL and 17.7 μL for 0.5 and 1.5 mm i.d. tubing, respectively. The actual volumes of each loop were measured by first weighing the loop dry and then again after filling with water.

Both injection valves are equipped with pneumatic activators mounted on opposite ends of the slide bar. When air pressure of at least 50 psi is switched from one activator to the other the state of the injection loop will change. The application or release of pressure to each actuator is governed by an AC activated, 3-way solenoid valve. The circuitry to control the two solenoid valves needed for each injection valve is shown in Figure 5. The circuit allows switching of each injection valve either by a logic signal from an I/O bit or manually with a push button. Two identical circuits were built, one for each injection valve, and were mounted in an aluminum box. The injection valves along with a pair of solenoid valves for each were all mounted in a single open-topped aluminum box.

A 4-way valve, identical to the type used for sample injection valves (see Appendix II) was equipped with pneumatic actuators. The circuitry and hardware assembled for switching the valve are identical

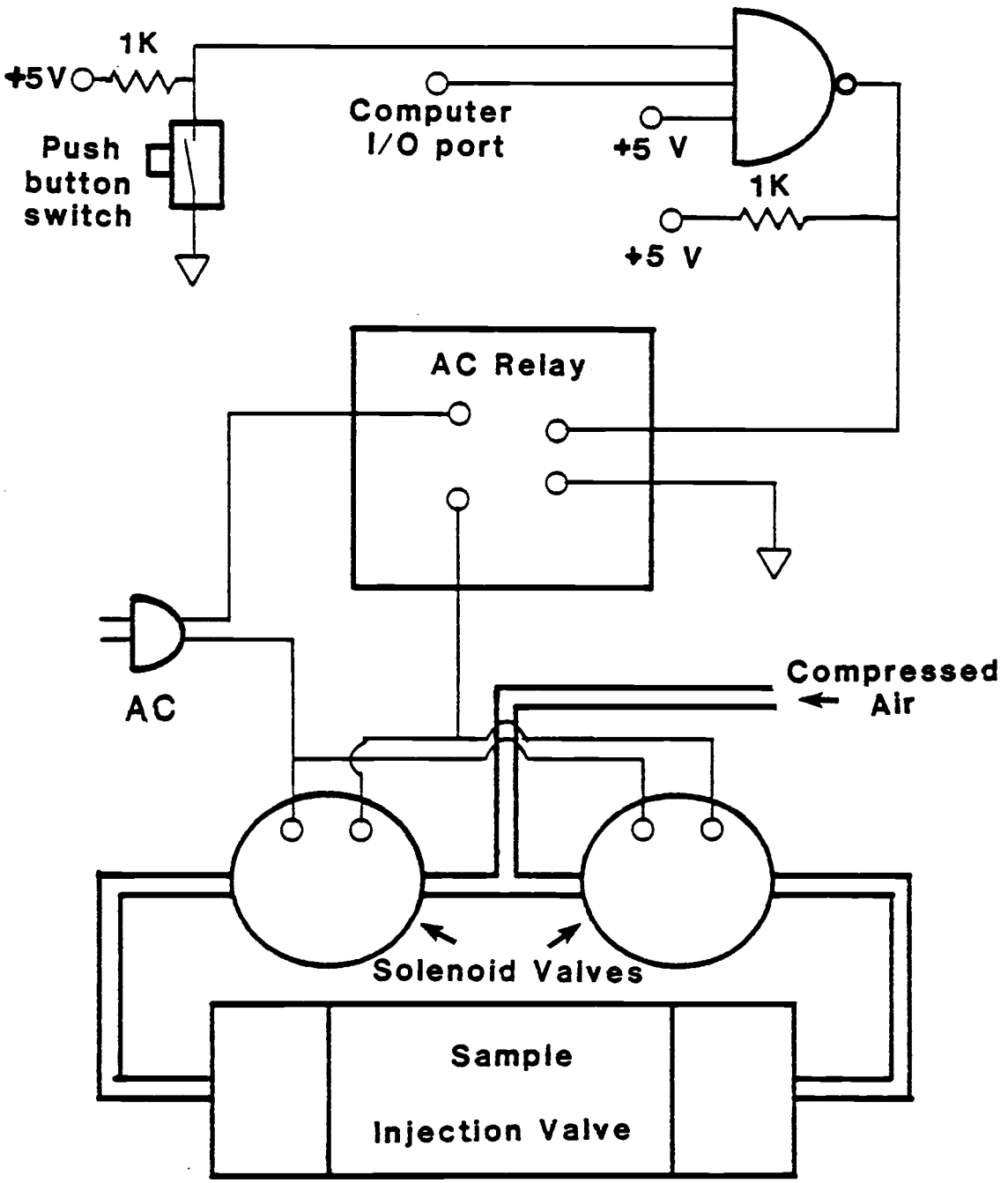

Figure 5. Diagram of the circuitry and hardware used to control a sample injection valve. Components are listed in Table I. The NAND gate used is an open-collector type (3-input type used because no 2-input gates were available).

to those for the injection loops except that direct connection was made between the +5 V control pin of the AC relay and an I/O line on the KIM system. This simplifies the circuit since no NAND gate is required along with the +5 V source needed to provide power. This simplification allows the 4-way valve to be more mobile and versatile for a variety of different uses.

The first and most important application of the 4-way valve was to divert the carrier stream around the flow cell during stopped-flow measurements (see Figure 6). This option for stopping flow has several advantages over the alternate method, that of stopping the pumps, as will be discussed in the Results section. The 4-way valve was also used as a 3-way valve (by blocking one port with a plug) to automatically switch between two different solutions for filling the reagent loop (see Figure 4).

For the automatic introduction of multiple samples and standards into the sample injection loop an autosampler was added to the system. A remanufactured Technicon Sampler III (100) was chosen because it is reliable, inexpensive and easily adapted to computer control. The Sampler III features a 40 vial sample tray for which 3 mL vials were purchased. The probe arm was fitted with a 35 cm section of 0.5 mm i.d. teflon tubing connected to the injection valve. The length of tubing within the probe arm was adjusted so that when sampling, the tube would reach the bottom of each vial. The rinse receptacle on the Sampler III was connected to a large separatory funnel to provide water for rinsing the tube and sample loop between samples.

The operation of the Sampler III is a simple, two step process. The probe arm extends out and down into the sample vial when two leads

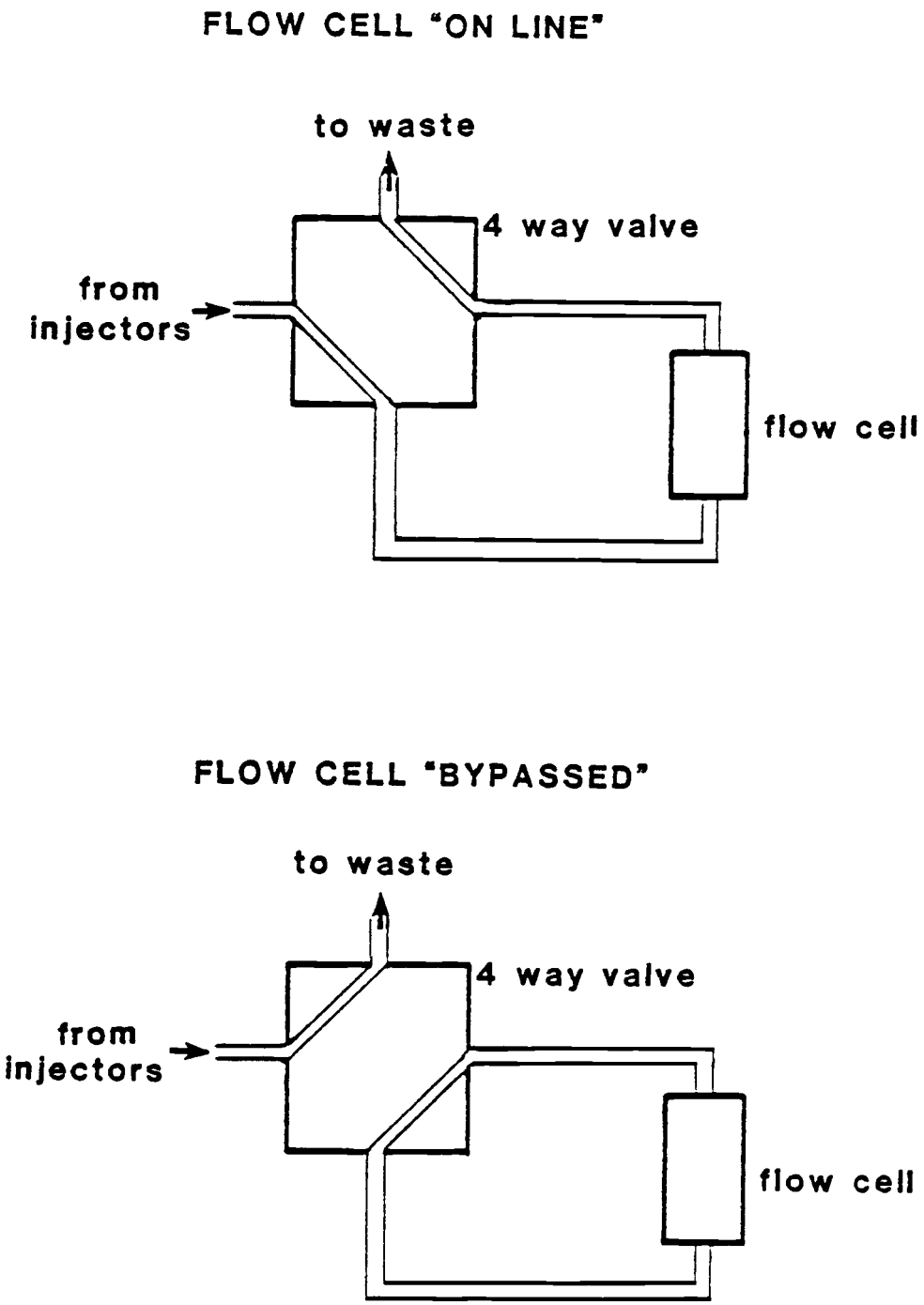

Figure 6. Operation of the 4-way valve for bypassing flow around the flow cell.

from the autosampler are connected. Breaking this connection causes the arm to return to the rinse receptacle and the sample tray to advance clockwise to the next vial. Operation of the Sampler III was placed under computer control by using a circuit specially designed for that purpose by Dean Marino. A complete description of the circuit is available elsewhere (101). The circuit accepts TTL logic signals from an I/O line of the computer which causes the circuit to switch a reed relay to open or close the connection between the two leads. Additional connectors on the box containing this circuitry provide access to TTL signals for synchronization of other devices with the autosampler.

The fluorescence flow cell used in this system was a model designed for fluorescence detection for HPLC. The dimensions of the cell housing are 12.5 mm x 12.5 mm x 57 mm not including the inlet and outlet fittings. The intensity of fluorescence radiation from the cell is enhanced by two mirrors mounted on the inside walls of the housing opposite the excitation and emission windows. The sample cavity is contained within a square bar of fluorescence-grade fused silica. The cross section of the 20 μL sample cavity is square (1 mm x 1 mm) which minimizes the amount of scattered light reaching the detector. The inlet and outlet tubing (0.25 mm i.d., 1.5 mm o.d.) were made of stainless steel and were equipped with ferrule-type high pressure fittings.

Several modifications were required to match the flow cell to the FIA system and the fluorometer. The cell housing was raised by attaching a 6 mm x 12 mm x 12 mm block to the bottom in order to center the sample cavity in the excitation beam. Clip-on slits of various sizes were made to attach to the cell windows to optimize the spectral

properties of the cell. The stainless steel inlet and outlet tubing was replaced with 0.5 mm i.d. teflon tubing. This allowed the use of ¼-28 thread fittings to make the flow cell compatible with the rest of the FIA system. The larger diameter teflon tubing reduced the amount of pressure drop across the cell which adversely effected stopped-flow measurements. Black tape was wrapped on the inlet tube over the length that passes through the interior of the cell housing to eliminate background fluorescence from the Teflon.

A homemade fluorescence flow cell was constructed using parts from an absorbance flow cell housing and fuzed silica tubing (2 mm i.d.). Initial studies of the cell showed that its performance was inferior to that of the commercial flow cell. No further testing or use was made of the homemade cell.

The tubing selected to connect the various components of the FIA system had to meet several requirements. Dispersion must be minimized to obtain maximum concentrations of sample and reagent upon arrival at the flow cell. Pressure drop or flow restriction by the tubing must also be minimized especially for stopped-flow measurements. Inertness, maximum mixing efficiency and good thermal transfer properties are also important considerations. In general, larger i.d.'s and longer lengths will increase dispersion while small i.d.'s will show increased pressure drops.

Teflon tubing was used for all flow paths involving solutions that would eventually pass through the cell. Connectors and fittings used throughout the system were made with an electrically-heated flanging tool and with ¼-28 thread Teflon fittings. These fittings are compatible with all components and two sizes are available for 1.5 and

3.0 mm o.d. tubing. Table III summarizes the tubing used in this system. The choice of the diameter of tubing between the tee and the flow cell and for the injection loops will be discussed in the Results and Discussion section.

Tubing used between the H_2O reservoir and the pumps and on to the injection valves was all 1.5 mm i.d. teflon tubing. Larger tubing is practical for this portion of the system since dispersion is irrelevant and minimizing pressure drop is important. At higher pumping rates (greater than 3 mL/min) cavitation and out-gassing of the carrier stream entering the pumps can be a problem. These problems are reduced by using larger diameter tubing between the reservoir and the inlet to the pumps and by elevating the reservoir several feet above the pumps.

Software for FIA System

Computer control was emphasized in the design and construction of the FIA system so that the operation of the system could be controlled by software. This allows more convenient optimization of the operating parameters and more versatility in the mode of operation. The software is responsible for input of variables from the operator, control and timing of all FIA operations, data collection, calculations and display of results. For convenience, the main program written to accomplish these tasks is in BASIC while machine language subroutines are utilized for data collection and for control of the FIA components.

The operational sequence controlled by software is summarized in Figure 7. As can be seen, first the values of variables used by the

Table III

Summary of Tubing Used in FIA System

Connection [a]	Tubing i.d. (mm)	Tubing Length (cm)
Carrier Stream Reservoir to Pumps	1.5	100
Pumps to Injection Valves	1.5	45
Autosampler to Sample Injection Valve	0.5	35
Reagent Reservoir to Reagent Injection Valve (when not using 3-way valve)	1.5	30
Reagent Reservoir(s) to 3-way Valve (when used)	1.5	25
3-way Valve to Reagent Injection Valve	0.5	35
Injection Valves to Vacuum	1.5	100
Bypass loops	0.5	5
Reagent Injection Valve to Tee	0.5	15
Sample Injection Valve to Tee	0.5	14
Tee to Flow Cell	0.5	14
Flow Cell to Waste	0.5	40

a Refer to Figure 4

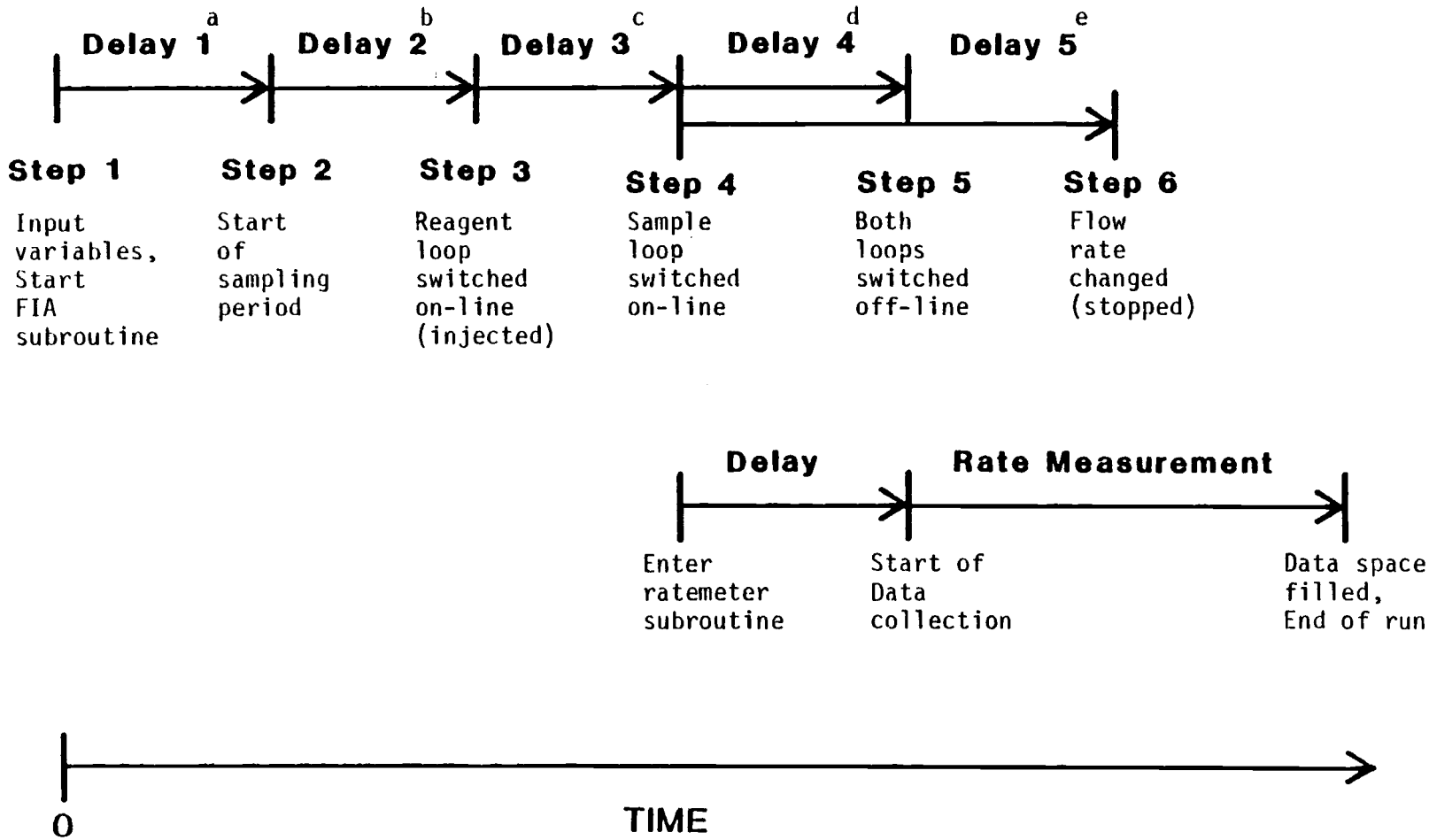

Figure 7. See caption on p. 43

Figure 7. Sequence of events for a Typical FIA run.

[a]Initial rinse period, also allows pumps to attain the desired flow rate.

[b]Sampling period, autosampler in sample mode, 3-way valve switched to allow reagent to enter reagent loop.

[c]Delay between injection of reagent and sample loops. This allows adjustment of the overlap of the plugs.

[d]Delay to allow the full volume of the loops to enter the carrier stream, depending on loop volume and flow rate.

[e]Delay between switching loops off-line and changing flow rate (usually flow is stopped).

This diagram was not drawn to scale and the lengths of each segment are not proportional to the actual delay times. See Results and Discussion for more details of the actual time periods used.

program are entered. The sample and reagent loops are filled, followed by the injection of the contents of each loop into its own carrier stream. At this point (Step 4) the ratemeter subroutine is entered and the ratemeter delay (DELAY) is begun. For continuous-flow applications, the measurement period is started prior to the arrival of the merged plugs at the flow cell in order to get a measurement of the baseline. For stopped-flow, kinetics-based measurements using FIA, baseline measurements are usually unnecessary so the ratemeter delay is extended until just after Step 6 is completed. At this point the merged plugs have entered the flow cell and flow has been stopped so that meaningful data can be collected.

The operation of the program will now be described in more detail. In Step 1, the program first asks the operator whether single or multiple runs are to be made and the number of multiple runs. Next the values of variables for rate or magnitude measurements, delay periods and finally pump flow rates are entered for later use by the main program and by the subroutines.

The rate measurement variables are equivalent to those in the BASIC ratemeter program described earlier. Values for MEASNO, TIME, DELAY and SELECT are input by the operator and are converted by the program into the proper form before being entered (POKEd) into the ratemeter subroutine. The main program also requests input of the amount of memory space to be used for data collection.

The main program then requests input of the five delay periods of the FIA routine. The time values for each of the 5 delay periods are individually requested by the main program. After input by the operator each value is converted to the proper form for use by the FIA

subroutine. These converted numbers are POKEd by the main program into specific memory locations where they may be accessed by the FIA subroutine. A description of how the timing is conducted will be presented in the discussion of the FIA subroutine.

The last variables to be requested for input are the initial and final flow rates for both the sample and the reagent pump. The software is designed so that not only the initial flow rate may be selected but also a change in flow rate of either or both pumps may be executed any time after the injection of the sample. A total of 4 values in units of mL/min are input by the operator and then are converted to the proper form for loading into the I/O ports assigned for control of pumping rates. Refer to Table II for the assignment of specific I/O lines for computer control of flow rates. The flow rates to be input by the operator are restricted to values between zero and 4.4 mL/min in increments of 0.2 mL/min. A description of the routine used by the program to convert the input values into the proper form can be found in Appendix III.

After all variables have been entered and the proper conversions performed, the main program asks the operator if a run should be initiated. After the operator initiates the run, the program jumps to the FIA machine language subroutine to start the sequence of operations. The FIA subroutine, including the necessary timing routines, is contained in memory between $0400 and $0520, just above the ratemeter subroutine (see Figure 2). The subroutine carries out the 6 steps described in Figure 7, each step separated in time by the specific delay period requested by the operator. Execution of these 6 steps is accomplished by changing the output of I/O ports A and B as

described in Table IV. To change the output of one or more lines while retaining the contents of all other lines in the I/O port requires the use of addition and subtraction commands. For example, if PA1 is to be changed from high to low (switching reagent injection loop on line) the value in port A is first loaded into the accumulator. The number 2 is subtracted from the value in the accumulator changing bit 1 from 1 to 0 but changing no other bits. This value is then loaded back into port A causing the reagent injection valve to switch while all other I/O lines and devices remain unaffected. The first 4 steps of the FIA procedure are executed as a series of additions and subtractions of the initial value placed in I/O port A.

The intervals between each step are timed by the computer using two different approaches, depending on the requirements of each situation. Timing for the delay periods 1 thru 3 is performed with a downcounting register ($1707) located on the 6530 IC chip on the KIM board. Operation of the register and the software used in this application are identical to the timing routines utilized in the Ryan ratemeter (91). The software compares the number of downcounts (0.25 s periods) to the total number required to make up the requested delay time. These values are obtained from consecutive memory locations ($00E9 to $00EB) which were loaded by the main program following the input of delay times by the operator.

A different approach is taken for the last 2 steps of the FIA run. Here delay periods 4 and 5 are timed without the direct participation by the computer as with the method using registers on the 6530 chip. This is accomplished by using the timing registers located on the 6522 VIA chip which can perform unattended timings by utilizing interrupts

Table IV

I/O Assignments for Control of Valves and Autosampler

I/O Bit on 6522	Device Connected To It	Logic Signal at Bit	State of the Device
PA0	Autosampler	0	Rinsing
		1	Sampling
PA1	Reagent injection valve	0	Bypass loop on line
		1	Reagent loop on line
PA2	Sample injection valve	0	Bypass loop on line
		1	Sample loop on line
PB5	4-way valve for flow cell bypass	0	Flow cell on line
		1	Flow cell bypassed

to signal the end of each selected time period (102). This method allows the computer to proceed with data collection or other duties during the last 2 delay periods. For example, measurements can be made of the baseline prior to the arrival of the merged plug at the flow cell since the computer is not occupied with counting the number of 0.25 s downcounts.

This mode of timing is accomplished by using two 16 bit downcounting registers on the 6522 which are tied together by connecting I/O bits PB6 and PB7. The lower 16-bit register (Timer 1) is programmed to operate in a free run mode where a pulse is output at PB7 once every 0.1309 s. The pulse from PB7 will enter PB6 where it will decrement the value in the upper 16-bit register (Timer 2). In this manner, timing periods of up to 142 minutes may be produced by placing various values into Timer 2. For FIA applications, periods of zero to 33 s are usually sufficient so values between 00 and $FF are loaded into the lower byte ($8008) and 00 into the upper byte ($8009) of Timer 2. The main program loads the appropriate delay value (# of 0.1309 s periods) into specific memory locations during the input of FIA delay times. The FIA subroutine takes the delay value and enters it into the lower byte of Timer 2 and loads $FF into both upper and lower bytes of Timer 1 to initiate the timers. Once the timers have been started, the computer may proceed with other duties. When the value of Timer 2 reaches zero an interrupt is requested, stopping the program in progress and causing a jump to an interrupt service routine.

The execution of the last 2 steps of the FIA routine are performed by interrupt service routines. When the computer responds to the interrupt, the location of the service routine is obtained from the

interrupt vectors ($17FE, $17FF). The first service routine will execute Step 5 of the FIA routine by adding the number 6 to the value in I/O port A thus setting PA1 and PA2 high. The first service routine must also load the interrupt vectors with the location of the second service routine. The interrupt flag must be cleared and the value of the time remaining for Delay 5 must be loaded into Timer 2 before control is returned to the program halted by the interrupt.

The second interrupt service routine will be called at the end of Delay 5. This routine will change the values of the I/O lines which control the flow rates. This is done by first subtracting the values of the initial flow rates from Ports A and B then adding the appropriate values for the final flow rates. The flow rate is normally changed to zero for both pumps in order to conduct stopped-flow measurements. After changing the flow rate, the service routine clears the interrupt flag and control is again returned to the halted program.

An interrupt can be requested at any time during the execution of the ratemeter subroutine and following the service routine the program will proceed unharmed from the point where it was halted. The service routines are executed very quickly (approximately 20 μs) relative to the data collection routine (0.25 s) so no significant errors are caused in data collection. The only instance where an interrupt can interfere with the operation of the system is during the readout of a rate or magnitude valve to the CRT and printer. The interrupt will interfere with data transmission and cause incorrect letters or numbers to be displayed. This problem can be avoided by temporarily disabling the interrupt during the PRINT commands of the main program.

Following Step 4 of the FIA routine, control is returned to the main BASIC program where the jump is made to the ratemeter subroutine. Except for the two interrupt service routines executed sometime during the remaining part of the run, the operation of the ratemeter software is nearly identical to the BASIC ratemeter program described earlier. Data are collected and either rate or magnitude values are calculated by the subroutine. Following the calculation, the jump is made back to the main program in order to print out the result. The major difference between the original BASIC ratemeter program and the FIA-ratemeter version is that the later keeps track of the number of interrupts called. Once two interrupts have been called the main program disables the 6522 interrupt request line thus preventing any additional interrupts from being called. The main program will also record a message on the readout device that the flow rate change was executed during the just-completed measurement period. This allows the operator to pick out which values were recorded before and after the flow rate was changed.

The end of the FIA run occurs when the selected amount of memory space has been filled with data. What happens next depends on whether the system is being used in the single or multiple run mode. If the single run mode had been selected (at the start of the program), the program would then ask the operator whether measurements should be recalculated and what changes to make in the recalculations. If recalculation is not requested or after all the desired recalculations are completed, the program returns to the start and again requests if single or multiple runs are desired. At this point the operator can

also choose whether to change the value of any variable or repeat the run using the same parameters.

If the multiple run mode had been selected, the second run would start immediately after completion of the first run, using the same parameters. With this mode, no option is available to recalculate the results of each run since data from each successive run is written over data from the previous run. At the end of the requested number of multiple runs, the program again returns to the start and again asks which mode to use for the following runs and whether parameters are to be changed.

Three Loop Merging Zones System

Brief studies were conducted with an additional injection valve to investigate the use of merging 3 separate plugs into the carrier stream. This 3rd valve was set up in identical fashion to the one used for injecting reagent except that no 3-way valve was included. Computer control of the 3rd valve was accomplished in a different manner than for the reagent injection valve. Since this was only a temporary study, the valve was set up for computer control by the most convenient means available. All I/O lines of one of the 6522 VIA were used for other purposes so a connection was made between the 3rd valve and a control line from the autosampler control box. This signal switched the 3rd loop off-line for filling during the sampling period and injected the 3rd loop simultaneously with the sample loop.

A 3rd pump was set up to carry solution from the 3rd injection valve to the 4-port merging manifold (Dionex Inc.). This additional

pump was a positive displacement, valveless pump identical to the two original pumps except it was not designed for computer control. Flow rates were adjusted manually and temporary computer control for stopped-flow studies was set up with a TTL-switched AC relay (101) connected between the pump power cord and an AC outlet.

EXPERIMENTAL

Introduction

This section covers the preparation of solutions and experimental conditions used for studies included in this thesis. The general instrumental parameters used for fluorometric measurements with the Wilson and Ryan ratemeters are presented. The preparation of stock solutions used for each type of enzymatic assay and for interference studies are listed along with the procedures and specific measurement parameters for each. The latter part of this section describes instrumental conditions used for FIA methods in addition to procedures for optimizations and routine analysis.

General Solution Handling

All solutions were prepared using double deionized water prepared by a Millipore Milli-Q system fed by house deionized water (all further references to H_2O will refer to this grade of water). All chemicals were reagent grade except where noted. The glassware and plasticware used in these experiments were all cleaned prior to use as previously described (2). Dilutions of stock solutions and the addition of reagents to the sample cell were conducted with Eppendorf pipets equipped with disposable tips. When adding solutions to the cuvette, care must be taken to flow solutions down the side of the cell to avoid formation of bubbles in the cell. The stir

bar within the cuvette should not be started until at least 2 mL of solution is present in the cell to prevent bubble formation. The cuvette was rinsed 4 times with H_2O between runs.

Instrumental Parameters

The following parameters were used for the fluorometric measurement of NADH in a 1 cm square fused silica cuvette mounted in the Wilson (or Ryan) fluorometer. Changes made for the measurement of resorufin or for fluorometric measurements conducted with the FIA system will be discussed later.

General instrumental conditions were set as follows unless specified otherwise:

excitation wavelength:	366 nm
excitation bandpass:	17 nm (2 mm slit width)
emission wavelength:	468 nm (with emission monochromator)
emission bandpass:	12 nm (1.4 mm slit with emission monochromator)
	10 nm (with emission interference filter)
feedback resistor for current-to-voltage converters	10 M Ω with a 0.1 uF feedback capacitor chosen for one second electronic time constant
PMT voltage:	800 V (current gain of 10^6)
Temperature of water bath to control cell temperature:	25 °C

Studies of NADH Fluorescence

Initial Studies

Studies of the use of the Wilson fluorometer for fluorometric measurement of NADH began with obtaining excitation and emission spectra. Following the selection of optimum excitation and emission wavelengths, a calibration curve was made in order to determine each parameter such as the detection limit and upper limit of linearity. Initial studies included remaking the calibration curve using separate sets of NADH standards made up in each type of buffer required for the different enzymatic assays to be studied. The preparation of each buffer is described in the table of stock solutions made up for the respective assay. The effect of changing temperature and pH on NADH fluorescence was also studied. Measurements were also made using NADPH to compare its spectral properties to NADH.

It was observed that NAD^+ and $NADP^+$ were major contributors to the reagent blank signal for assays which produce NADH. Studies were therefore made on the fluorescence from a range of NAD^+ and $NADP^+$ standards. Absorbance measurements at 366 and 468 nm were made on the same set of standards.

NADH Fluorescence Interference Study

Since it was intended to measure NADH fluorescence in a human serum matrix, interference studies were conducted using the individual major components of serum. The components of the enzymatic

assays were tested in a similar manner. The supplier and the method of preparing the stock solutions used in the interference study are given in Table V. The procedure for conducting NADH interference measurements is listed below:

1. Add 2 mL of 2.56 x 10^{-6} M NADH and 1 mL buffer to the cuvette, measure fluorescence, rinse.
2. Add 2 mL buffer and 1 mL of the interferent solution, measure fluoresence, rinse.
3. Add 2 mL of 2.56 x 10^{-6} M NADH and 1 mL of the interference solution to the cuvette, measure fluorescence, rinse.

Repeat steps 2 and 3 for at least 3 different concentrations of the interferent. Magnitude measurements using an 8 s integration time were made following an 8 s delay period. The buffer used for interferent solutions was 0.05 M Tris, pH 8.5.

If the results of the interference study showed that a substance caused a reduction of the net NADH fluorescence, then absorbance measurements were made on the interferent. These were done with the Cary 118 spectrophotometer where absorbance measurements were made on several concentrations of the interferent at both the fluorescence excitation and emission wavelengths (366 and 468 nm, respectively).

The solutions of globulin-type serum proteins contained considerable amounts of particulates. To remove the particulates, reconstituted protein fractions of $_1$, $_2$ and globulin were centrifuged for 5 min at maximum speed using a clinical centrifuge

Table V

Stock Solutions for the NADH Interference Study

Stock Solution and Concentration	Source and Catalog #	Method of Preparing the Stock Solution
Acetoacetate - 20 mg/dL	Sigma A-3642	Dissolve 20 mg in 100 mL of buffer
Albumin - 5 g/dL	Sigma A-2386	Dissolve 0.5 g in 10 mL of 0.85% NaCl
Ascorbic Acid - 4 mg/dL	Sigma A-7506	Dissolve 4 mg in 100 mL of buffer, protect from light
Bilirubin - 30 mg/dL	Sigma B-4126	Dissolve 30 mg in 2 to 3 mL of 0.1 M NaOH, Na_2CO_3, dilute to 100 mL with buffer
Cholesterol - 25, 50 and 100 mg/dL	Abbott Labs Inc. HDL Cholesterol stds.	Made up according to package instructions
Creatinine - 6 mg/dL	Sigma C-6257	Dissolve 6 mg in 100 mL of buffer
Fibrinogen - 150 mg/dL	Sigma F-1003	Dissolve 30 mg with 2 mL of 3% NaOH, dilute to 20 mL with buffer
β-d-Glucose - 200 mg/dL	Sigma G-5250	Dissolve 200 mg in 100 mL buffer
α_1-Globulin - 1 g/dL	U.S. Biochemical Corp., Fraction IV-1	Dissolve 0.2 g in 20 mL of 0.85% NaCl
α_2-Globulin - 1 g/dL	U.S. Biochemical Corp., fraction IV-4	Dissolve 0.2g in 20 mL of 0.85% NaCl

Table V (continued)

β-Globulin - 1 g/dL	U.S. Biochemical Corp., Fraction III	Dissolve 0.2 g in 20 mL of 0.85% NaCl
γ-Globulin - 1.4 g/dL	U.S. Biochemical Corp. Fraction II	Dissolve 0.14 g in 10 mL of 0.85% NaCl
Hemoglobin - 10 mg/dL	Sigma H-7379	Dissolve 10 mg in 100 mL of buffer
β- Hydroxybutyrate - 20 mg/dL	Sigma H-6501	Dissolve 20 mg in 100 mL of buffer
β-Lipoprotein - 240 mg/dL	U.S. Biochemical Corp., Fraction III-Ø	Lipoproteins are permanently denatured by lyophilization. Thus, are not easily dissolved. Method used: dissolve 48 mg in 2 mL EtOH, dilute to 20 mL with 94 mg/dL glycine in 0.85% NaCl
L-Phenylalanine - 2 mg/dL	Sigma P-2126	Dissolve 2 mg in 100 mL of buffer
Pyruvate - 18 mg/dL	Sigma P-2256	Dissolve 18 mg in 100 mL of buffer
L-Tyrosine - 4 mg/dL	Sigma T-3754	Dissolve 4 mg in 0.5 M HNO_3, dilute to 100 mL with buffer
L-Tryptophan - 300 mg/dL	Sigma T-0254	Dissolve 300 mg into 100 mL of buffer
Uric Acid - 8 mg/dL	Sigma U-2625	Dissolve 8 mg in 100 mL of buffer (heat gently to dissolve)
Urea - 31 mg/dL	Sigma U-1250	Dissolve 31 mg in 100 mL of buffer

(International Equipment Company). To measure if any protein was lost by centrifugation, a total protein test (A-Gent Total Protein kit, Abbott Laboratories, Inc.) was run on both centrifuged and non-centrifuged portions of each protein solution. The tests were ran according to package instructions using albumin solutions as standards.

Table VI shows the list of serum standards used for a variety of different studies conducted for this thesis. Each standard was reconstituted according to package directions. Interference measurements using the procedure described previously were made on a range of dilutions of certain serum standards. The spectral properties of several different dilutions of serum standards Versatol, Versatol-A and Q-PAK Serum II were studied by measuring the fluorescence using the optimum conditions for NADH measurement (see page 54). Absorbance measurements at 366 and 468 nm were made on the same range of dilutions using the Cary 118 spectrophotometer.

Enzymatic Assays

Kinetic Assay for EtOH

Stock solutions used for these studies are listed in Table VII. The procedure for addition of reagents and samples to the cuvette is shown below:

1. 1.0 mL of the buffer solution
2. 0.5 mL of the ADH solution

Table VI

Commercial Serum Standards and Controls

Name of Standard	Source	Preparation for Use
Versatol	General Diagnostics	Dissolve in 5 mL H_2O dilute with buffer to desired concentration
Versatol-A	General Diagnostics	Dissolve in 5 mL H_2O dilute with buffer to desired concentration
Versatol-A alternate	General Diagnostics	Dissolve in 5 mL H_2O dilute with buffer to desired concentration
Enzatrol Enzyme Control	American Hospital Supply Corp.	Dissolve in 3 mL H_2O dilute with buffer to the desired concentration
Q-PAK Control Serum I	Hyland Diagnostics	Dissolve in 5 mL H_2O dilute with buffer to desired concentration
Q-PAK Control Serum II	Hyland Diagnostics	Dissolve in 5 mL H_2O dilute with buffer to desired concentration
Qualify I	American Monitor Corp.	Dissolve in 10 mL H_2O dilute with buffer to desired concentration
Qualify II	American Monitor Corp.	Dissolve in 10 mL H_2O dilute with buffer to desired concentration

3. 1.0 mL of the EtOH sample or standard

4. 0.5 mL of the NAD^+ solution

Upon addition of the last reagent (NAD^+), the reaction is initiated and the ratemeter is triggered. After an 8 s delay the 16 s rate measurement begins. For blank measurements buffer is used in place of the ethanol solution, except for serum blanks where unspiked serum dilutions were used. For precision studies the autoinjector was used to deliver 0.5 mL of the NAD^+ solution. Optimization studies were conducted using the same procedure, but with varying concentrations of ADH and NAD^+ added to the cuvette.

Kinetic Assay for Glucose

Preliminary studies of this assay were conducted with a commercial reagent kit, A-Gent-Glucose U.V. Test Kit (Abbott Laboratories, Inc.). Each reagent vial was prepared by adding 6 mL of H_2O. The procedure for the addition of solutions to the cuvette is listed below:

1. 1.0 mL of H_2O

2. 1.0 mL of the glucose standard or sample

3. 1.0 mL of the reagent

All solutions were added with Eppendorf pipets and the ratemeter was triggered immediately after the addition of the last solution. Rate measurements were made over six consecutive 8 s periods after an 8 s delay period.

Table VII

Stock Solutions for EtOH Assay

Solution	Source and Catalog #	Method of Preparing Stock Solution
EtOH standard 0.17 M	U.S. Industrial Chemicals	1 mL of absolute ethanol diluted to 100 mL with H_2O. Further dilutions were made using buffer.
NAD+ 0.012 M	Sigma: N-7004	Dissolve 0.218 g in 25 mL of buffer, made up fresh each day.
ADH - 20 units/mL	Sigma: A-7011	Dissolve 1.4 g in 25.5 mL of phosphate-glycine buffer, stored at 2°C until used.
Phosphate buffer pH = 7.5	Mallinckrodt: Na_2HPO_4 - #7917 NaH_2PO_4 - #7892	Dissolve 0.75 g of both Na_2HPO_4 and NaH_2PO_4 in 1 L H_2O. Adjust pH to 7.5 with 0.5 M NaOH. Stored at 2°C until used.
Phosphate-glycine solution, 0.04 M glycine	Glycine: MCB GX-205	Dissolve 0.3 g glycine in 100 mL phosphate buffer. pH does not change measurably upon addition of glycine.
Tris buffer 0.10 M, pH = 8.5	Sigma: Trizma Base: T-3253 Trizma HCl: T-1503	Dissolve 4.42 g Trizma HCl and 8.72 g Trizma Base in 1 L H_2O. This combination results in a solution of pH 8.5.
Pyrophosphate buffer 0.12 M pH = 8.5	Mallinckrodt: #7960	Dissolve 53.6 g of $Na_4P_2O_7 \cdot 10\ H_2O$ in 1 L H_2O. Adjust to pH 8.5 with H_3PO_4.

Further studies of this assay required the use of solutions containing the individual components of the reagent mixture. The stock solutions made up for this purpose are listed in Table VIII. The use of separate portions of the reagent mixture allows the concentration of the major components to be optimized. The procedure for addition of reagents to the cuvette is listed below:

1. 0.5 mL of the hexokinase solution
2. 0.5 mL of the G-6-PDH solution
3. 0.5 mL of the NAD^+ solution
4. 1.0 mL of the glucose standard or sample
5. 0.5 mL of the ATP solution

The ATP solution is added to initiate the reaction via the autoinjector. For routine analysis the enzyme solutions are combined so that 1 mL of combined enzyme mixture is added to the cell. Rate measurements of an 8 s duration were made following an 8 s delay period. Serum standards were analyzed using the same procedure. The ATP solution was replaced by buffer solution for blank measurements.

Kinetic Assay for Lactate Dehydrogenase (LDH):

The stock solutions used for the study of fluorescence monitoring for LDH assays are listed in Table IX. The procedure for the addition of reagents and samples into the cuvette is shown below:

1. 1 mL of the NADH solution
2. 1 mL of the LDH standard or sample
3. 1 mL of pyruvate solution

Table VIII

Glucose System Stock Solutions

Solution	Source and Catalog #	Method of Making Stock Solution
β-d-glucose - 100 mg/dL	Sigma: G-5250	Dissolve 100 mg in 100 mL of saturated benzoic acid solution
ATP - 0.03 M	Sigma A-5394	Dissolve 0.54 g in 30 mL of buffer
NAD+ - .012 M	Sigma: N-7004	Dissolve 0.218 g in 25 mL buffer
Hexokinase - 40 units/mL	Sigma: H-1131	Dissolve 6 mg in 19.5 mL of buffer
Glucose-6-PO_4 - Dehydrogenase 80 units/mL	Sigma: G-5885	2.6 mL buffer added to one vial (209 units) of G-6-PDH
Tri ethanolamine (Tri.EA) buffer - 0.075 M	Sigma: T-1502	Dissolve 13.96 g in 1 L H_2O Adjust pH to 7.5 with HCl
Other chemicals needed for an optimum assay:		Add the respective quantities of the 4 chemicals to 1 L of Triethanolamine buffer:
Mg Aspartate 0.0012 M	Sigma: A-9506	0.515 g
Na_2CO_3 0.0165 M	Mallinckrodt:7521	2.62 g
$K_2C_2O_4$ 0.009 M	Mallinckrodt:7052	2.28 g
Na citrate 0.005 M	Mallinckrodt:0754	1.81 g

This combined solution is used as the buffer to dissolve and dilute the first 5 solutions on this list.

Table IX

LDH System Stock Solutions

Solution	Source and Catalog #	Method of Making Stock
Pyruvate 3 mM	Sigma: P-2256	Dissolve 33 mg in 100 mL of buffer
NADH 25.6 µM	Sigma: 304-102	Dissolve 2 mg (preweighed vial) in 100 mL of buffer
Lactate Dehydrogenase (LDH) 99 units/mL	Sigma: L-2500	Obtained as a liquid suspension. Dilute 200 µL of the suspension to 20 mL with buffer
Tris buffer 0.05 M pH 7.2	Sigma: Trizma HCl - T-3253 Trizma Base - T-1503	Add 0.67 g Trizma base with 7.02 g Trizma HCl. Dissolve and dilute to 1 L with H_2O
Q-PAK Serum II	Hyland Diagnostics	See Table VI for method of preparation. Dilutions were made with buffer

All solutions are added via Eppendorf pipets and upon addition of the pyruvate solution the reaction is initiated. A 16 s rate measurement is used following an 8 s delay. The standards used for the calibration curve were made by diluting a serum standard, Q-PAK Serum II, (Hyland Diagnostics, Inc.) to achieve a range of LDH activity levels. For blank measurements, buffer solution was used in place of the pyruvate solution.

Kinetic Assay for Creatine Kinase (CK)

Initial studies of the use of fluorometric monitoring for measurement of CK activity were done with the commercial assay kit, A-Gent U.V. CPK Kit (Abbott Laboratories). The premixed reagent vials were prepared according to package directions but were diluted a factor of 2 in the fluorescence cell as compared to the suggested procedure used for absorbance monitoring. The procedure for adding solutions to the cuvette is shown below:

1. 1 mL of the kit reagent
2. 1 mL of H_2O
3. 1 mL of a CK sample or standard

The CK standards used for these preliminary studies were dilutions of lyophilized enzyme obtained from rabbit muscle (Sigma - #C-3755, see Table X). Dilutions of the CK stock solution were made up using a 1 to 40 dilution of a serum standard, Versatol (General Diagnostics). Rate measurements of an 8 s duration following a 40 s delay gave optimum results for these initial studies.

Table X

Stock Solutions for the CK Assay

Solution	Supplier and Catalog #	Method of Making the Stock Solution
ADP 0.013 M	Sigma: A-2754	Dissolve 0.06 g in 10 mL of buffer
AMP 0.15 M	Sigma: A-1752	Dissolve 0.556 g in 10 mL of buffer
Phosphocreatine - 0.09 M	Sigma: P-6502	Dissolve 0.230 g in 10 mL of buffer

For Routine Assays

Combined Substrates Solution:

Compound	Grams added to Mixture	Resulting Concentration (mM in Solution)
NAD+	0.0866	3.00
β-d-glucose	0.2162	30.0
ADP	0.025	1.0
PO_4-creatine	0.230	22.5
AMP	0.0887	6.0
NaF	0.0302	18.0
Mg Acetate	0.1704	30.0

Combine the above compounds, dissolve and dilute to 40 mL with buffer. This solution should be made fresh daily.

Table X (continued)

Coupling Enzymes: Hexokinase - 7 U/mL	Sigma: H-1131	Dissolve 1.8 mg hexokinase, plus one vial (210 units) of G-6-PDH in 32 mL of buffer
G-6-PDH - 6 U/mL	G-5885	
CK standard Stock = 10 U/mL	Sigma: C-3755	Dissolve 1.0 mg in 10.4 mL of the albumin-monothioglycerol solution. Dilutions of the stock are also made with albumin-monothioglycerol solution
Albumin-monothio-glycerol solution	Sigma: Albumin-A-4503 Mono - M-1753	Dissolve 700 mg of monothioglycerol and 60 mg of albumin in 200 mL of buffer
BIS-TRIS buffer 0.20 M pH = 6.6	Sigma: B-9754	Dissolve 42.2 g of (Bis 2-hydroxy-ethyl) amino-tris (hydroxymethyl) methane (BIS-TRIS) in 1 L H_2O. Adjust pH to 6.6 with 5M HCL
MES buffer 0.083 M pH = 7.05	Sigma: M-8250	Dissolve 16.2 g of 2 [N-morpholino] ethane sulfonic acid (MES) in 1 L H_2O. pH is adjusted to 7.05 with 20% NaOH solution

The major components of the reagent which had not been studied previously in the glucose assay were made up in separate solutions (see Table X), and the fluorescence signals from each were measured. The blank reaction which was creating an elevated blank fluorescence signal was investigated by using separate solutions of ADP, AMP and the coupling enzymes.

Any parameter of the CK assay which does not affect the fluorometric measurement of NADH was selected according to the optimum conditions stated in reference 103. These included the selection of the optimum pH and type of buffer (pH = 6.6, BIS-TRIS buffer) and optimum enzyme activator, monothioglycerol, which was used in combination with albumin for use as a diluent for samples and standards. The stock solutions used for routine studies of the CK system are shown in Table X. The order of addition of reagents to the cuvette for a typical CK assay is as follows:

1. 1 mL of the combined substrates solution
2. 1 mL of the coupling enzymes solution
3. 1 mL of the CK standard or sample

For the optimization of the ADP concentration, the above procedure was modified such that 0.5 mL of the combined substrates solution (minus ADP) and 0.5 mL of the ADP solution were first added to the cell. All solutions were added to the cell with Eppendorf pipets.

A 16 s rate measurement was made following a 20 s delay period. The water bath temperature was increased to 30 °C for all studies of the CK system.

Studies of Resorufin Fluorescence and Formation

Initial Studies

The instrumental settings used for the fluorometric measurement of resorufin were 10 MΩ for R_F and 0.1 μF for C_F for both the PT and PMT current-to-voltage converters. The wavelengths and slit widths were 550 nm and 2 mm, respectively, for the excitation monochromator and 580 nm and 2.5 mm, respectively, for the emission monochromator. For studies of the decrease of NADH by NADH oxidase activity the instrumental settings were identical to those used for all previous NADH fluorometric measurements. Water bath temperature was kept at 25 °C. Measurement times of 8 s were used for both equilibrium and reaction rate measurements for the initial studies of the resorufin system. Absorbance measurements of the various solutions used in the resorufin system were made with the Cary 118 spectrophotometer at 550 and 580 nm.

The stock solutions used for these studies are listed in Table XI. Since reagent grade resorufin was not available commercially, studies were conducted on the reaction products from the mixture of resazurin, NADH and diaphorase. For all spectral studies, the reaction mixture contained a great excess of NADH to insure the

Table XI

Stock Solutions for Studies of Resorufin

Solution	Source and Catalog #	Method of Preparing Stock Solution
Resazurin 1.5 mM	Eastman Kodak Co. C-2106	Dissolve 3.8 mg in 10 mL buffer
Diaphorase 1.58 unit/ mL	Sigma D-2381	Dissolve 2.9 mg in 10 mL of the enzyme diluent
Enzyme diluent	Albumin - Sigma - A-4503 Flavin mononucleotide: Sigma - F-6750	Dissolve 5 mg albumin, 0.438 g KCl and 5 mg flavin mononucleotide in 20 mL of buffer
Tris buffer 0.05 M pH = 7.5	Sigma Trizma HCl-T-3253 Trizma Base T-1503	Dissolve 6.35 g of Trizma HCl and 1.18 g Trizma base in 1 L H_2O. This combination results in a solution of pH 7.5
Phenazine methosulfate (PMS) 65 μM	Sigma: P-9625	Dissolve 6 mg in 100 mL H_2O (made up like in Anal. Biochem. Vol. 1, p. 317)
NADH 0.64 mM	Sigma: 340-102	Dissolve 10 mg in 20 mL of buffer

reaction would yield a high percentage of resorufin. The procedure for the addition of reagents to the cell is as follows:

1. 1 mL of the resazurin solution
2. 1 mL of diaphorase solution
3. 1 mL of the NADH solution

All solutions were added to the cuvette with Eppendorf pipets. NADH is added last to maximize the yield of resorufin due to the reaction between NADH and oxygen in the presence of diaphorase.

Resorufin System Coupled to the CK Assay

All instrumental settings are identical to those used for the initial studies of resorufin except that the water bath temperature was raised to 30 °C.

The stock solutions used for this assay are nearly identical to the reagents used for the NADH-monitored CK assay and the initial resorufin experiments. Both the combined substrates solution and the coupling enzymes solution were made up to twice the concentration used in the NADH-monitored assay so that the final in-cell concentration would be equal for both studies. The concentration of ADP in the combined substrates solution was reduced to 3×10^{-4} M to lower the blank fluorescence signal. The concentration of the diaphorase solution was increased to match the in-cell activity used in the initial resorufin studies (0.1 unit/mL). MES buffer was used rather than BIS-TRIS since the latter appeared to react with resazurin. The preparation of MES buffer is included in Table X.

The procedure used for the addition of reagents and samples to the cell is listed below:

1. 0.5 mL of combined substrates solution
2. 0.5 mL of the coupling enzymes solution
3. 1 mL of the resazurin solution
4. 100 µL of the diaphorase solution
5. 1 mL of the CK sample or standard

The use of 4 separate solutions of different parts of the total reagent allows individual measurement of the effects of each solution on the blank reaction. All solutions were added with Eppendorf pipets. A 16 s rate measurement was made following a 20 s delay for mixing and for the maximum reaction rate to be achieved.

Flow Injection Analysis Studies

Instrument Settings

The settings listed below were used for the fluorometric measurement of NADH when using the flow cell. The major difference between these settings and those used for the cuvette is that the emission monochromator was replaced with an interference filter.

Excitation wavelength:	366 nm, 2.0 mm slit width
Emission wavelength:	480 nm interference filter bandpass = 10 nm
Feedback resistors and and capacitors for the PT and PMT current-to-voltage converters:	$R_F = 10^M\Omega$ $C_F = 0.1$ µF

PMT voltage:	800 V
Water bath temperature:	25 °C

Optimization of Fundamental FIA Operations

The general method used for optimizing the flow rate and delay periods utilizes injections of a fluorophore, normally 1.28×10^{-5} M NADH, and observation of the peak profile obtained on a chart recorder. Delay periods and flow rates were conveniently varied by entering new values into the software. The specific procedure for optimizing each individual parameter is described in greater detail below.

Initial Delay Periods. Initial delay periods are required to allow for adequate rinse-out of the flow cell between runs, complete filling of the injection loops and proper overlap of the sample and reagent plugs upon merging. The first delay period allows extra time between runs for more complete rinsing of the flow cell and it allows sufficient start-up time for the pumps after a stopped-flow measurement. The required rinse time between runs can be measured from the peak profiles obtained from injections of a fluorophore.

Optimization of the sampling period requires adjustment of both the flow rate of the withdrawal stream and the delay time for sampling. Withdrawal stream flow rates are adjusted with a needle valve between the injection valve and the vacuum collecting flask. After a reasonable withdrawal rate is set, the delay period is

optimized by maximizing the peak area from injections of a fluorophore. For the day to day set-up of the system the sampling time or withdrawal rate are adjusted by observing the volume of solution withdrawn from a sample vial. As a rule of thumb, the volume withdrawn should be 2 to 3 times greater than the injection loop volume.

Optimization of the overlap of the reagent and sample plugs was done by observing the combined peak profile from injections of a fluorophore by both injection valves. By varying the delay between the injection of the reagent and sample loops, the degree of peak overlap can be adjusted. For small volume injection loops ($\leq$ 200 µL) the maximum combined peak height indicates the maximum overlap. For large volume loops ($>$ 200 µL) the measurement of the combined peak half-width is a more effective gauge of the degree of overlap. The minimum half-width corresponds to the maximum overlap to the two plugs. For studies of optimum overlap, a flow rate of 2.0 mL/min. per pump was used.

For studies conducted to optimize the other parameters and for a majority of the routine assays, the following initial delay periods were used:

Start-up delay period	=	20 s
Delay for sampling	=	15 s (for 550 µL loop)
Withdrawal flow rate	=	8 to 10 mL/min.
Delay between injections	=	0.25 s

Flow Rate Optimization. Adjustments of the flow rate of each pump are made to obtain the desired mixing ratio of the sample to reagent. The ratio of peak heights from injections of a fluorophore in large volume loops is a measure of the mixing ratio. For a 1 to 2 ratio of sample to reagent the peak heights from separate injections of NADH using equal-volume loops are equalized by adjusting the flow rate of one pump.

A study was conducted to show the effect of flow rate on the peak profile of injections of NADH in order to predict throughput and minimum wash-out periods. For continuous-flow kinetic assays the optimum flow rate will depend on the delay period of the reaction being monitored. The effect of flow rate on the run to run precision was studied by using repetitive injections of NADH over a range of flow rates.

Modes of Measurement. The FIA system was designed so that both continuous-flow and stopped-flow methods could be used for either kinetic or equilibrium measurements. The general procedures for conducting stopped-flow and continuous-flow (dual peak) kinetic measurements are listed below:

Dual Peak Method:

1. Measurement of the blank:
   a. Merge a sample plug with a plug of reagent (this reagent is lacking a non-fluorescent cofactor or enzyme).

b. The merged plug is sent to the flow cell and the peak is integrated. This value corresonds to a blank signal.

2. Measurement of the reaction:

a. Merge a second plug of sample with a plug of reagent (this reagent is complete).

b. The merged plug is carried through the flow cell and the peak is integrated.

The rate value is calculated by taking the difference between the two integration values. The reaction time is equal to the time between the mixing of the two plugs and arrival at the flow cell.

Stopped-Flow Method:

a. Sample and reagent plugs are injected and merged.

b. The merged plug is carried to the flow cell.

c. Flow is stopped either by halting the pumps or by-passing flow around the flow cell.

d. After a short delay for flow to completely stabilize, the reaction rate is measured.

Since stopped-flow and continuous-flow measurement methods are effected differently by changes in certain parameters, further optimization studies were conducted specifically with one method or the other. The optimization studies using a stopped-flow method will first be described. The general operating parameters for stopped-flow studies are listed below:

Flow rate	=	2.0 mL/min per pump
Initial delay period	=	20 s
Delay for sampling	=	15 s (500-600 µL loops)
Delay between injection of loops	=	0.25 s

The delay period for on-line rinsing of the sample and reagent loops was adjusted so the loops were switched off-line 1 s prior to stopping flow. Optimization of the position of the plug within the flow cell during stopped-flow measurements was made by varying the delay time between injection and stopping flow. Precision studies were made by making repetitive injections of NADH and measuring the steady state signal after stopping at a particular point on the plug. Twelve runs were made for each different position on the plug so that the optimum position could be selected.

The effect of changing injection loop volumes on stopped-flow measurements was investigated with injections of NADH using a variety of different loop volumes. The delay period was adjusted for each loop volume so that flow would be stopped at the top of the peak where the concentration is maximum. The effect of loop volume on run to run precision was studied in a similar manner where the stopped-flow steady-state measurement of NADH was repeated 12 times per loop volume.

A bypass loop was set up to allow better precision in stopping flow reproducibly at the same position on the injected plug. The precision of making repetitive stopped-flow measurements with the

bypass loop was studied with injections of NADH. An identical series of measurements were made using pump shut-off to stop flow, thus a direct comparison of the two methods could be made.

For all stopped-flow optimization studies the steady state signal levels from NADH were measured with an 8 s measurement time following an 8 s delay after switching off the flow.

For the optimization of the dual peak kinetic method (continuous-flow) similar optimization studies were conducted. The general operating parameters for the studies of the dual peak method are the same as those used for the stopped-flow study except for the delay periods used after the injection of the sample. The delay prior to switching both injection loops back off line was longer than the delay period used for stopped-flow. The delay for the period between injection and stopping flow is irrelevant since no change in flow rate was used in these studies.

The optimization studies for the dual peak method included observing the effect of changing the injection loop volume on the integration of peaks produced by plugs of NADH. A study was made of the optimum integration period for the dual peak method by measuring 550 µL injections of NADH using a range of integration periods centered around the top of the peak.

Optimization and Performance of the Flow Cell

Spectral studies of the flow cell were conducted with stopped-flow measurements of solutions injected via a 550 µL sample loop.

The operating parameters of the FIA system are listed below:

Flow Rate (per pump)	=	2.0 mL/min
Initial Delay Period	=	20 s
Delay for Sampling	=	15 s
Delay Between Injection of Loops	=	0.25 s
Delay for On-line Rinsing	=	15 s
Delay Between Injection and Stopping of flow	=	16 s

Eight second steady-state measurements were made following an 8 s delay after pumps were stopped. For rate measurements a 16 s measurement was made following a 16 s delay. Studies of the attenuation of NADH fluorescence by serum standards were conducted by injecting various dilutions of Q-PAK Serum II via the sample loop (550 μL) and 12.8 μM NADH via the reagent loop (600 μL). Stopped-flow measurements were made on the drifts seen with NADH, NAD^+ and a 1 to 10 dilution of Q-PAK Serum II.

Kinetic Assay for EtOH Using the FIA System

The kinetic measurement of EtOH developed using the cuvette were adapted to the FIA-fluorometer. The following list shows the conditions used for this assay for both stopped-flow and dual peak methods used in this study.

1. FIA parameters:

   The flow rate and all delay times are identical to those used in the flow cell study

2. Measurement times:

Stopped-flow method	=	16 s rate measurement following a 16 s delay period
Dual Peak Method	=	8 s integration per peak beginning 10 s after injection

Solutions. See description of stock solutions in Table VII. NAD^+ and ADH are combined into one solution and injected via the 600 µL reagent loop. EtOH samples and standards are injected via the 550 µL sample loop. For the optimization of ADH and NAD^+ concentrations an EtOH standard was injected via the reagent loop.

CK Assay Using the FIA System

The CK assay monitored by NADH fluorescence was adapted for use in the FIA ratemeter. A stopped-flow measurement method was the only practical method for use with this assay since a 32 s lag time requires a 32 s delay time. The FIA parameters are identical to those used for stopped-flow measurements of the EtOH assay (see p. 80). The optimum measurement period was a 16 s rate measurement following a 32 s delay to allow the maximum reaction rate to be reached. The stock solutions used in this study were previously listed in Table X. The major change in the reagent solution was that the ADP concentration was increased to 2.4 mM in the final reagent mixture. A complete reagent mixture (combined substrates plus coupling enzymes) was injected via the 600 µL reagent loop and CK samples and standards were injected by the 550 µL sample loop.

Three Injection Loop System

Initial Studies

The instrumental settings for the fluorometer are identical to those used for other FIA studies involving NADH (see p. 73). Initial studies of the 3 loop system involved optimization of the FIA operating parameters by using injections of NADH (12.8 μM). Flow rates were adjusted to produce a 1 to 1 to 1 mixing ratio for the 3 loops by observing the peak heights of each injection loop and adjusting the flow rate of the third pump until all peak heights were equal. Peak overlap was maximized by the procedure described earlier. Pump stoppage was used to conduct stopped-flow measurements and the delay period was adjusted to stop flow on top of the peak (center of merged plug in flow cell). The results of these optimizations are shown below.

Flow Rate (per pump)	=	1.4 mL/min.
Initial Delay Period	=	20 s
Delay for Sampling	=	15 s
Delay between Injection of the Reagent and Sample Loops	=	0.25 s
Delay for On-line Rinsing	=	18 s
Delay between Injection and Stopping of Flow	=	19 s

Assay for EtOH Using the 3 Loop System

Stock solutions were made up according to Table VII. A 16 s rate measurement was made following a 16 s delay. The NAD^+ solution (2 mM in-cell) was injected via the third injection loop (1000 µL), while the ADH solution (1.7 U/mL in-cell) was injected via the reagent loop (600 µL). Ethanol samples and standards were injected with the sample injection loop (550 µL).

RESULTS AND DISCUSSION

NADH Fluorescence Studies

Initial Studies

Initial studies of the fluorescent characteristics of solutions of NADH were carried out to evaluate its utility for fluorescence monitoring in enzymatic assays. Excitation and emission spectra for NADH were taken and agreed with published spectra (40). From observation of the emission spectrum, the optimum emission wavelength was selected to be 468 nm. A wavelength of 366 nm was chosen as the optimum excitation wavelength since it produced the greatest fluorescence signal. Even though the molar absorptivity of NADH is over 60% less at 366 nm than at its absorbance maximum of 340 nm, the greater intensity at 366 nm from the Xe-Hg lamp makes the later (366 nm) the optimum excitation wavelength.

Fluorometric steady-state measurements were made on NADH solutions made up in 5 different buffers which are commonly used for enzymatic assays. A separate NADH calibration curve was produced for each buffer with the results of this study listed in Table XII. It appears that the net NADH fluorescent signals are independent of the type of buffer used (except for MES). The higher temperature (30 °C) used for the measurement of NADH in MES caused an approximate 9% decrease in the net NADH fluorescence as compared to results using

Table XII

NADH-Buffer Study[a]

Parameter Measured	Pyrophosphate	TRIS	Tri. E.A.	MES (at 30°C)	BIS-TRIS
Slope of Calibration Curve (counts per mM)	6.3×10^4	6.3×10^4	6.3×10^4	5.7×10^4	6.7×10^4
Average Blank Signal (counts)	5.4×10^3	4.5×10^3	6.6×10^3	1.9×10^4	6.8×10^3
SD of Blank Measurement (counts)	31	47	36	425	98
Theoretical Detection Limit (μM)	9.8×10^{-4}	1.5×10^{-3}	1.1×10^{-3}	1.5×10^{-2}	2.9×10^{-3}
SD of Blank Measurements, Run-to-Run (counts)	70	150	100	450	---
Practical Detection Limit (μM)	2.2×10^{-3}	4.8×10^{-3}	3.4×10^{-3}	1.6×10^{-2}	---

[a]Conditions used for this study: λ_{ex} = 366 nm; λ_{em} = 468 nm; temp. = 25° (except MES); O.A. #1 and #2: R_f = 10MΩ, C_f = 0.1μF; excitation slit = 2.0 mm; emission slit = 1.4 mm; 8 s measurement time

other buffers at 25 °C. Since the temperature coefficient for NADH is -1.6% per °C (13), the decrease in NADH fluorescence for MES is probably a temperature effect rather than a function of the type of buffer used.

The blank signals and standard deviations (SD) vary with the different buffers, therefore there is a difference in the theoretical detection limits of NADH in the five buffers. The detection limits for NADH in each buffer tested is shown in Table XII. The two detection limits shown in the table are defined below:

$$\text{Theoretical Detection Limit} = \frac{2 \times \text{SD of the blank signal}}{\text{Slope of the calibration curve}}$$

$$\text{Practical Detection Limit} = \frac{2 \times \text{blank-to-blank SD}}{\text{Slope of the calibration curve}}$$

The blank to blank SD is obtained from repetitive measurements on multiple blanks where the blank solution is removed, the cell rinsed and fresh buffer returned to the cell between measurements. Pyrophosphate, Tris and Triethanolamine buffers show significantly higher blank to blank SD's as compared to the SD of measurements made on a single blank. It was observed that these buffer solutions were sensitive to bubble formation when removed from the refrigerator and not allowed to equilibrate at room temperature for several hours. Perhaps degassing the buffers prior to use or greater care in sample handling would improve the blank to blank SD and reduce the practical detection limits. Kinetic measurements are not effected by changes in the blank signal levels from run to run and therefore kinetic

measurements of NADH should not be as sensitive as steady state measurements to deviations in the blank signal level.

As a comparison the detection limit for NADH using absorbance monitoring at 340 nm was calculated. The molar absorptivity of NADH at 340 nm is 6.2×10^3 $(cm\ M)^{-1}$. Assuming the detection limit is the concentration yielding an absorbance of 0.0002, the detection limit by absorbance would be approximately 3.2×10^{-2} μmol/L or about 30 times worse than the fluorescence detection limit using the pyrophosphate buffer.

For all five buffers tested, the range of linearity extends to about 25 μM of NADH at which point the fluorescence signal is ~5% below the value predicted by extrapolation of the linear portion of the curve. This yields a linear dynamic range of over 4 orders of magnitude for NADH in buffer measured at 25 °C. As the temperature is increased the dynamic range will be reduced but is still over 3 orders of magnitude at 30 °C using the MES buffer.

The fluorescence signals from solutions of NADPH were measured using the identical conditions as for NADH. The net fluorescence signals from equal concentrations of NADH and NADPH differ by less than 3%. This is consistent with reports in the literature which indicate their fluorescent properties are identical (13).

The effect of changes in pH and temperature on NADH fluorescence was also studied. The net fluorescence was measured for a series of solutions ranging from pH 6.2 to 9.4, each containing an identical

concentration of NADH. The relative standard deviation (RSD) of the net signals of the series of solutions was 1.9% while the RSD of repetitive measurements of NADH solutions at a constant pH was 1.8%. It appears that pH changes between 6.2 and 9.4 will have no measureable effect on NADH fluorescence. The literature confirms this observation stating that NADH is stable between pH 6.5 and 9.0 but becomes increasingly unstable at higher and lower pH's (13).

The effect of changes in temperature on NADH fluorescence was studied. The results showed that the net fluorescence signal would drop by nearly 2% for a 1 °C increase in temperature. The reported relative temperature coefficient for NADH is 1.6% per °C (13). The different between these values may be due to uncertainties in measuring the actual in-cell temperature during measurement.

The optimum measurement periods for monitoring steady-state NADH fluorescence were 8 and 16 s. Shorter measurement periods where the integration time was less than 8 s showed higher relative noise levels. Measurement periods greater than 16 s provided no improvement in the relative noise levels since drifts due to heating effects and lamp fluctuations became significant. For an 8 s steady-state measurement of an NADH concentration near 10 μM the RSD is typically 0.1 to 0.4% for a single run and 1 to 2% for repetitive runs.

NAD^+ and $NADP^+$ Fluorescence Studies

Any assay involving the enzymatic production of NADH must include NAD^+. It was determined that the net fluorescence from a

solution of NAD^+ is 0.09% of the net signal from an equal concentration of NADH when using identical measurement conditions. Even though the fluorescence signal is low relative to NADH, the concentrations of NAD^+ used in typical enzymatic assays (0.2 to 2 mM) makes it the major contributor to the reagent fluorescence signal. The net signal levels of equal concentrations of NAD^+ and $NADP^+$ show a 40% lower signal for $NADP^+$, perhaps due to the higher purity of the $NADP^+$. This difference is not significant enough to make $NADP^+$ the preferred choice for fluorometric measurements, especially since it is nearly 8 times more expensive than NAD^+.

Since increases in the blank signal level causes greater blank noise levels and higher detection limits, the concentrations of NAD^+ and $NADP^+$ must be minimized. The effect of changing the NAD^+ and $NADP^+$ concentration on the noise level of the blank was studied by measuring the SD of the blank signal from a range of concentrations. The results are listed in Table XIII. At concentrations above 1 mM, the noise increases by a factor greater than the square root of the signal level, indicating both signal shot and source flicker noise are significant. These noise values can be used for optimization studies for enzymatic assays which utilize NAD^+ or $NADP^+$. The NAD^+ concentration giving the maximum value for the ratio of the reaction rate vs. blank noise level will be optimum for the kinetic assay.

Absorbance measurements of NAD^+ and $NADP^+$ at 366 nm show molar absorptivities of approximately 10 L/(mol-cm) for both cofactors. At concentrations above 5 mM the absorbance at 366 nm becomes high

Table XIII

Blank Noise Levels vs. NAD^+ and $NADP^+$ Concentrations

NAD^+ Concentration in cell (mM)	Within Run SD[a] (counts)
Buffer only in cell	40
0.01	54
0.10	62
0.50	182
1.0	308
10.0	1214

$NADP^+$ Concentration in cell (mM)	Within Run SD[a] (counts)
Buffer only in cell	40
0.06	67
0.60	124
1.0	233
6.0	1053

[a]SD from 9 repetitive 8s integrations

enough to cause attenuation of NADH fluorescence by lowering the intensity of the excitation beam (pre-filter effect). It is therefore important to keep the concentration of either of these co-factors below 5 mM in order to obtain the maximum NADH fluorescence signals.

NADH Interference Study

The objective of this study was to determine the effects of human serum on the fluorometric measurement of NADH. Figure 8 shows a fluorescence emission spectra of two diluted serum standards and NADH. Serum contributes a major amount of blank fluorescence signal and hence blank noise which significantly increases the detection limit of NADH compared to measurements made in buffer. Figure 9 shows the absorption spectra of two different serum standards and of bilirubin. The absorbance of serum at 366 and 468 nm causes significant pre-and post-filter effects which attenuate NADH fluorescence signals.

Solutions were prepared of the individual constituents of serum so that the effect of each component on NADH fluorescence could be tested. Only the major components were tested (normal serum concentrations greater than 0.5 mg/dL). Also only endogenous species were considered. Reference 15 contains a table of the major components found in serum and the normal concentration range of each. This was used as the guide for this portion of the interference study. The concentrations of the species tested were increased until

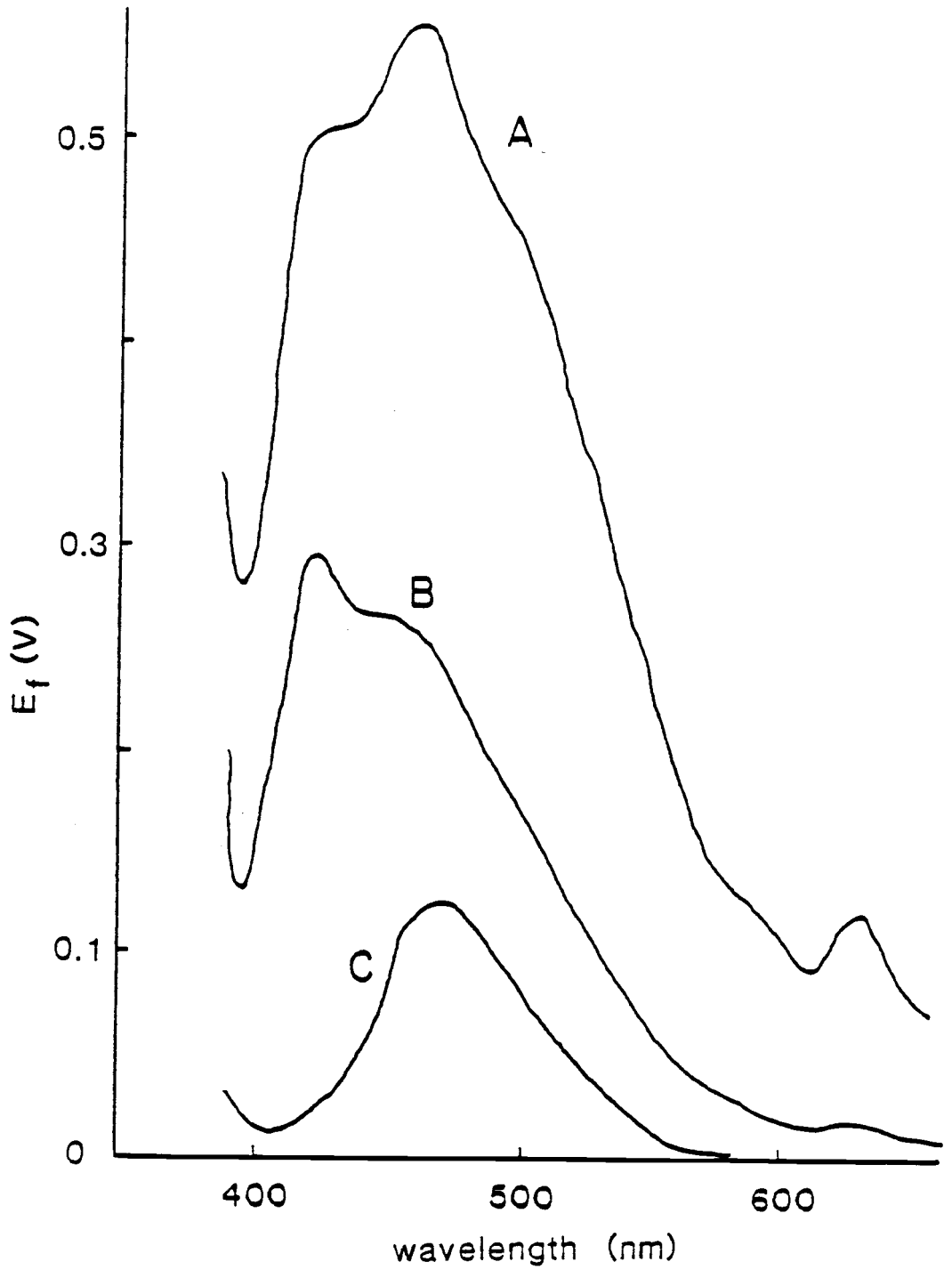

Figure 8. Fluorescence emission spectra of serum standards and NADH. Excitation wavelength set at 366 nm. A) Q-PAK Serum II, B) Enzatrol, C) 1 μM NADH. Both serum standards were diluted 1 to 90 for the in-cell concentration

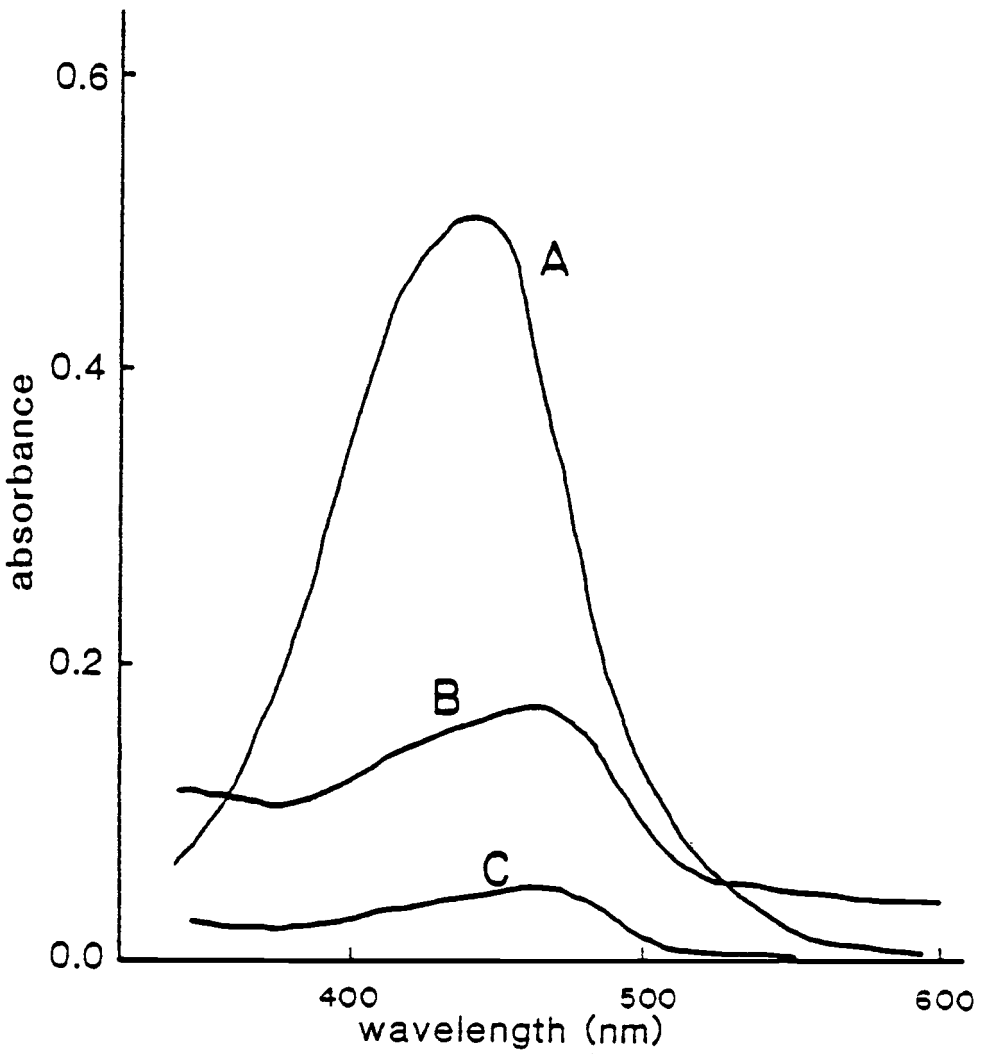

Figure 9. Absorption spectra of serum standards and bilirubin. A) bilirubin, 1 mg/dL (in-cell), B) Q-PAK Serum II, C) Enzatrol. Both serum standards were diluted 1 to 30 in-cell.

significant interference was observed or until the tested concentration was above a reasonable normal level. The individual components and reagents of the enzymatic assays used in this research were also tested for NADH interference using the same technique.

The results of the interference study are summarized in Table XIV. In this study, interference was defined as either a positive or negative deviation of greater than 2% of the signal obtained from pure NADH in buffer. This value was chosen because the run-to-run RSD of measurements of NADH in buffer was approximately 2%. The serum protein solutions (albumin, globulins) and bilirubin were found to cause significant spectral interference and were further tested to determine their mode of interference. The native fluorescence of each type of serum protein was measured using the optimum conditions for NADH. The absorptivity of each protein solution and bilirubin was calculated from measurements made at both 366 and 468 nm. The results of these measurements are recorded in Table XV. The absorptivity of all species was calculated using concentrations terms of mg per dL since these are the units most commonly used in clinical chemistry. Serum proteins cause interference both by increasing the level of background fluorescence and by attenuating NADH fluorescence. Bilirubin shows no native fluorescence under these measurement conditions but its absorbance at 366 and 468 nm causes serious pre- and post-filter effects with its post filter effect being the more significant. The broad peak between 400 and 500 nm in the absorption spectra of serum standards (see Figure 9) is due to the presence of bilirubin in serum.

Table XIV

Results of Interference Studies

Serum Component	Normal[a] Levels in serum (mg/dL)	Highest Concentration Tested (mg/dL in cell)	Total[b] Measured Signal Relative to 1 μM NADH (%)	Percent[c] Recovery of net NADH Fluorescence (%)
Acetoacetate	0.2-0.5	6.0	99	100
Albumin	3500-5000	100	314	99
Ascorbic Acid	0.6-2.0	1.3	101	100
Bilirubin	0.2-1.0	1.0	54	54
Cholesterol	130-250	33	101	99
Fibrinogen	∿ 0 in serum	50	124	94
β-D-Glucose	50-200	67	99	100
α_1-Globulin	200-400	50	403	88
α_2-Globulin	400-900	50	416	90
β -Globulin	600-1100	50	344	98
γ-Globulin	500-1700	100	180	85
Hemoglobin	∿ 0 in serum	3.3	82	82
β-Hydroxybutyrate	0.1-0.5	6.6	99	100
L-Lactic Acid	3.0-7.0	3.0	100	100
β-Lipoprotein	300-500	16	175	94
L-Phenylalanine	0.8-1.8	0.7	99	99
L-tyrosine	0.8-1.3	1.3	100	100
Uric Acid	3.5-7.2	2.7	100	100
Urea	10-40	10.5	100	100

Table XIV (continued)

Serum Component	Normal[a] Levels in Serum (mg/dL)	Highest Concentration Tested	Total[b] Measured Signal Relative to 1 μM NADH (%)	Percent[c] Recovery of net NADH Fluorescence (%)
Reagents Used in Enzymatic Assays				
ADH	-	266 U/mL	217	100
ATP	-	3 mM	98	100
HK and G-6-PDH	-	2 U/mL	100	100
NAD^+	-	60 mM	383	50
AMP	-	50 mM	99	99
PO_4- creatine	-	30 mM	101	100
ADP	-	4.4 mM	101	100
Pyruvate	-	10 mM	99	100

[a]According to values listed in Reference 15.

[b]$\frac{(\text{Signal of NADH plus Serum Component})}{(\text{Signal of NADH})} \times 100$

[c]$\frac{(\text{Signal of NADH + Serum Component - Signal of Serum Component})}{(\text{Net Signal of NADH})} \times 100$

Table XV

Spectral Properties of Interferents

Interferent[a]	Slope ($\frac{counts}{mg/dL}$)	Unit Absorptivities (dL/(mg-cm)) 468 nm	365 nm
Albumin	1.4×10^{3}	1.2×10^{-5}	7.3×10^{-5}
γ-globulin	4.6×10^{2}	4.2×10^{-4}	6.0×10^{-4}
β-globulin	6.1×10^{3}	1.6×10^{-3}	2.2×10^{-3}
β -globulin (centrifuged)	5.5×10^{2}	4.8×10^{-5}	1.1×10^{-4}
α_1-globulin	7.2×10^{3}	7.9×10^{-4}	1.4×10^{-3}
α_1-globulin (centrifuged)	6.7×10^{3}	2.8×10^{-4}	7.3×10^{-4}
α_2-globulin	7.2×10^{3}	7.8×10^{-4}	1.3×10^{-3}
α_2-globulin (centrifuged)	6.7×10^{3}	2.7×10^{-4}	7.2×10^{-4}
β-Lipoprotein[b]	3.4×10^{3}	5.0×10^{-4} (1.7×10^{-3})	5.5×10^{-4} (2.4×10^{-3})
Bilirubin	~ 0	0.76	0.17

[a] Solutions made up in 0.2 M buffer pH = 7.5

[b] The absorbance values are taken from ref. 121 since there was incomplete dissolution of the lipoprotein stock solution. The fluorescence value and the absorbance values in parenthesis are the actual measured values.

Several problems were encountered in the interference study of individual serum components. Commercial serum protein fractions were used to study the spectral properties of the different types of serum proteins. The purity of the commercial fractions is quite poor, especially for the different classes of globulins. For example, the purity of the α_1-globulin fraction was only 51%, according to the predictions in reference 104, with the bulk of the remaining protein being α_2-globulin. The α_2-globulin fraction also had a similar purity with α_1-globulin being most of the remaining protein. Spectral studies showed nearly identical spectral properties for the two fractions so it was assumed the two classes of proteins have very similar properties. The purity of other fractions was high enough (except for lipoprotein contamination) that the measured spectral properties could be considered equivalent to those of the pure protein type.

Lyophilized serum protein fractions and serum standards which contain lipoproteins show significant turbidity upon reconstitution. Lipoproteins are permanently denatured by lyophilization and therefore result in the formation of particulates when reconstituted (105-107). The presence of lipoprotein in the commercial protein fractions caused major increases in the fluorescence level and absorbance readings of these reconstituted solutions. To get more accurate measurements of the spectral properties of these fractions the reconstituted solutions were centrifuged to remove the particulates. Total protein tests were run on the solutions before and after

centrifugation to check if any protein was lost. The worst case was the β-globulin fraction which showed a loss of nearly 20% of the total protein after centrifugation, of which only 10% could be accounted for by the lipoprotein itself. The net loss of 10% was taken into account by adjusting the stated protein concentration. Table XV shows the change in spectral properties of the centrifuged samples which show lower absorbance and fluorescence values. The spectral properties of the centrifuged samples show lower absorbance and fluorescence values. The spectral properties of the centrifuged samples are assumed to be a much closer match to fresh solutions of each protein.

The turbidity of reconstituted serum standards is also caused by the denaturation of lipoproteins upon lyophilization (106). Particulates in reconstituted standards cause increased absorption over the entire spectrum. Figure 9 shows the difference in absorption between a serum standard which contains lipoproteins (Q-PAK Serum II) and another which does not (Enzatrol). Obviously the presence of the particulates increases the observed absorbance, especially at wavelengths greater than 500 nm where no "fresh" serum components cause absorption. The quality of the serum standard (whether lipoproteins are removed prior to lyophilization) can have a significant effect on the accuracy of fluorometric measurements and lower quality standards require greater dilution to eliminate pre-and post-filter effects.

Since kinetic methods provide automatic background fluorescence correction the blank absorbance rather than the blank fluorescence will be the greatest cause of errors. The simplest method of lower-

ing blank absorbance is to dilute the sample. The absorptivity of an interferent at the excitation and emission wavelengths can be used to predict the amount of dilution needed to lower the pre- and post-filter effects to below an observable level (2% attenuation). The following equation was used to estimate the concentration of an interferent, (c_i), which would cause a 2% attenuation of NADH fluorescence:

$$c_i = 0.0088/(\varepsilon_{366} + \varepsilon_{468}) \times 0.5 \text{ cm} \qquad (1)$$

An absorbance of 0.0088 corresponds to a transmittance of 0.98 (a 2% attenuation). The value of 0.5 cm is the average path length of an excitation or emission photon in the 1 cm square cuvette. ε_{366} and ε_{468} are the molar absorptivities of the interferent at 366 and 468 nm, respectively. This equation is valid only at low absorbances where Beer's Law is followed (108) and the values calculated for c_i are used only as rough estimates.

The values in Table XV and the listings of normal concentrations of serum constituents (15) were used to predict the dilution needed to reduce attenuation to less than 2% for each interfering species. The results are listed in Table XVI which shows that γ-globulin may cause the greatest portion of the total attenuation but the contribution from each interferent will be significant.

If a serum sample contained the maximum concentration of the normal range for each interferent the absorbance calculated using equation 1 would be 4.89. A dilution of 1 to 280 would be needed to reduce the expected attenuation to less than 2%. It is unlikely a

Table XVI

Predicted Dilutions to Eliminate Interference of Certain Serum Components

Species	Normal Range (mg/dL)	Predicted Concentration[b] which will cause a 2% attenuation (mg/dL)	Required[c] Dilution
Albumin	3000-5000	210	1 to 24
γ -globulin	700-1500	17	1 to 88
β -globulin[d]	600-1200	110	1 to 11
α_1-globulin[d]	200-400	18	1 to 22
α_2-globulin[d]	400-900	18	1 to 50
β -lipoprotein[a]	300-500	17	1 to 29
Bilirubin	0.2-1.0	.019	1 to 53

[a]Using literature values for fresh lipoprotein samples.

[b]Calculations were made using Table XV and equation 1.

[c]Dilution of the maximum concentration of the normal range to the level for a $\sim$2% attenuation.

[d]Using values from centrifuged samples.

serum sample would contain such levels of all the interfering species so this could be considered a worst case situation.

To test the validity of the values given in Table XV and the use of equation 1 for predicting the amount of attenuation, measurements were made of NADH in a range of different dilutions of Q-PAK Serum II. Table XVII shows the comparison of the predicted values to the percent attenuation actually measured by the fluorometer. The predicted attenuation was greater than the measured values for each dilution tested. Perhaps the estimates of the attenuation due to the particulates from lipoprotein were inaccurate since the absorption and scattering properties of these particulates is dependent on a variety of different parameters. The difference between the predicted and measured values is small enough that the predicted values could be used to estimate the dilution necessary to eliminate attenuation of NADH fluorescence. These predictions should be more accurate for fresh samples which are not effected by denatured lipoproteins.

Kinetic Assay for Ethanol

Introduction

The first system to be used for studies of fluorescence kinetic monitoring of enzymatic assays was the ethanol-alcohol dehydrogenase (ADH) reaction shown below:

$$EtOH + NAD^+ \overset{ADH}{\longleftrightarrow} CH_3CHO + NADH + H^+$$

Table XVII

Attenuation of NADH Fluorescence by a Range of Dilutions of Q-PAK Serum II

Serum Dilution[a] (in cell)	Expected %[b] attenuation	Measured % attenuation
1 to 240	3.3	2.5
1 to 180	4.7	3.7
1 to 150	5.6	4.5
1 to 120	6.9	5.9
1 to 90	8.8	7.2

[a] dilutions made using Tris buffer pH 7.5

[b] calculated using values in Table XV and concentrations listed on package insert.

A single enzyme system such as this is the simplest case and will therefore be suitable for initial studies since fewer parameters need be optimized. The specific rate equation which predicts the kinetic properties of ADH is found in reference (13). The equation is equivalent to the Michaelis-Menton equation for the above reaction except that inhibition constants are included.

Optimization

Experimental conditions such as pH and temperature used in this study are consistent with typical enzymatic assays for ethanol which use absorbance monitoring of NADH (11). Initial studies were conducted to optimize those conditions and parameters which may effect the use of a kinetic fluorescence method for the analysis of ethanol. The optimum rate measurement period was 16 s which gave the maximum value of the ratio of the measured rate vs. the blank noise. The rate measurement began after an 8 s delay which allowed complete mixing but still permitted the rate to be measured early in the course of the reaction, thus minimizing the effects of product inhibition. Using these conditions, less than 12% of the reaction has been completed by the end of the measurement period.

The dependence of the measured rate on the concentrations of NAD^+ and ADH was studied to determine their optimum levels. The results of the NAD^+ optimization study are shown in Figure 10. The increase in the observed rate with increasing NAD^+

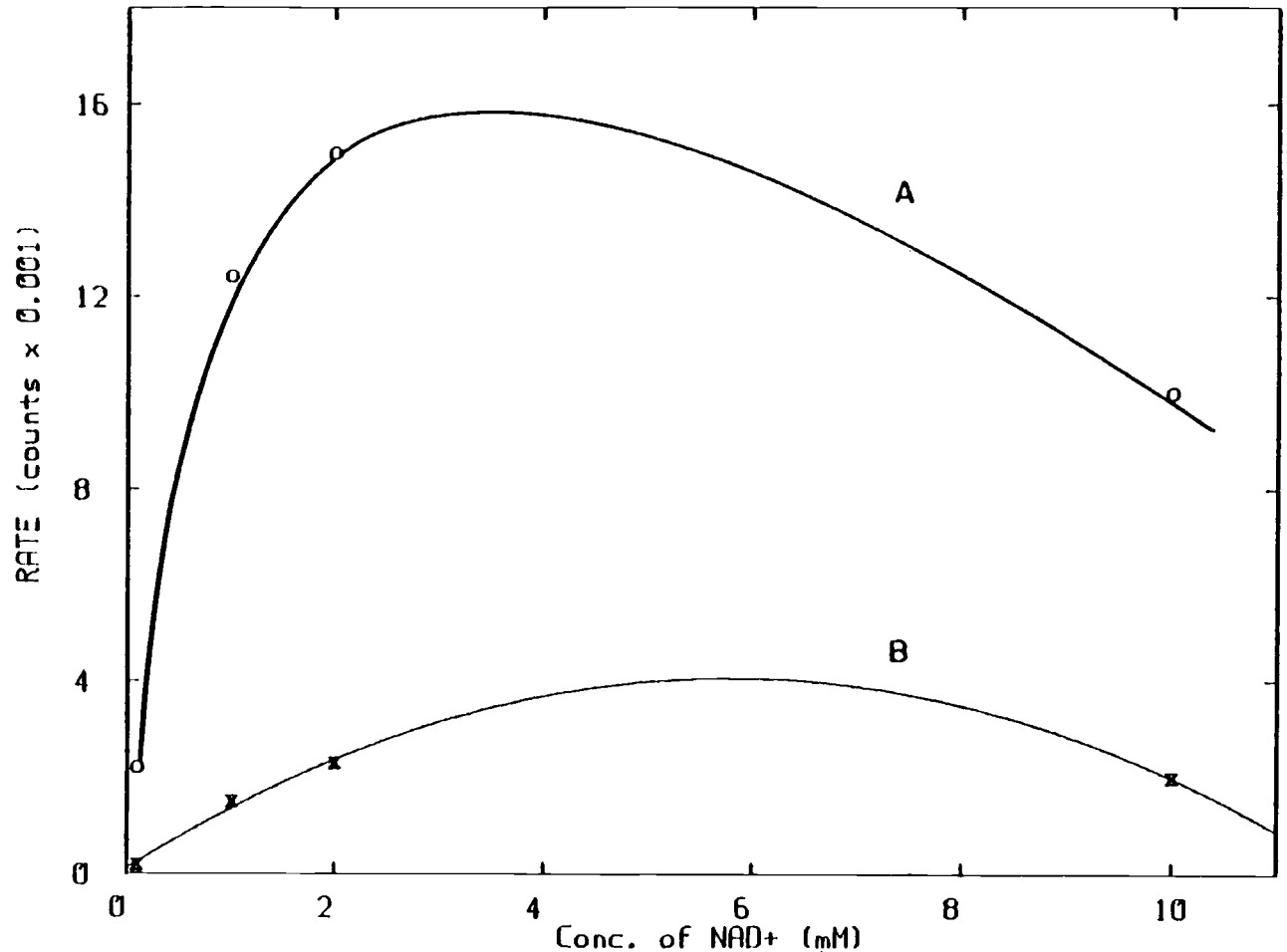

Figure 10. NAD^+ optimization for the ethanol assay. NAD^+ concentrations refer to the in-cell levels. A) 17 μM ethanol in-sample (rate values minus blank rates), B) Blank rates (buffer used in place of ethanol sample). ADH activity (in-cell) was 3.3 U/mL.

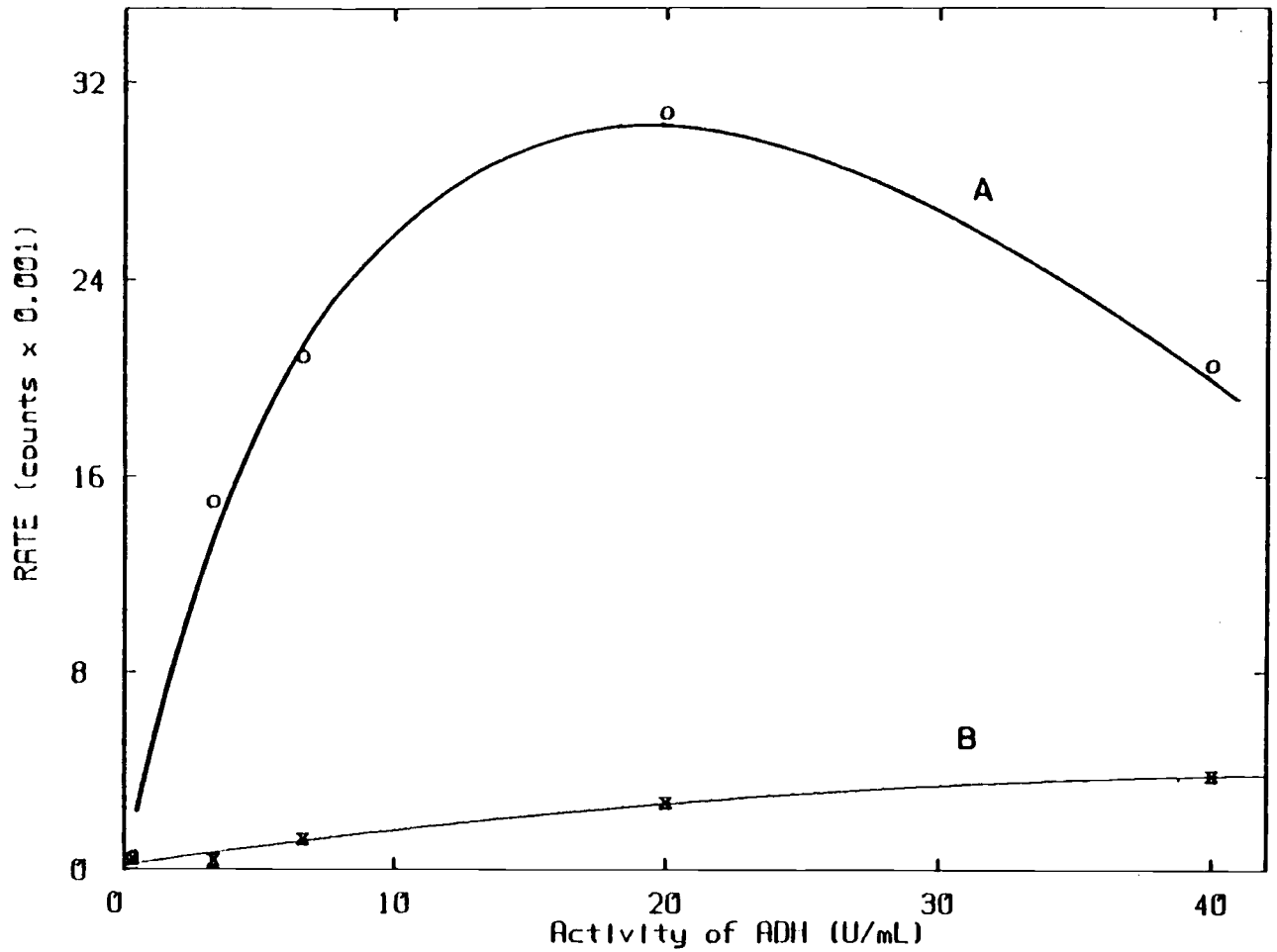

Figure 11. ADH optimization for the ethanol assay. The ADH levels reported here are the in-cell activities. A) 17 μM ethanol in-sample (rate values minus blank rates). B) Blank rates (buffer used in place of the sample solution). NAD^+ concentration was kept at 2 mM, in-cell.

concentration between 0.1 and 2 mM is equivalent to what would be predicted by the rate equation for ADH (109). When the NAD^+ concentration was increased beyond 5 mM a decrease was seen in the observed rate. This is due in part to the pre-filter effects seen with NAD^+ concentrations of 4 mM and above. NADH fluorescence is attenuated, thus the reaction rate appears to decrease. The ADH rate equation also predicts inhibition of the reaction by NAD^+ at levels above 5 mM; this also will contribute to the decreasing rate (109).

The increased blank signal and noise level at higher NAD^+ concentrations must be considered when selecting the optimum concentration. The noise values in Table XIII and the data from Figure 10 can together be used to calculate a maximum for the ratio of the measured rate vs. blank noise. The resulting optimum concentration of NAD^+ was 2 mM, which should provide the best detection limit for the kinetic assay of ethanol.

Changing the concentration (activity) of the ADH in the cuvette caused a change in both the net reaction rate of an ethanol standard and the rate of the blank reaction. The blank reaction is observed when NAD^+ and ADH are mixed in the cell even in the absence of added ethanol. It was learned from the supplier that ethanol contamination of the enzyme itself was common and unavoidable in the purification process. The blank reaction will cause a non-zero intercept in the calibration curve if the blank rate is not subtracted from the rate value of each standard. The presence of the blank reaction will not

cause errors in the measurement of samples if the blank reaction is accounted for in the determination. At ADH concentrations of 4 U/ml and below, the noise level in the blank reaction is nearly equal to that for measurements made on NAD^+ alone in the cell. The effect of increasing the ADH activity on the blank reaction is shown in Figure 11.

The effect of the ADH activity on the observed reaction rate is shown in Figure 11. The rate equation for ADH predicts that the true initial rate should be directly proportional to the ADH activity in the cell. The results of this study show that the observed rate is proportional to the ADH activity only up to a level of 6 to 7 U/mL. Above this concentration the measured rate levels out and at higher concentrations the observed rate begins to decrease. At ADH activities above 7 U/mL in the cell, the observed rate is no longer the initial rate since a significant portion of the reaction will have taken place during the delay period prior to measurement. As the ADH level is increased, more of the reaction will take place prior to measurement and therefore less and less of the original ethanol will be present by the start of the measurement period. The blank reaction does not show this same maximum since each increase in the ADH level also increases the concentration of the contaminating ethanol.

Several articles (110,111) have pointed out the advantages of operating under conditions yielding the maximum measured rate (18 to 25 U/mL of ADH for this system). Changes in pH, temperature or other

factors which would effect the enzyme activity would have less effect on the measured rate when working at this maximum, and therefore precision should improve. Studies made on the ethanol-ADH system using the maximum ADH level (20 U/mL) gave ethanol detection limits that were equivalent to those measured with the ADH concentration near 4 U/mL. At activity levels above 3 to 4 U/mL the noise in the blank rate increases more than the observed rate of an ethanol standard, thus the detection limit is increased.

Calibration Curve

A calibration curve of the measured rate vs. the ethanol concentration was made up using the optimum conditions and is plotted in Figure 12. The results of this study are summarized below:

Slope of Calibration Curve (counts per μM ethanol in standard)	=	690
Average Blank Rate (counts)	=	467
SD of Repetitive Measurements of the Blank Rate (counts)	=	432
Theoretical Detection Limit for Ethanol (μM, in sample)	=	1.3
Upper Limit of Linearity (μM)	=	230
RSD of Repetitive Runs (using 17 mM Et^{OH})	=	3%

The average blank reaction was subtracted from the measured rate of each standard.

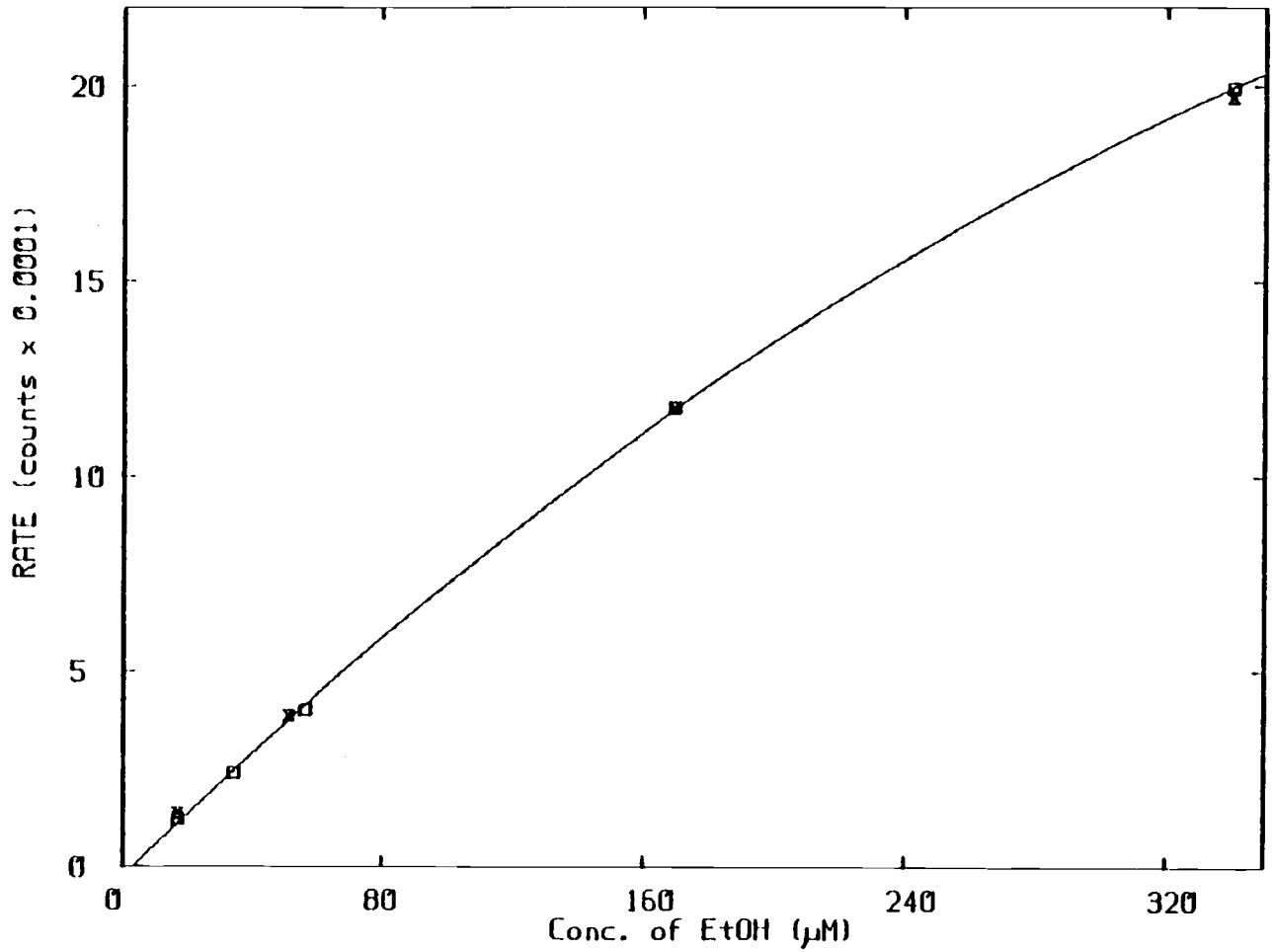

Figure 12. Calibration curve for the ethanol assay. ◻) Ethanol standards made up in Tris buffer, ⧗) Ethanol standards made up in a 1 to 200 dilution (in-sample) of Versatol serum standard (1 to 600 in-cell). 2 mM NAD^+, 3.3 U/mL ADH in-cell.

Calculations were conducted to determine the average amount of NADH produced during a reaction equivalent to that for an ethanol concentration at the detection limit. At the ethanol detection limit (1.3 μM) the average NADH concentration produced during the measurement period (NADH present at the end of the first 8 s of the 16 s measurement period) was calculated to be 0.017 μM.

The theoretical detection limit for NADH for a 16 s rate measurement was calculated from repetitive 8 s steady-state measurements of a 2 mM NAD^+ solution which would show the equivalent noise level of the blank. The SD of these measurements was 356 counts which corresponds to a detection limit of 1.2×10^{-2} μM for NADH using an 8 s steady-state measurement. Since a 16 s rate measurement is equivalent to the difference between two 8 s steady-state measurements, the SD of a 16 s rate measurement of the blank solution should be $\sqrt{2} \times 356$ or 498 counts. Since the SD increased by the $\sqrt{2}$, the theoretical detection limit would also increase by the same proportion, resulting in 1.6×10^{-2} μM for the detection limit for NADH using a 16 s rate measurement. In other words, the reaction rate equivalent to the ethanol detection limit should theoretically produce an average concentration of 1.6×10^{-2} μM NADH during the measurement period. This theoretical detection limit corresponds well to the calculated average NADH concentration produced at the ethanol detection limit.

The upper limit of linearity for the kinetic assay of ethanol is defined as the concentration showing a 5% deviation from the

expected linear value. Using the Michaelis-Menton equation the theoretical ethanol concentration which should show a 5% deviation from first order kinetics can be calculated.

$$V_o = \frac{V_{max} \times [EtOH]}{K_m + [EtOH]} = 0.95 \times \frac{V_{max}}{K_m} \times [EtOH]$$

With 0.013 M as the value of K_m, the value for ethanol is calculated to be 0.69 mM. The upper limit of linearity measured from the calibration curve is approximately 0.23 mM, which would correspond to an in-cell concentration of 0.077 mM for ethanol. This difference between the observed and the expected limit of linearity indicates other factors are effecting the system.

From calculations using the chart recordings from reactions of ethanol standards the approximate concentration of NADH produced at the upper limit of linearity (0.23 mM) was calculated. The results showed that no greater than 7 μM NADH was present by the middle of the measurement period, which indicates that the non-linearity was not due to exceeding the limit of linearity for NADH fluorescence, 25 μM. The cause of the non-linearity must be due to effects on the chemistry of the system. Reference 109 describes a study conducted on the inhibition effects of the products of the ethanol reaction on ADH. Acetaldehyde at concentrations near 10 μM and above can cause inhibition of ADH, thereby reducing the observed reaction rate. Since the level of acetaldehyde at the upper limit of linearity has reached 7 μM, the effects of enzyme inhibition should become significant. For maximum linear range with this type of system, it

is important to measure the reaction rate as soon after mixing as possible.

For equilibrium assays, complexing agents such as semicarbazide are used to remove acetaldehyde and thereby allow greater yields. With the fluorometric kinetic assay of ethanol, the reaction rate was reduced by 30% upon the addition of 33 mM semicarbazide. Further experiments were not performed to study this inhibition and semicarbazide was not used in any subsequent assays. Even if product inhibition could be prevented without effecting the reaction rate, the limit of linearity could only be increased by a factor of 4. At this level of activity the concentration of NADH produced during the measurement period would reach 25 μM, which is the upper limit for fluorescence measurements of NADH.

Measurements were made on diluted serum standards spiked with ethanol using the same conditions as in previous studies. The results are shown in Figure 12 and are summarized below:

Slope of Calibration Curve (counts/ M EtOH in sample)	=	690
Average Blank Rate (counts)	=	370
SD of Repetitive Measurements of the Blank Rate (counts)	=	277
Theoretical Detection Limit for Ethanol (μM, in sample)	=	0.82
RSD of Repetitive Runs (using 51 μM ethanol)	=	2.5%

The analysis of ethanol in a 1 to 600 dilution of a Versatol serum standard showed results which are basically the same as with standards made up in buffer. The range of interest for ethanol in blood is from 0.05 to 0.15% (w/v) or 1 to 3 x 10^{-2} M. A dilution of the sample by a factor of 600 will put the in-cell concentration of ethanol within the linear range. This degree of dilution eliminates any pre-or post-filter effects and reduces the net steady-state fluorescence of the serum blank to about 0.3 times the NAD^+ signal. This small change in the blank signal should not have a significant effect on the noise in the blank, so no major difference should be seen in the detection limit for ethanol.

Kinetic Assay for Glucose

Introduction

The second enzymatic assay to be adapted to fluorescence kinetic monitoring was the determination of glucose utilizing the hexokinase (HK)-glucose-6-phosphate dehydrogenase (G-6-PDH) system. The reactions involved are given below:

$$\text{Glucose} + \text{ATP} \xleftrightarrow{\text{HK}} \text{ADP} + \text{Glucose-6-PO}_4$$

$$\text{Glucose-6-PO}_4 + \text{NAD}^+ \xleftrightarrow{\text{G-6-PDH}} \text{6-phosphogluconate} + \text{NADH} + \text{H}^+$$

The K_m values for the substrates in this system are 0.1 mM for ATP and glucose, 0.5 mM and 0.1 mM for glucose-6-phosphate and NAD^+, respectively.

This system was studied to show if fluorescence kinetic monitoring could be used with a system more complex than a single

enzyme system, such as the ethanol assay. More parameters must be adjusted for optimum performance since twice the number of reagents are required for the analysis.

Instrumental settings used for studies of the glucose system were identical to the ethanol assay except that an 8 s measurement time was used. A scouting study showed no significant difference between 8 s and 16 s measurements in terms of the relative noise levels, so the 8 s period was used since it provides faster analysis times.

Commercial reagent kits (Abbott Laboratories, Inc.) designed for equilibrium absorbance monitoring of glucose were used for the initial studies of the glucose system to provide a rapid way to determine the feasibility of using fluorescence kinetic monitoring for glucose analysis. The results of the analysis of glucose standards using the commercial reagent are shown below:

Slope of Calibration Curve (counts per mg/dL in standard)	=	6.1×10^3
SD of Blank Measurements (counts)	=	234
Theoretical Detection Limit (mg/dL in standard)	=	0.076
Upper Limit of Linearity, -5% Deviation (mg/dL in standard)	=	1.4
RSD of Repetitive Runs (at 1.0 mg/dL)	=	3%

To conserve reagent, its final concentration in the cuvette was diluted by a factor of 3 as compared to the concentration recommended by the manufacturer. The resulting in-cell concentration of the

major components of the commercial reagent are; 0.5 mM of NAD^+, 0.6 mM of ATP, 0.26 U/mL of HK, 0.52 U/mL of G-6-PDH and 0.4 mM for Mg^{2+}.

Optimization

These initial studies showed that the glucose assay could be successfully monitored by a fluorescence kinetic method. The next step was to study the effect of changing the concentration of the major components of the reagent in order to determine their optimum levels. The first study was of the effect of the NAD^+ concentration on the measured rate of a glucose standard (see Figure 13). The results show an increase in the measured rate as the NAD^+ concentration is increased up to about 3 mM. Above this level the observed rate levels off, but at concentrations above 5 mM the observed rate begins to decline with increases in NAD^+. At these higher concentrations the NAD^+ begins to cause pre-filter effects due to its absorbance at 366 nm. A NAD^+ concentration of 2 mM was chosen as optimum in terms of the ratio of the observed rate vs. the blank noise level.

Figure 14 shows the results of the ATP optimization studies. As would be expected, the observed rate increased as the concentration of ATP was raised up to 0.5 mM, at which point the measured rate began to level off. Above 1 mM the observed rate began to decline as the ATP level was further increased. Reference 112 describes how elevated levels of ATP can competitively inhibit HK, thus lowering the rate of phosphorylation. Since ATP has no effect

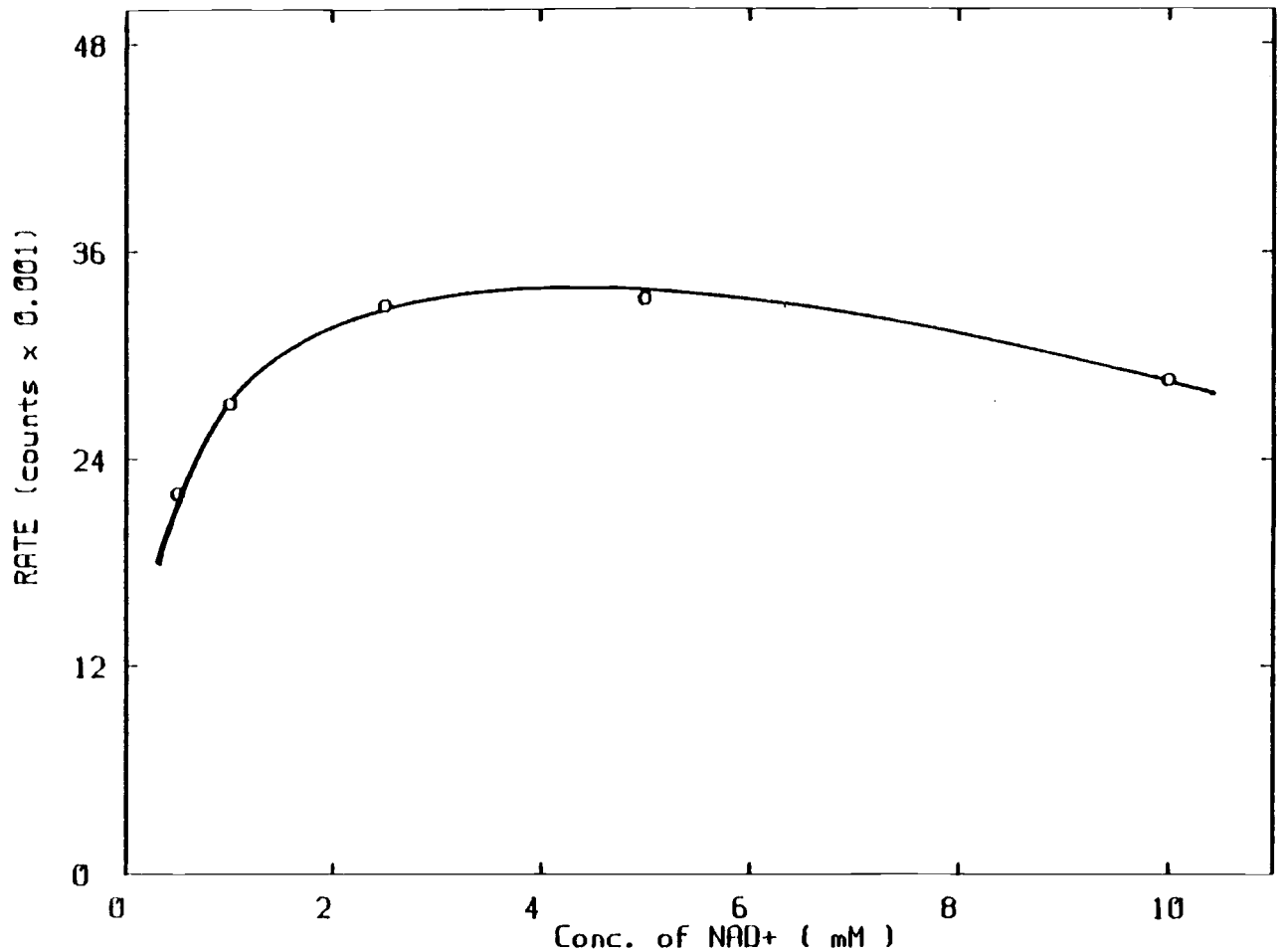

Figure 13. NAD^+ optimization for the glucose assay. The NAD^+ levels reported here are the in-cell concentrations. The in-cell concentrations of other major components were 0.33 mg/dL glucose, 1 mM ATP, 0.33 U/mL HK and 0.66 U/mL G-6-PDH.

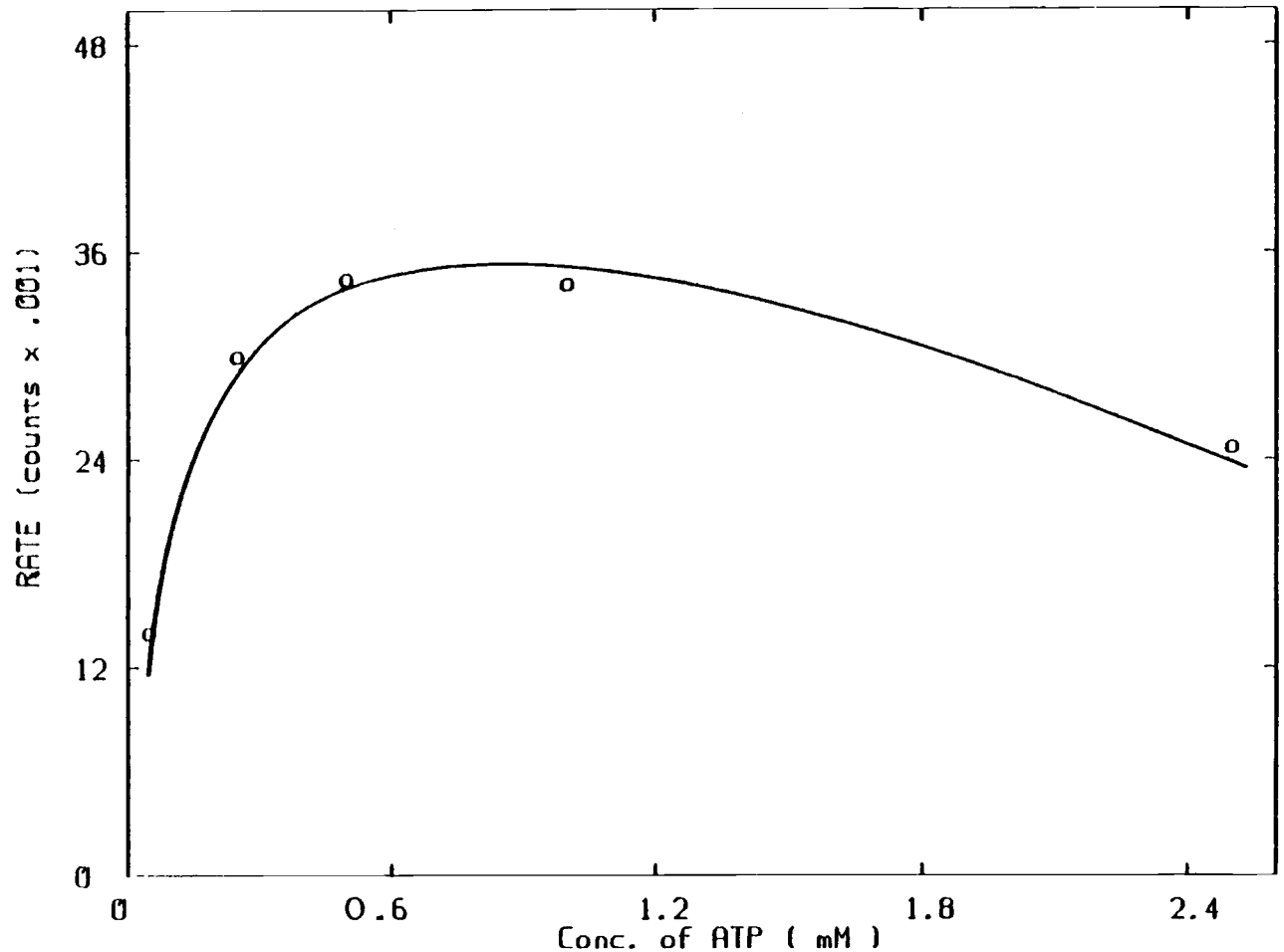

Figure 14. ATP optimization for the glucose assay. The ATP levels reported here are the in-cell concentrations. The in-cell concentrations of the other major components were 2 mM NAD^+, 0.33 mg/dL glucose, 0.33 U/mL HK and 0.66 U/mL G-6-PDH.

on the blank noise, it is necessary to only consider which concentration gives the maximum rate when choosing the optimum concentration. An in-cell concentration of 1 mM was therefore selected as optimum.

The major shortcoming seen in the initial studies using the commercial reagent was that a 32 s delay period was needed to achieve the maximum measured rate. To decrease this lag between mixing and reaching the maximum rate, an increase in the observed activity of the G-6-PDH is necessary. Both the concentration of the enzyme and of NAD^+ can effect the observed activity of the G-6-PDH reaction. It was shown in a previous study that 2 mM NAD^+ gave the maximum observed activity, so it was held at this level while the effect of changing the G-6-PDH level on the measured rate and the lag time was observed. The results of the G-6-PDH optimization are shown in Table XVIII. These results show a reduction in the lag time with increases in G-6-PDH activity until the level of the enzyme had reached 0.8 U/mL, above which no significant change was seen in the observed rate. At 0.8 U/mL the optimum delay period was reduced to 8 s, which was sufficient time for both complete mixing and for the measured rate to reach its maximum.

Another factor in the system that can effect the activities of both the G-6-PDH and HK enzymes was the Mg^{2+} concentration (112,113). The concentration of Mg^{2+} used for the optimization studies (1.2 mM) was a factor of 3 greater than that present in the commercial reagent used for initial studies. This certainly had an effect on the

Table XVIII

Optimizations of G-6-PDH and HK[a]

Enzyme Concentration in-cell (U/mL)	Approximate Delay to Reach Maximum Rate	Measured Rate using an 8 s delay (counts x 10^{-3})
G-6-PDH:		
0.2	16 s	48
0.8	8 s	88
2.0	8 s	92
20	4 to 8 s	94
HK:		
0.17	8 s	24
0.83	8 s	92
8.3	8 s	58

[a] For the G-6-PDH optimization the HK level was 0.83 U/mL. For the HK optimization the G-6-PDH level was 2.0 U/mL. For both studies the concentrations of other components were; 1 mM ATP, 5 mM NAD^+, 1.2 mM Mg^{2+}.

increased reaction rates and lower lag times observed during the optimizations, as compared to the initial studies with the commercial reagent. Reference 112 reports that 1.2 mM Mg^{2+} is optimum for this study.

An optimization study was conducted for the HK activity using identical conditions as for the G-6-PDH study (see Table XVIII). The results were equivalent to what was seen in the optimization of ADH (refer to p. 107). The observed activity increased with higher activities of HK until a maximum was reached near 3 U/mL and began decreasing at HK activities above that level. At such fast reaction rates a significant portion of the total glucose is used up prior to the measurement period, thus a lower reaction rate is observed.

For the selection of optimum concentrations of HK and G-6-PDH, a compromise must be made between the desired sensitivity of the method and the cost of each assay. At enzyme levels of 3 U/mL and 0.8 U/mL for HK and G-6-PDH, respectively, the best detection limit will be obtained but the cost per run would be nearly 1.00$. Reducing the enzyme levels to 0.33 U/mL and 0.66 U/mL, respectively, would cut the cost to less than 20¢ per run,[a] while increasing the detection limit by about a factor of 4. This higher detection limit (0.028 mg/dL of glucose) is more than adequate for serum analysis (see p. 125).

The G-6-PDH used in the commercial reagent was the type derived from yeast and is usable only with $NADP^+$ as the cofactor. High

---

[a] Prices quoted from the 1982 Sigma Catalog, Sigma Chem. Co., St. Louis, MI

quality $NADP^+$ needed for fluorometric monitoring is nearly a factor of 8 more expensive than comparable NAD^+.[a] It was therefore decided to use a type of G-6-PDH derived from the bacteria, Leuconostoc Mesenteroides, which functions equally well with NAD^+ or $NADP^+$ (114).

Calibration Curve

After the optimum parameters had been established, the operation of the system was tested by making up a calibration curve using glucose standards diluted with saturated benzoic acid solution. The benzoic acid in solution stabilizes the glucose. The results are plotted in Figure 15 and are summarized below:

Slope of Calibration Curve (counts per mg/dL of standard)	=	2.8×10^4
SD of Blank Measurements (counts)	=	388
Theoretical Detection Limit (mg/dL in sat'd benzoic acid)	=	0.028
Upper Limit of Linearity (mg/dL)	=	1.6
RSD of Repetitive Runs (at 0.5 mg/dL)	=	3%

Comparing these results to those from the initial studies using the commercial reagent shows a factor of 3 improvement in the detection limit. The optimization of both ATP and NAD^+ and the

---

[a] Prices quoted from the 1982 Sigma Catalog, Sigma Chem. Co., St. Louis, MI.

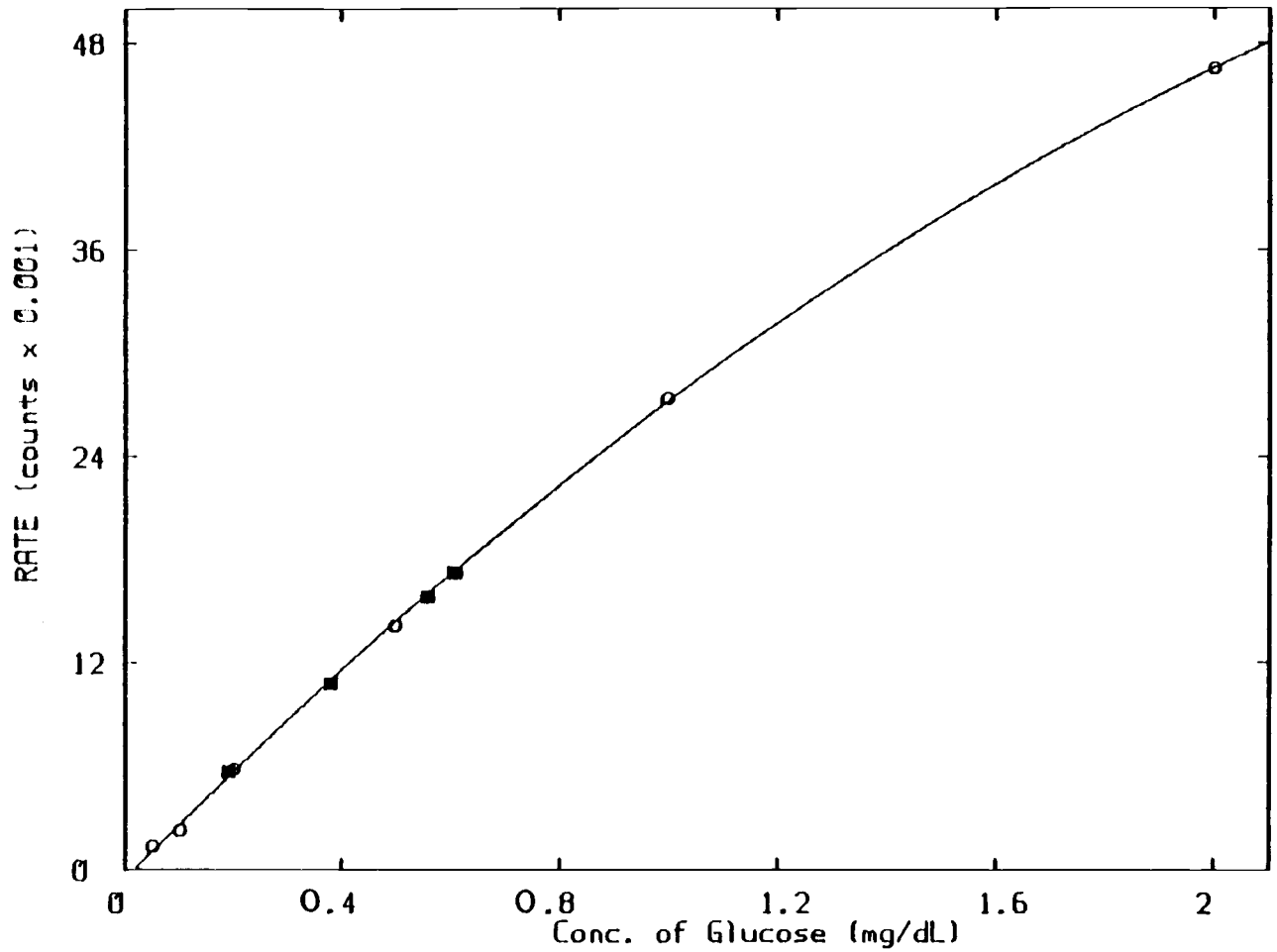

Figure 15. Calibration curve for the glucose assay. The glucose levels reported here are in-sample concentrations (prior to addition to cuvette). o) Glucose standards in sat'd benzoic acid, ■) 1 to 500 dilutions (in-sample) of serum standards (see Table XIX). Other components = 2 mM NAD^+, 1 mM ATP, 0.33 U/mL HK and 0.66 U/mL G-6-PDH.

increase in the concentration of Mg^{2+} helped to increase the observed reaction rates without a proportional increase in the blank noise. The concentrations of the enzymes used for the optimized calibration curve (0.33 U/mL HK and 0.66 U/mL G-6-PDH) are only 30% higher than the concentrations of the enzymes present in the cell during the studies with the commercial reagent (0.25 U/mL HK, 0.52 U/mL G-6-PDH). As was observed in the enzyme optimization studies, the detection limit could be lowered if higher enzyme levels were used, but at the expense of higher costs per assay.

Calculations using the chart recordings of the calibration runs were made to estimate the amount of NADH produced during the measurement period at the glucose detection limit. From this the average concentration of NADH produced during the measurement period was calculated to be 0.016 μM. The theoretical detection limit for NADH in the blank solution using an 8 s rate measurement was determined to be 0.018 μM. Since these two values are nearly equal, it can be concluded that under these conditions, the detection limit for glucose is a function of the detectability of NADH. Decreased blank noise or greater signal per unit concentration of NADH would improve the detection limit for glucose.

The concentration of glucose in the sample solution corresponding to a measured rate of 5% below the expected value was estimated from Figure 15 to be 1.6 mg/dL. This upper limit of linearity was nearly equal for both the optimized system and for the commercial reagent. It can therefore be concluded that the upper

limit is independent of the relative reaction rates, at least for these experimental conditions. Using the rate equation for HK, an ordered, single displacement reaction (115), the limit of linearity can be calculated in the same manner as for the ethanol-ADH system (see p. 111). The value determined by this method is 23 mM of glucose, which corresponds to 1.3 mg/dL in the sample or standard solution, which is close to the experimental value determined from the plot of the calibration curve. The working range for the glucose assay using these conditions is 0.03 to 1.3 mg/dL glucose in the sample solution.

To test the use of this system for glucose analysis in a serum matrix, serum standards were made up and tested using the optimum conditions used for glucose standards. Using buffer as diluent, 1 to 500 dilutions of each serum standard were made prior to analysis in order to obtain glucose levels within the linear range and to minimize spectral interferences. For typical levels of serum glucose of 50 to 200 mg/dL, a minimum dilution of 1 to 200 would be needed to put the diluted samples within the linear range. The results of these assays are included in the calibration curve in Figure 15. Table XIX shows the yields of glucose compared to the reported concentrations for the serum standards in the diluted samples. These experimental values compare well to the reported values given by the manufacturers. The only significant change seen in the analysis of glucose in serum compared to glucose standards in saturated benzoic

Table XIX

Glucose Assay of Serum Standards

Type of Serum Standard	Reported Concentration (after a 1 to 500 dilution) mg/dL	Experimentally Measured Glucose Concentration mg/dL
Versatol A	0.39 ± .03[a]	0.39 ± .02 [b]
Versatol A Alternate	0.61 ± .05	0.63 ± .03
Q-PAK Serum I	0.19 ± .02	0.21 ± .02
Q-PAK Serum II	0.56 ± .04	0.57 ± .03

[a] The
by the manufacturer for the undiluted glucose level.

[b] Reported values are the average of 2 runs. The RSD for measurements of glucose in this range of concentrations is typically 5%, which was used to calculate the error in these measurements.

acid solution was that the noise level of the blank increased. The worst-case serum blank (Q-PAK Serum I) gave a standard deviation of 546 counts. This increased the glucose detection limit to 0.04 mg/dL which was still well below the lowest expected glucose level.

The enzymatic fluorescence kinetic method was shown to be effective for glucose analysis in serum since large dilutions are possible, which eliminate nearly all serum spectral interferences. An additional advantage of large dilutions is that much smaller serum quantities are required, which is important since normally only limited quantities of serum are available.

Fluorometric Assay for Lactate Dehydrogenase

A brief study was made of measuring the activity of lactate dehydrogenase (LDH) with fluorescence monitoring. The reaction catalyzed by LDH is shown below:

$$\text{Pyruvate} + \text{NADH} + \text{H}^+ \xleftrightarrow{\text{LDH}} \text{NAD}^+ + \text{Lactate}$$

The K_m values for LDH are; 6.7 mM for lactate, 0.16 mM for pyruvate, 0.25 mM for NAD^+ and 11 μM for NADH (11).

Previous studies have shown that fluorescence monitoring can be used for measurement of LDH activity in serum (57, 116). These methods utilized the reverse reaction so that the increase in fluorescence from NADH is monitored to determine the activity. For this brief study the reaction in the forward direction was monitored

so that the decrease in NADH fluorescence could be used to measure LDH activity to show the characteristics of rate measurements made where the fluorophore concentration is decreasing.

Initial studies involved optimizing the cofactor concentrations (pyruvate and NADH) for the greatest sensitivity and maximum reaction rates. Ideally for an enzyme assay the cofactor concentrations should be adjusted so that the rate equation reduces to $V_o = V_{max}$ where the observed rate is equal to the maximum enzyme activity. For pyruvate, the concentration could be raised above the K_m value without causing major problems with the system. The optimum level was chosen as 1 mM which, according to reference 117, should give the maximum rate and minimal substrate inhibition for LDH.

The optimum concentration of NADH must be below the upper limit of linearity for NADH fluorescence (25 μM) in order for the rate measurements to be valid. Optimization of NADH also requires a compromise between the reaction rate and the noise level of the blank due to NADH fluorescence. Table XX shows the noise levels of the blank and the observed reaction rates of a 1.4 mU/mL LDH standard for a range of NADH concentrations. The NADH concentration yielding the maximum for the ratio of the observed rate vs. the blank noise is 2.8 μM. This concentration should provide the greatest sensitivity and therefore the lowest detection limit and it is well below 25 μM.

At an NADH concentration of 2.8 μM the observed reaction rates are only a fraction of the total activity possible from the enzyme in the cell. This can be shown from calculations using the Michaelis-

Menton equation where K_m for NADH is 11 μM and the NADH concentration is 2.8 μM,

thus:

$$V_o = \frac{V_{max} \times [NADH]}{K_m + [NADH]} = V_{max} \times 0.21$$

This shows that the observed rate, V_o, will only be 1/5 of the maximum enzyme activity, V_{max}.

A convenient way to produce a calibration curve and to test this method of LDH assay in a serum matrix was to make various dilutions of a serum standard (Q-PAK Serum II) to produce a range of LDH activities. Reference 116 states that this method can be used to make up valid calibration curves for LDH. The concentration of LDH in each diluton was calculated using the reported activity in the undiluted serum, 89 mU/mL at 25 °C. The results of these assays are shown in Figure 16 and are summarized below:

Slope of calibration curve for the 3 lower concentrations (counts per mU/mL)	=	1×10^4
SD of the serum blank 1 to 150 dilution in cell (counts)	=	815
Theoretical detection limit (mU/mL in the cell)	=	0.16
Observed limit of linearity (mU/mL in the cell)	=	0.9

The noise level of the blank increases by 50% when the 1 to 150 dilution of Q-PAK Serum II is added to the NADH in the cell. The theoretical detection limit is therefore a factor of 1.5 times higher

Table XX

Optimization of NADH Concentration[a]

NADH in-cell (μM)	SD of Blank (counts)	Observed Reaction Rate (counts)	Ratio of rate to SD of Blank
0.28	154	733	4.8
0.85	345	1771	5.1
2.8	557	3308	5.9
8.5	1236	3804	3.1

[a] In-cell concentrations were; 1 mM pyruvate, 1.4 mU/mL LDH. For blank measurements, buffer was used in place of LDH. Reaction rates and SD's were calculated using 16 s rate measurement times.

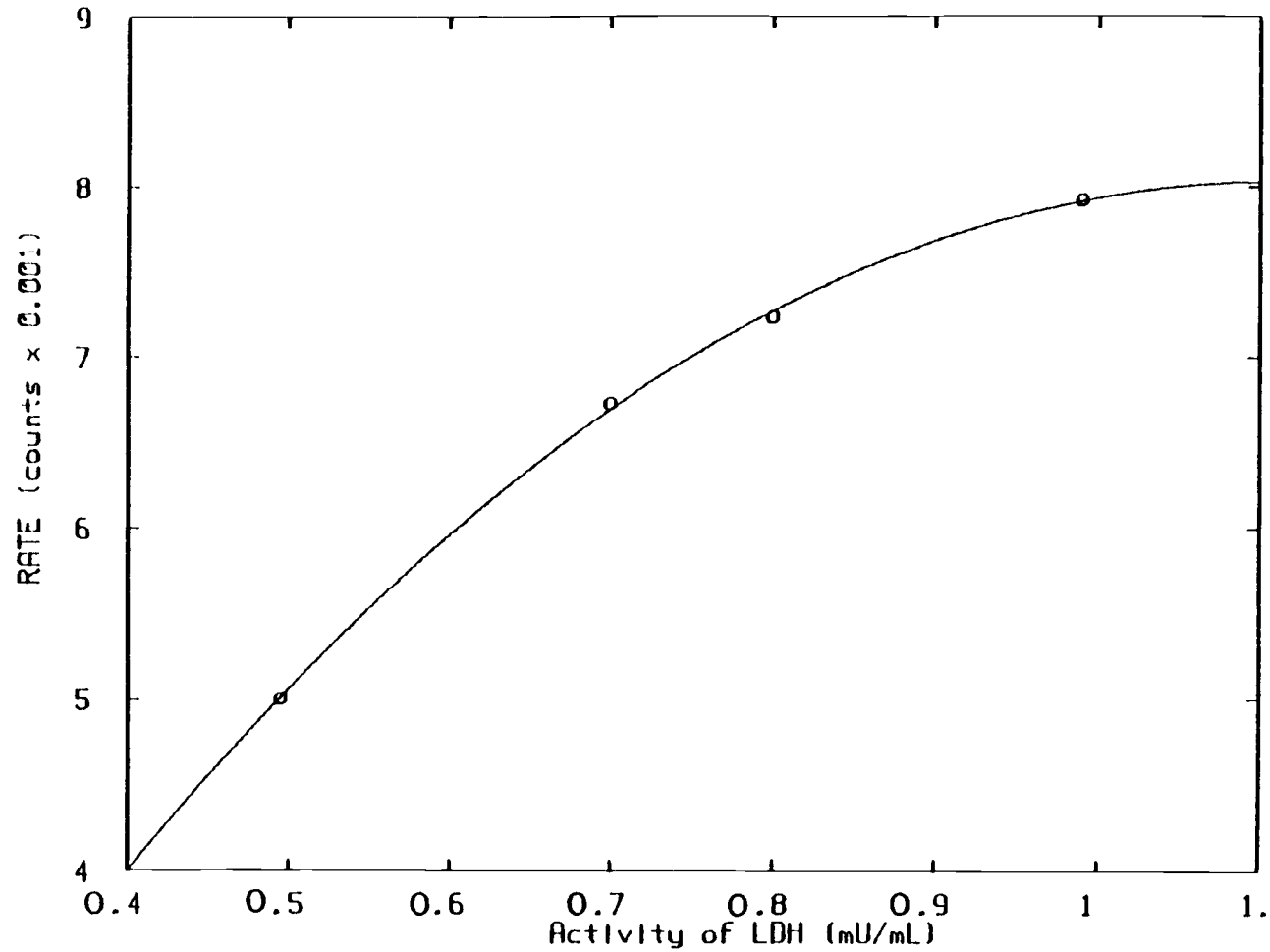

Figure 16. Calibration curve for the LDH assay. The LDH levels reported here are the in-cell activities. The LDH standards were made up using a range of dilutions of Q-PAK Serum II. The reported rate values are of the decrease in signal per unit time. Other concentrations = 2.8 μM NADH and 1 mM pyruvate (in-cell).

when measuring serum standards as compared to solutions of LDH made up in buffer.

From Figure 16 it can be seen that at the highest concentration tested (1 to 90 dilution), the observed rate had dropped by 9.5% from the value expected from linear extrapolation. The predicted attenuation of NADH due to serum absorbance, when measured in a 1 to 90 dilution of Q-PAK Serum II was 7.2% (see Table XVII). The observed nonlinearity is due primarily to the attenuation of NADH fluorescence rather than a decrease in the reaction rate itself. For samples where spectral interference is not a factor, nonlinearity will occur at reaction rates where a significant portion of the NADH is used up by the middle of the measurement period. Using the Michaelis-Menton equation, the concentration of LDH causing a 5% deviation from linearity can be estimated. As shown on p. 129 the observed rate, V_o, is 0.21 times V_{max} at an NADH concentration of 2.8 μM. For a 5% decrease in linearity, 0.21 must reduce to 0.19 which corresponds to a decrease of 0.18 μM in the NADH concentration. The observed reaction rate (V_o) which would convert 0.18 μM NADH to NAD^+ in the 16 s period between mixing and the middle of the delay period is calculated to be 0.68 mU/mL. This corresponds to an in-cell concentration of LDH (V_{max}) of 3.3 mU/mL under these reaction conditions. The theoretical linear range would be from 0.16 to 3.3 mU/mL for LDH.

The normal range of LDH in undiluted serum is 0.085 to 0.19 U/mL (15). A dilution of 1 to 150 of serum in the cell would result in

concentrations of 0.57 to 1.3 mU/mL which would fit well with the linear range of this technique. With certain diseases however, the level of LDH may reach ten times the normal levels which would result in activities well above the linear range. Using this fluorescence technique, accurate measurements of high levels of LDH can not be made without making additional dilutions and rerunning the assays.

It is obvious that this system may not be the optimum method for measuring LDH activity in serum. As a comparison, the theoretical detection limit and upper limit of linearity for the fluorometric measurement of the reverse reaction were calculated. Using the reverse reaction the blank signal and noise level will be a function of the NAD^+ concentration in the cell. To match the blank signal and noise level of 2.8 μM NADH, 2.5 mM NAD^+ must be present in the cell. From calculations using the Michaelis-Menton equation and assuming lactate is at a saturating concentration, the detection limit for LDH, using the reverse reaction, was estimated to be 0.04 mU/mL when using 2.5 mM NAD^+.

Estimations of the theoretical limit of linearity for the reverse reaction were made by assuming the controlling factor would be the limit of linearity of NADH fluorescence, 25 μM. In other words, the limit of linearity for the LDH assay would occur at a reaction rate which would produce 25 μM NADH by the middle of the measurement period. Using the rate equation, the upper limit of linearity was calculated to be 94 mU/mL. The resulting theoretical linear range would be from 0.04 to 94 mU/mL for LDH.

Even though these values are estimates, they still illustrate the advantage of measuring enzymatic assays in the mode where the concentration of the fluorophore is increasing.

Creatine Kinase Assay

Introduction

Fluorescence monitoring of NADH can be used to measure the activity of the enzyme, creatine kinase (CK) by coupling the CK reaction with additional enzymatic reactions as shown below:

$$\text{Creatine phosphate} + \text{ADP} \xleftrightarrow{\text{CK}} \text{creatine} + \text{ATP}$$

$$\text{ATP} + \text{glucose} \xleftrightarrow{\text{HK}} \text{ADP} + \text{glucose-6 phosphate}$$

$$\text{Glucose-6-phosphate} + \text{NAD}^+ \xleftrightarrow{\text{G-6-PDH}} \text{6-phosphogluconate} + \text{NADH} + \text{H}^+$$

The Michaelis constants for CK are as follows; 16 mM for creatine, 0.8 mM for ADP, 0.5 mM for ATP and 5 mM for creatine phosphate.

The purpose of this study was to investigate the use of fluorescence kinetic methods for complex assays requiring 3 reaction steps to produce a fluorophore. This particular assay was chosen because some familiarity had already been gained about this system from studies of the glucose assay. As can be seen, the two coupling

reactions in the system are identical to the reactions used in the glucose assay.

The first studies conducted with this system utilized commercial reagent kits (Abbott Labs Inc.) designed for absorbance monitoring of CK activity. CK standards were made up using purified CK enzyme which had been derived from rabbit muscle. The results of this study are shown below:

Slope of Calibration Curve (counts per U/mL in cell)	=	1.3×10^6
SD of Blank Measurements (counts)	=	864
Theoretical Detection Limit (mU/mL in cell)	=	1.3
Upper Limit of Linearity (mU/mL in cell)	=	54

The in-cell concentrations of the major components of the commercial reagent were; 0.5 mM ADP, 1 mM NAD^+, 7.5 mM glucose, 19 mM phosphocreatine, 0.83 U/mL HK and 1.6 U/mL G-6-PDH. A delay time of 40 s was required when using this commercial reagent in order for the measured 16 s rate to reach its maximum.

Optimization

References 118 and 119 discuss in length the optimum conditions for measuring CK activity using absorbance monitoring of NADH. For this study these same optimum conditions were used except for those which might effect the fluorescence measurements of NADH. The two parameters that did have an effect on the fluorescence monitoring

were the concentrations of both NAD^+ and ADP. The optimum concentrations for the other major components are listed in the caption of Figure 17.

Previous studies with the ethanol system had shown that a 2 mM concentration of NAD^+, in-cell, would be optimum for this type of fluorometric kinetic method. A brief study showed this same concentration was optimum for the CK assay as well. Reference 119 also reports 2 mM as the optimum NAD^+ concentration for absorbance methods.

It was shown that the concentration of ADP in the reagent mixture affected the blank signal from the reagent. This was first discovered when the sum of the net fluorescence of each separate component of the reagent was compared to the fluorescence of the complete mixture, which was much higher. The cause of this high blank signal was investigated by measuring the fluorescence of various combinations of the components. It was found that the ADP was contaminated with ATP or a similar compound which was reacting by the two coupling reactions to form NADH. The NADH produced in this manner caused the blank signal to be a factor of two higher than expected for the sum of the net fluorescence of each component of the commercial reagent. This high blank signal caused the theoretical detection limit for CK to be a factor of 2 higher than originally predicted.

Since much of the blank fluorescence was found to be a function of the purity of ADP, a study was made of the ATP concentration in

several different types of ADP (extracted from different sources). The lowest relative level of ATP was found in a type of ADP extracted from yeast (Sigma Chem. Co., Cat. #4386) which, when tested using the HK G-6-PDH reaction, contained only 0.10% ATP (mol/mol).

This type of ADP was then used in an optimization study where the blank noise level was measured and compared to the reaction rate of a CK standard, for a range of ADP concentrations. The results are shown in Table XXI. The optimum was chosen to be 0.3 mM of ADP in-cell since this concentration showed the maximum value for the rate vs. blank noise ratio. This optimum may change depending upon the relative concentration of ATP in a particular batch of ADP.

Calibration Curve

Using the optimum conditions (see Figure 17), a calibration curve was obtained by assaying a range of CK activities made up using the rabbit muscle enzyme. The curve is plotted in Figure 17 and the results are summarized below.

Slope of Calibration Curve (counts per U/mL, in cell)	=	4.5×10^6
SD of Blank Measurements (counts)	=	546
Theoretical Detection Limit (mU/mL in cell)	=	0.24
Upper Limit of Linearity (mU/mL in cell)	=	29
RSD of Repetitive Runs (using 8.3 mU/mL CK)	=	3.3%

Table XXI

Optimization of ADP Concentration

ADP Concentration in-cell (mM)	Observed[a] Reaction Rate (counts)	SD of Blank[b] Measurement (counts)	Ratio of rate/SD of Blank
No ADP	-	430	-
0.1	129,000	535	242
0.33	299,000	812	370
1.0	333,000	1182	280
3.3	292,500	2550	115
10	221,000	4392	50

[a]Using a 0.05 U/mL CK standard

[b]Calculated from 8 16 s rate measurements of the blank.

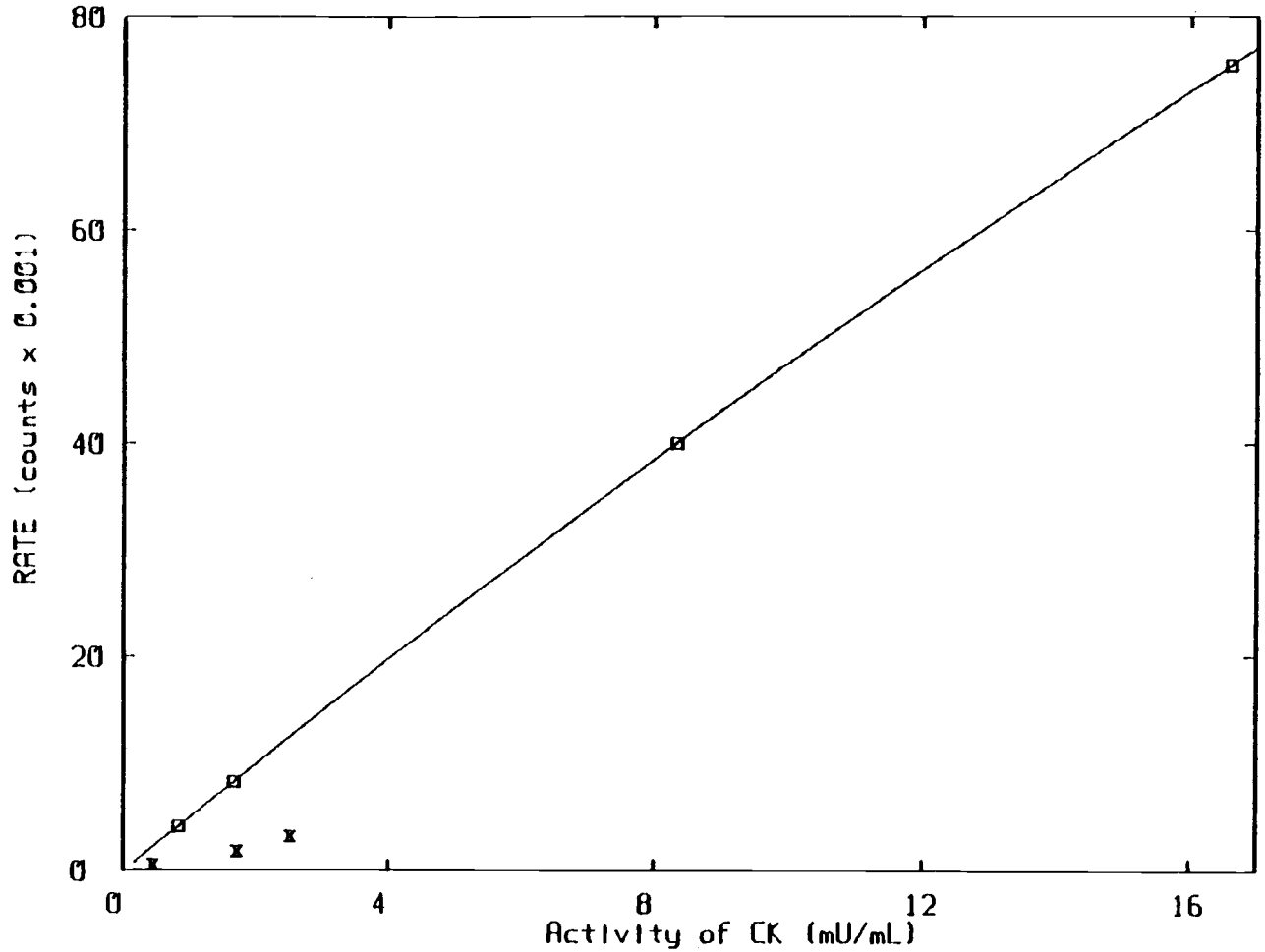

Figure 17. Calibration curve for the CK assay. □) Rabbit-muscle CK standards, ⧗) 1 to 160 dilutions in-cell, of Q-PAK Serum I, Q-PAK Serum II and Enzatrol (lowest to highest, respectively). The reported activities are in-cell activities. Other concentrations = 0.33 mM ADP, 10 mM PO_4-creatine, 10 mM glucose, 2 mM NAD^+, 2.4 U/mL HK and 2.0 U/mL G-6-PDH (in-cell).

A delay time of 20 s was needed to allow the observed reaction rate to reach a maximum. This is a significant improvement over the 40 s delay required when using the commercial reagent. This change is due to the factor of 3 increase in the activities of HK and G-6-PDH in the optimized reagent.

Other improvements over the commercial reagent are also apparent. The slope of the calibration curve has increased by a factor of 3 for the optimized assay and a decrease was seen in the blank signal and subsequent noise level. The greater slope was due to an increase in CK activity at pH 6.5 and use of a better activating agent, monothioglycerol. This observation is confirmed in reference 119 where the observed CK activity is increased by over a factor of 2 as compared to the Abbott reagent kit.

The lower blank signal was due to using a lower concentration and possibly better quality ADP in the reagent. The increased activity and lower blank noise helped to improve the detection limit by nearly a factor of 4.

The average concentration of NADH produced during measurement at the detection limit was calculated to be 0.025 μM. For comparison, the theoretical detection limit of NADH in this reagent blank would be 0.017 μM when using a 16 s measurement time. These two values are close enough to conclude that the ability to detect CK activity is limited by the detectability of NADH.

The upper limit of linearity for CK using this assay was measured to be 29 mU/mL in-cell. This value was estimated using a

calibration curve which included two, more concentrated standards not shown in Figure 17. Calculations estimate that the concentration of NADH by the middle of a 16 s measurement of 29 mU/mL CK would be 10 μM. This would correspond to a decrease of 3% in the ADP concentration and thereby reduce the reaction rate by approximately 3%. At 10 μM of NADH, there would be a 2% decrease from linearity for NADH fluorescence measurements. These two factors combined should account for the 5% non-linearity at 29 mU/mL of CK.

In addition to measuring the rabbit-muscle CK standards for the calibration curve, 3 different serum standards (diluted 1 to 160, in-cell were also assayed using the same conditions. The results of those measurements are included in Figure 17. Using those results the slope of a calibration curve and detection limit for the serum standards were calculated.

Slope of Calibration Curve (counts per U/mL in cell)	=	1.2×10^6
SD of Serum Blank Measurements (counts)	=	790
Theoretical Detection Limit (mU/mL, in cell)	=	1.3

As can be observed from the values of the slopes of the two calibration curves, there is a factor of 4 difference in the measured activities of the rabbit-muscle CK standards and those of the serum standards. Calculations made using the chart recordings of both types of standards show that the activities of the serum standards are much closer to what would be predicted by the Michaelis-Menton equation.

Several factors could have caused this discrepency in the observed rate of the two different CK standards. It is possible that the CK enzyme derived from rabbit muscle is affected differently by the optimized reaction conditions than was the CK present in the serum standards. In other words, the conditions used by the manufacturer to measure the activity of the rabbit-muscle enzyme may have been significantly different than the conditions used in the optimized assay. This would result in a large underestimate of the activity per unit weight of the commercial enzyme, thus causing the activity of the rabbit muscle standards to be higher than expected. In contrast, the assay conditions used to measure CK activity in the serum standards, as described by the supplier, are a close match to those used in the optimized system. It was concluded that the CK activities of the serum standards are a better match to the expected activities found in fresh serum samples. The values of the slope and the detection limit calculated for the serum standards are therefore more valid than those for the rabbit-muscle enzyme standards.

Since no serum standards were available with CK activities high enough to measure the upper limit of linearity, this value was estimated using the results of the assays of the rabbit-muscle enzyme standards. Since the relative activity of serum standards is a factor of 4 lower it can be estimated that the upper limit of linearity should be a factor of 4 higher than that for the rabbit-muscle standards. This would result in an upper limit of linearity

of 120 mU/mL, in-cell, for CK in serum and a range of linearity extending from 1.3 to 120 mU/mL.

The normal range of CK activity in undiluted serum is 12 to 65 mU/mL(15). If a dilution of 1 to 150 must be used to eliminate spectral interference, the resulting concentrations will be 0.08 and 0.43 mU/mL, which are both below the theoretical detection limit. It can therefore be concluded that since such large dilutions are required to eliminate spectral interference of NADH that this method of measuring CK activity may not be practical.

To lower the detection limit for CK in serum, it will be necessary to increase the measurement time. A measurement time of over 3 minutes would be required to obtain a detection limit for CK which was less than 0.1 mU/mL. Such long measurement periods mean that there is no significant advantage to using this fluorescence method compared to the absorbance method which requires measurement times on the order of 4 minutes (15). Other options for lowering the detection limit of the fluorescence method are to use higher purity ADP and in some way eliminate the interference without using such large dilutions of the sample. The use of a fluorophore with greater fluorescence signal and which is less affected by serum interference than NADH would also improve the detection limit for CK.

Resorufin Fluorescence Studies

Since NADH has a quantum efficiency of about 2%, a fluorophore with higher quantum efficiency could provide better detection limits

for enzymatic assays involving fluorometric monitoring. A fluorescent species known as resorufin has been used for the analysis of bile acids in biological samples (70,71). One of the first uses of the resazurin to resorufin reaction was found in reference 68 for the kinetic assay of dehydrogenases. The advantage of coupling this reaction to assays which produce NADH is that resorufin is a more fluorescent species and its optimum excitation and emission wavelengths (550 nm and 580 nm, respectively) are well above the wavelength region of serum spectral interferences. Since the reaction utilizes NADH, it can potentially be coupled to any system which produces NADH as the final product. This reaction is catalyzed by an enzyme known as diaphorase which will oxidize NADH or NADPH to NAD^+ or $NADP^+$ in the presence of an electron acceptor. In this application resazurin is serving as the electron acceptor as shown below.

$$H^+ + \text{resazurin} + NADH \xleftarrow{\text{Diaphorase}} NAD^+ + \text{resorufin} + H_2O$$

The K_m value of the diaphorase enzyme is 90 µM for NADH. No literature value of K_m for resazurin could be found so a study was made to observe the effects of changing the resazurin concentration on the rate of formation of resorufin (increase in fluorescence). The level of resazurin was increased from 0.05 to 10 µM, in-cell, which resulted in proportional increases in the rate of formation. This would indicate that the K_m for resazurin was at a concentration above 10 µM.

In the forward direction the diaphorase reaction is thermodynamically favorable so a high percent yield of resorufin is obtained.

Reagent grade resorufin was not available commercially so spectral studies were done on resorufin in a reaction mixture which had come to equilibrium. An excess of NADH was added to the mixture since NADH showed no fluorescence or absorbance in the spectral region of optimum resorufin fluorescence. Initial studies with this solution involved taking excitation and emission spectra for the selection of optimum excitation and emission wavelengths (see Figures 18 & 19). Wavelengths of 550 and 580 nm were chosen as optimum for the excitation and emission settings, respectively. A calibration curve was made and the results are shown in Table XXII along with the results of a similar study done on NADH. Absorbance measurements were made in a similar manner and the resulting molar absorptivities for resorufin were 2.3×10^4 and 2.5×10^4 L/cm mol at 550 and 580 nm, respectively.

Comparing the measurements of the PMT dark current for both the NADH system and the resorufin system shows that a much larger signal is obtained with the resorufin system. This is due to the divider circuitry responding to the factor of 5 decrease in intensity of the excitation beam at 550 nm as compared to that for 366 nm. The undivided PMT dark current is independent of the excitation beam but when connected to the divider the measured dark current will change according to differences in the excitation beam intensity. This

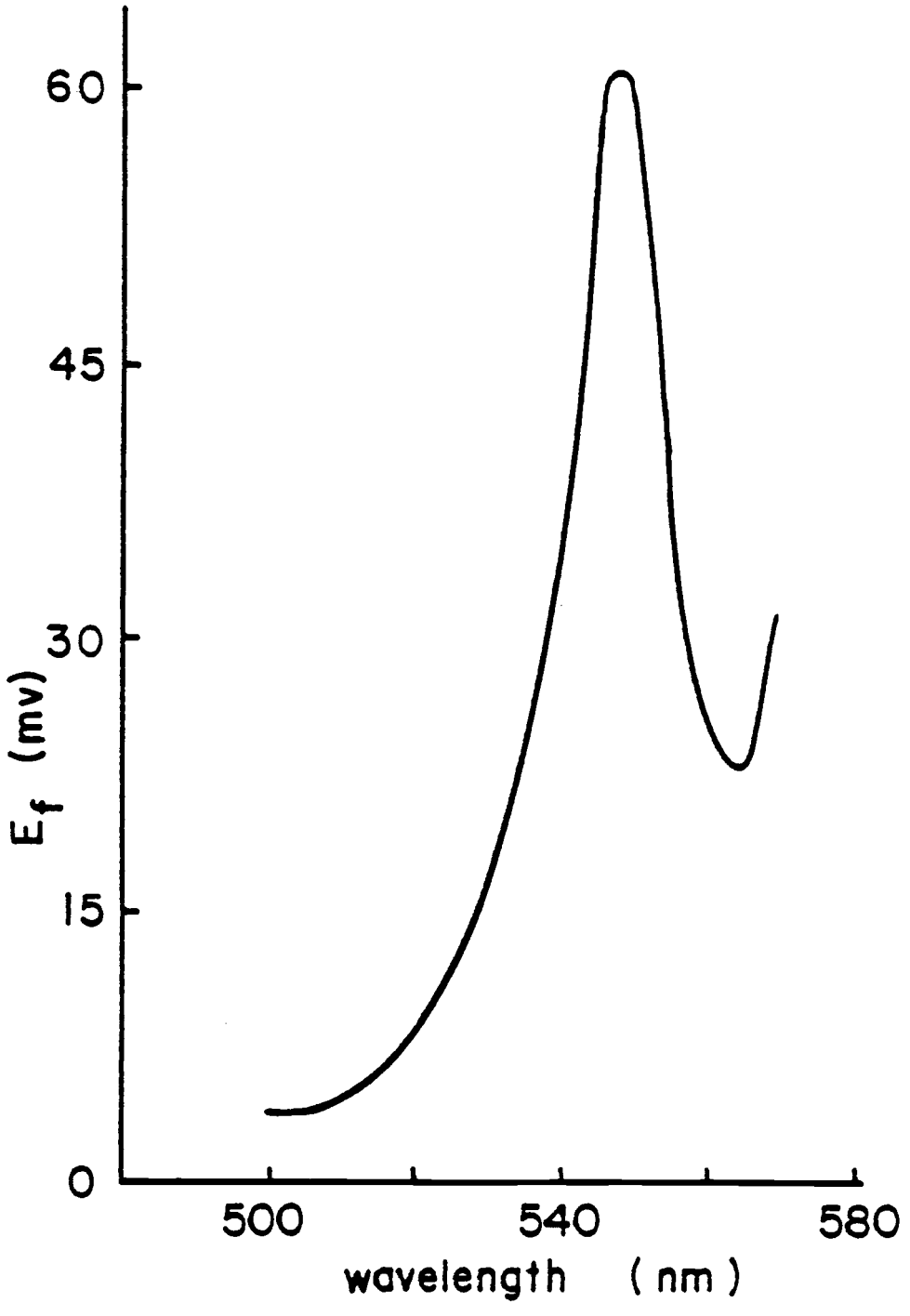

Figure 18. Fluorescence excitation spectrum for resorufin. Resorufin concentration, in-cell, is 0.043 μM. Emission wavelength set at 580 nm.

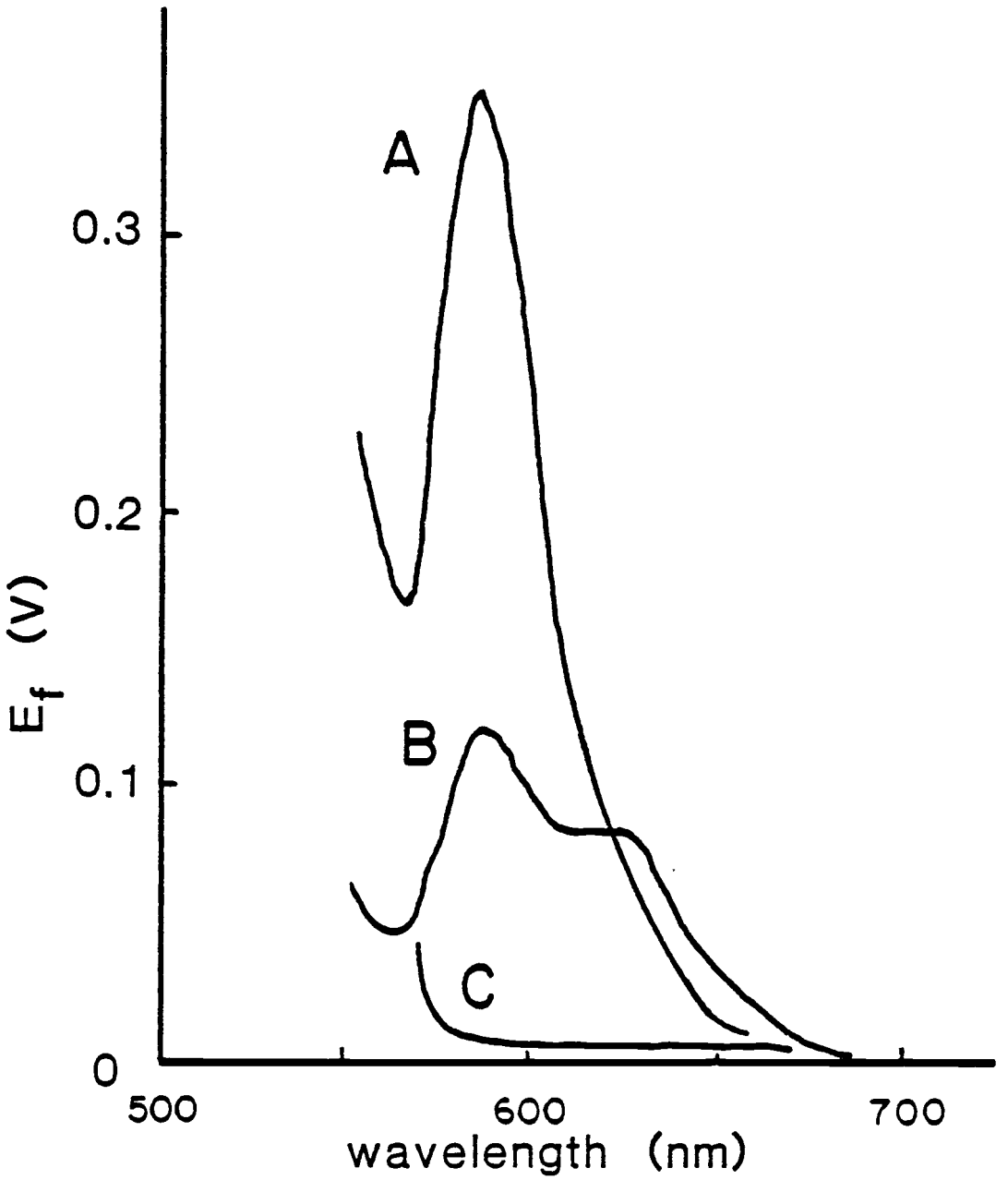

Figure 19. Fluorescence emission spectra. A) 0.043 µM resorufin, B) 0.5 µM resazurin, C) 1 to 90 dilution, in-cell, of Q-PAK Serum II. Excitation wavelength set at 550 nm.

Table XXII

Comparison of NADH and Resorufin as Fluorophores[a]

Parameter	NADH	Resorufin
Slope of Calibration Curve (counts per μM in-cell, 8 s MT)	6.3×10^{4}	2.4×10^{7}
Steady-state Measurement of Tris Buffer (counts)	5800	29,900
SD of the Buffer Signal (counts)	57	304
Theoretical Detection Limit in Tris Buffer (μM, in-cell)	2×10^{-3}	3×10^{-5}
Theoretical Detection Limit in a 1 to 90 Dilution of a Serum Standard (μM)	2×10^{-2}	5×10^{-5}
Upper Limit of Linearity (-5% deviation, μM)	25	1.4
PMT Dark Current Signal (8 s MT, counts)	4440	25,026
SD of Dark Current Signal (counts)	45	249

[a] C_f and R_f for all measurements are 0.1 μF and 10 MΩ, respectively. [f] PMT voltage set at 800 V.

effect causes the measured values of both the dark current and the net fluorescence of the buffer blank (Tris buffer in the cell) to be a factor of 5 higher for the resorufin system than for the NADH system. Along with higher signal levels when using the resorufin system, the noise in the dark current and buffer blank have also been magnified by about a factor of five.

The higher quantum efficiency and molar absorptivity of resorufin make up for the reduced intensity of the 550 nm excitation beam, thereby resulting in a much higher value for the slope of the calibration curve for resorufin. This more than compensates for the increased noise level of the blank, thus the theoretical detection limit for resorufin is 60 times lower than that for NADH (see Table XXII).

Fluorometric measurements of resazurin solutions using the optimum conditions for resorufin monitoring show nearly 4% of the fluorescence expected for an equal concentration of resorufin. This causes a large increase in the blank fluorescence signal when resazurin is added to the buffer solution. For a 1 μM solution of resazurin the net 8 s signal would be 9.7×10^5 counts as compared to 3×10^4 counts for the buffer. The SD of the signal from the 1 μM resazurin solution was 1440 counts as compared to 304 counts for the SD of buffer measurements. The detection limit of resorufin in a reaction mixture will therefore depend on the concentration of resazurin in the reagent.

The two maxima shown in the emission spectra of resazurin (see Figure 19) indicate that there is significant contamination of resazurin with resorufin. This fact has been confirmed by the manufacturer of resazurin (Eastman Kodak Co.). Higher purity resazurin would show a reduced fluorescence signal at 580 nm which will reduce the noise level of the blank and thereby improve the detection limit. Higher purity resazurin was not available commercially at the time these studies were conducted.

The upper limit of linearity (-5% deviation) for the resorufin calibration curve can be estimated by calculating the pre- and post-filter effects of μM concentrations of resorufin. The excitation and emission slits mounted on the cell holder are 2 mm and 5 mm, respectively. The resulting path length of excitation radiation passing through solution before entering the viewed volume is 0.25 cm and the path length of emission radiation leaving the viewed volume is 0.4 cm. For a 5% attenuation of fluorescence the combined absorbance for these two regions must be approximately 0.0223. The resorufin concentration (X) which would give a combined absorbance of 0.0223 was calculated to be 1.4 μM using the following equation:

$$X = 0.0223/((0.25\ cm \times 2.3 \times 10^4\ L/mol\text{-}cm)+(0.4\ cm \times 2.5 \times 10^4\ L/mol\text{-}cm))$$

The highest concentration of resorufin tested was 0.43 μM which showed less than 3% non-linearity.

The use of resorufin as a fluorophore eliminates many of the spectral interference problems encountered when making fluorometric measurements of NADH in a serum matrix. The blank fluorescence from

serum when exciting at 550 nm is insignificant in comparison to the serum fluorescence signals obtained with a 366 nm excitation wavelength. Figure 19 shows the emission spectrum of a 1 to 90 dilution of Q-PAK Serum II. The level of serum fluorescence is only slightly higher than the buffer fluorescence signal at 580 nm. The detection limit for resorufin therefore does not increase significantly when making measurements in a serum matrix.

A study was made of the pre- and post-filter effects seen when measuring the fluorescence of resorufin in various dilutions of serum standards. Even though the major components of serum show very little absorbance above 530 nm, particulates found in reconstituted serum standards cause significant scattering which attenuates both the emission and excitation radiation (see absorption spectra of serum standards, Figure 9). These effects are less than that from the absorption of serum proteins and bilirubin at 366 and 468 nm but are still significant. A diluton of 1 to 60 is required to lower the attenuation of resorufin fluorescence by Q-PAK Serum II to 3% compared to a dilution of 1 to 180 for a 3% attenuation of NADH fluorescence. Serum II could be considered a worst case situation since fresh serum should not contain the same amount of particulates, and therefore scattering should be greatly reduced.

Studies of the conversion of resazurin to resorufin showed that the order of addition of the reagents to the cell affected the equilibrium fluorescence level. It was discovered that a blank reaction was proceeding when NADH and diaphorase are combined. The

diaphorase is catalyzing a reaction which is oxidizing NADH even in the absence of resazurin. Since no other species were present to accept electrons the reaction must be reducing oxygen to hydrogen peroxide. The data sheet which was sent with the diaphorase states that a small level of NADH oxidase activity (0.7% of the diaphorase activity) is present. The reaction catalyzed by NADH oxidase is shown below:

$$H^+ + NADH + O_2 \xleftrightarrow{\text{NADH oxidase}} NAD^+ + H_2O_2$$

Under the conditions of these experiments, the concentration of dissolved oxygen in the buffer solution is estimated to be 0.1 mM. This is several orders of magnitude greater than the typical concentrations of resazurin (10^{-6} M) therefore the NADH oxidase activity is much more significant than 0.7% of the maximum diaphorase activity. Kinetic measurements of NADH show that the activity of NADH oxidase (negative rate observed when NADH and diaphorase are mixed) is about equal to the observed diaphorase activity (difference between negative rates measured with and without resazurin in the reaction mixture) when the resazurin concentration is 0.5 μM. By increasing the resazurin concentration to 5 μM, the ratio of the diaphorase rate to the NADH oxidase rate increases to 10 to 1. Both reactions appear to be first order with respect to NADH within the range of 0.004 to 0.2 μM NADH when 5 μM resazurin is used. Since both reactions are first order with respect to NADH, the NADH oxidase activity will not cause errors in rate measurements of NADH or NADH-

producing reactions but would reduce the sensitivity of the measurement method.

The effect of using different buffers with the diaphorase system was studied to see if this reaction could be coupled to all the NADH-producing assays described earlier. Four different buffers were tested (BIS-TRIS, Tris, MES and phosphate) all at pH 7.5. Tris, MES and phosphate buffers all showed equivalent results in terms of diaphorase activity and equilibrium fluorescence signals from equal concentrations of resorufin. The use of BIS-TRIS buffer resulted in very erratic reaction rates and very high blank fluorescence signals. It was also noted that the stock solution of resazurin made up in BIS-TRIS had changed color. It was concluded that BIS-TRIS (bis [2-Hydroxyethyl] amino-tris-[hydroxymethyl] methane) must react with resazurin and is therefore not suitable for use in assays coupled to the diaphorase reaction.

A study was made of using other reagents in place of diaphorase to catalyze the conversion of resazurin to resorufin in hopes of eliminating the NADH oxidase reaction. Reference 120 reports the use of a variety of compounds which serve as electron carriers for the reduction of tetrazolium salts by NADH. Phenazine methosulfate (PMS) was reported to be a good substitute for diaphorase in this type of reaction. An experiment was conducted where diaphorase was replaced by PMS for the reduction of resazurin to resorufin. The results showed that PMS successfully catalyzes the formation of resorufin but it also catalyzes a reaction similar to that of NADH oxidase. The

ratio of the diaphorase reaction rate to the NADH oxidase rate for the diaphorase enzyme was nearly equal to the ratio of the equivalent reaction rates for PMS under identical conditions. It appears there is no benefit in using PMS rather than diaphorase to catalyze this reaction.

Coupling the Diaphorase System to the CK Assay

In order to test the use of fluorometric measurements of resorufin for kinetic monitoring of serum assays, the diaphorase system was coupled to the CK assay. The CK assay system which was used for NADH fluorescence monitoring had to be modified before being coupled with the resazurin-resorufin reaction. MES buffer had to be substituted for BIS-TRIS since it was observed that resazurin reacts with the latter. The concentration of ADP had to be decreased since the concentration of NADH resulting from the ATP contamination of ADP would cause an unacceptable blank signal when coupled to the diaphorase system. The decreased ADP concentration will reduce the activity of the CK enzyme such that a compromise must be made between CK activity and the noise level of the blank. An in-cell concentration of 0.05 mM ADP was selected as optimum since it offered the highest rate to blank noise ratio.

The results of the assay are shown in the calibration curve in Figure 20 and are listed below:

	C-3755 Standards	Serum Standards
SD of Blank Measurements (counts)	778	767
Slope of Calibration Curve (counts per U/mL, in-cell)	6.2×10^7	1.7×10^7
Theoretical Detection Limit (mU/mL, in-cell)	0.025	0.09
Upper Limit of Linearity (5% deviation)(mU/mL in cell) (estimated from calibration curve)	0.6	Not measured

The maximum rate was observed in the 2nd 16 s measurement period but it was also observed that the first 16 s measurement period would provide a higher upper limit of linearity and faster total measurement times. It should be possible to reduce the lag time by increasing the activity of the coupling enzymes (hexokinase and G-6-PDH).

The reduced concentration of ADP (0.05 mM) would lower the observed CK activity to 0.06 times V_{max}, according to calculations using the Michaelis-Menton equation. The reaction rates of the serum standards show an actual rate (calculated from the chart recordings) of 0.09 times their maximum reported CK activities while the standards made with CK from rabbit-muscle showed 0.37 times the expected maximum activity. This is consistent with the results of CK analysis using NADH fluorescence monitoring where the rabbit-muscle enzyme standard showed 4 times more activity than would be predicted.

The blank fluorescence level for this system is produced primarily by the fluorescence from resazurin and the resorufin

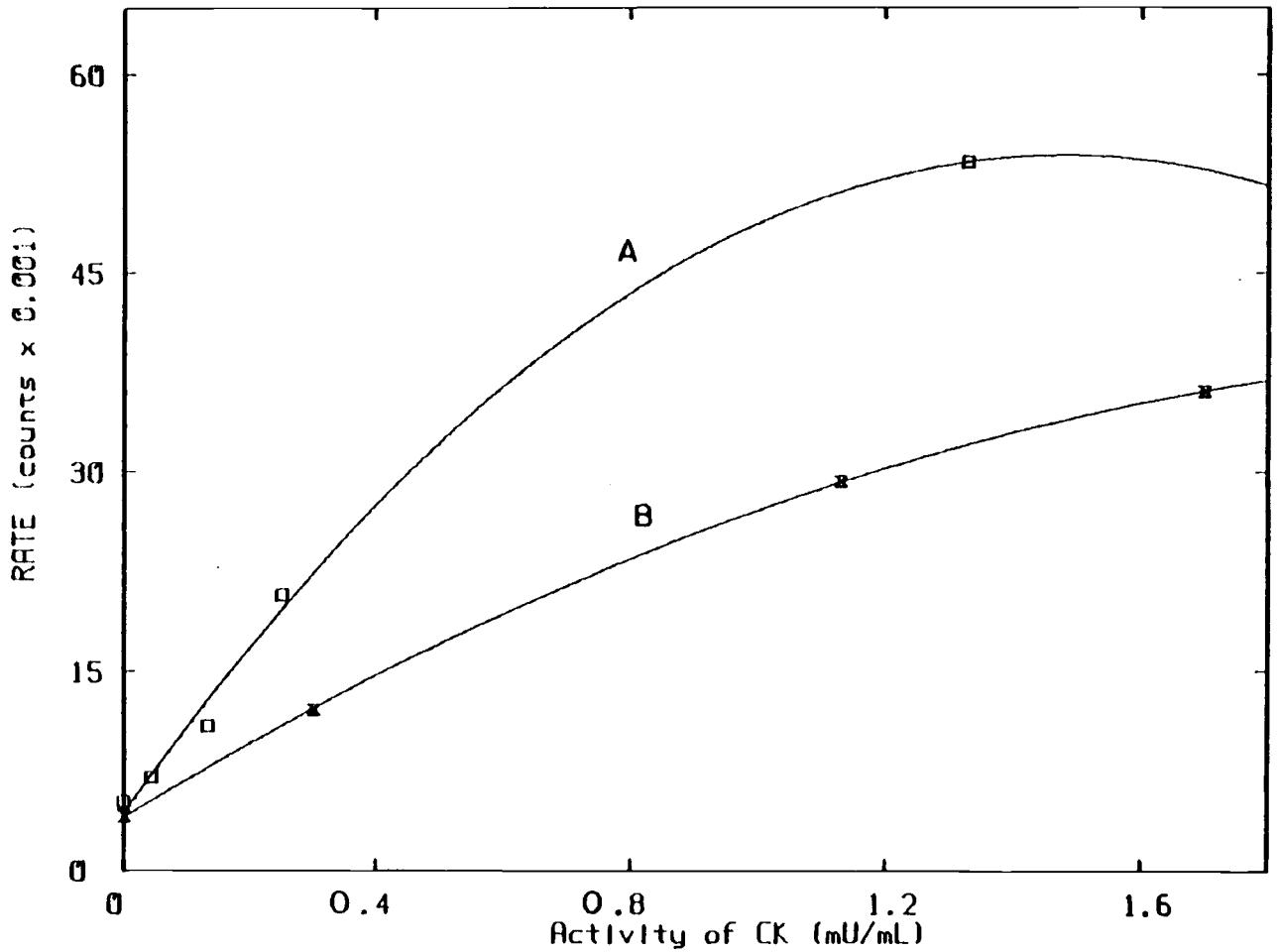

Figure 20. Calibration curves for the CK assay using resorufin monitoring. A) Rabbit-muscle standards, B) 1 to 180 dilutions, in-cell,of Q-PAK Serum I, Q-PAK Serum II and Enzatrol (lowest to highest activities, respectively). The reported CK levels are the in-cell activities.

generated by NADH from the ATP contamination. The noise level of the blank is unaffected by the addition of a serum sample since the fluorescence signal of serum is insignificant when exciting at 550 nm. The difference in detection limits between the serum standards and the rabbit-muscle CK stanadards is due to the difference in observed activity levels (slope of the calibration curves) rather than a change in the blank noise level. Comparing the detection limit for serum standards when monitoring NADH fluorescence (1.3 mU/mL in-cell) to the detection limit for resorufin fluorescence monitoring (0.09 mU/mL, in-cell) shows the significant improvement in sensitivity when using the resorufin method. As already noted, resorufin is less sensitive to the pre- and post-filter effects of serum, therefore only a 1 to 60 dilution in-cell is required, which is 3 times less than the dilution needed for NADH monitoring. With resorufin monitoring, the expected range of CK activity in the cell will be 0.2 to 1.08 mU/mL for assays of normal serum. These values are above the detection limit (0.09 mU/mL) which is a significant improvement over what was observed for NADH monitored assays.

Calculations were made using the chart recordings from the calibration runs to find the factor controlling the upper limit of linearity. At the observed upper limit of linearity (0.6 mU/mL of rabbit-muscle enzyme), the concentration of resorufin produced by the middle of the measurement period was estimated to be 0.033 μM. The formation of 0.033 μM resorufin would be equivalent to a decrease of 6% in the concentration of resazurin. It can be shown that this

change in the resazurin concentration would be responsible for the 5% non-linearity.

The CK concentration of the serum standards was not high enough to test the upper limit of linearity but an estimate can be made by using the results of the rabbit-muscle CK standards. The activity of serum CK is a factor of 4 less than that for the rabbit-muscle standards so it can be assumed that 4 times as much serum CK will be needed to cause the 5% non-linearity. The upper limit of linearity for serum CK should be near 2.4 mU/mL.

Since resazurin contributes a large fraction of the blank fluorescence even at a concentration of 0.5 μM it will not be possible to increase the upper limit of linearity without a proportional increase in the blank noise and therefore a higher detection limit. In order to improve the dynamic range of this technique the fluorescence of resazurin must be reduced. Perhaps the fluorescence level of resazurin could be reduced via a clean-up procedure to remove the resorufin.

A blank reaction is observed when the albumin-monothioglycerol solution is used for blank measurements. Initial experiments showed that the blank reaction was not present when the coupling enzyme solution was replaced with buffer. It was concluded that something present in the albumin-monothioglycerol solution was reacting via the coupling reactions to produce NADH which in turn was oxidized to form resorufin. Further studies were not done to more fully isolate the source of the blank reaction. This same reaction was probably

present in the NADH-monitored CK assay but the activity level of the blank reaction (equivalent to 0.07 mU/mL of rabbit-muscle CK) would have been below the detection limit for rabbit-muscle CK, 0.24 mU/mL. The blank reaction causes a non-zero Y-intercept in the calibration curve but does not appear to effect the linearity of the curve.

The SD of measurements of the blank reaction was 778 counts (the value reported on p. 155) while the SD of the reagents without the albumin-monothioglycerol solution gave an SD of 650 counts. This difference is not significant enough to state that the blank reaction has a major effect on noise level and the detection limit. The blank reaction rate could be minimized by reducing the amount of the albumin-monothioglycerol solution added to the final reaction mixture. This was not studied nor the effect this might have on CK activity since monothioglycerol is used as the activating agent for CK.

Optimization and Performance of the FIA Fluorometer

Introduction

The remainder of the Results and Discussion section will deal with the characteristics and performance of the FIA fluorometer. The results from the initial studies of the fundamental operating parameters (flow rate, delay times, etc.) will be presented first. The performance of the flow cell itself will be discussed next followed by the application of this system to the kinetic assay of ethanol. The ethanol system was studied in detail to determine optimum operating conditions and the performance of the FIA system for kinetic methods in general. The fluorometric assay for CK was also adapted to this system. The last part of this discussion will briefly describe the operation and performance of this system when a 3rd injection loop was included.

Initial Studies

The first studies conducted with the FIA fluorometer were to learn about the basic operating parameters of the system. Variables such as delay times, flow rates, tubing diameters and modes of measurement can each affect the performance of the system. The initial studies were made using injections of a fluorophore (NADH) to generate the signals by which the optimizations were made. The discussion of these initial results will be in the order of events of a typical run. First, those factors that effect sampling and injecting will be discussed followed

by a discussion of the delivery of the injected plugs of solution to the flow cell. The last part of the initial studies section will deal with the two modes used to measure the injected plugs once they have arrived at the flow cell.

Conducting these initial studies showed that the optimum setting for many parameters depended on the mode of operation of the system. There are basically two different modes of operation for this system, the stopped-flow mode and the continuous-flow mode. These two modes correspond to two different approaches to making kinetic measurements. Refer to the Experimental section, p. 77 for a description of these two operations. The following discussion of optimum parameters will discuss both modes of operation, when applicable.

The first operation of the system during a typical FIA run is to enter an initial delay period to allow for sufficient rinse-out of the flow cell between runs. This period is also needed for the pumps to reach their maximum flow rate since the pumps are started slowly and are accelerated up to the desired flow rate during a 15 s time period. This delay for pump acceleration is not needed for continuous-run modes except for the first run. Part of the time required for cell rinse-out and pump acceleration can be included in the sampling period. The initial delay period therefore need only be long enough to make up the difference between the sampling time and the start up time. For most of the studies described in this section, the initial delay was set at 20 s to insure complete rinse-out and full flow rates even for very short sampling times.

Optimization of Injections

Proper filling of the injection loops and optimum performance of the injector depend on several factors. For optimum filling of the injection loops, 2 to 3 loop volumes of solution should have been drawn through the loops. This is achieved by adjusting both the sampling delay period and the withdrawal rate of the vacuum system. A withdrawal flow rate of 8 to 9 mL/min was the fastest rate usable without causing air to leak into the withdrawal stream. At this withdrawal rate a 15 s sampling time was needed to properly fill a 600 µL injection loop.

In order to get the maximum signal levels from plugs of solution injected into the carrier stream, it is important to minimize the dispersion of the plugs. It was therefore necessary to keep the dispersion caused by the injection itself at a minimum. The diameter of tubing and the volume of the loop used for the injector, can affect the dispersion of injected plugs. It was observed that an injection loop made of 1.5 mm i.d. tubing showed measureably more dispersion upon arrival at the flow cell than an equal volume loop made of 0.5 mm i.d. tubing. The disadvantage of using tubing of 0.5 mm i.d. or less is that flow restriction and pressure drop become significant. The observed filling rate of large volume loops (less than 400 µL) made of 0.5 i.d. tubing was slower by a factor of 2 or 3 as compared to 1.5 mm i.d. loops when using samples of high viscosity such as serum or protein solutions. As would be expected, the volume of the injection loop affects the observed dispersion of the plug. Figure 21 shows that loop volumes greater than 400 µL show no measurable dispersion or

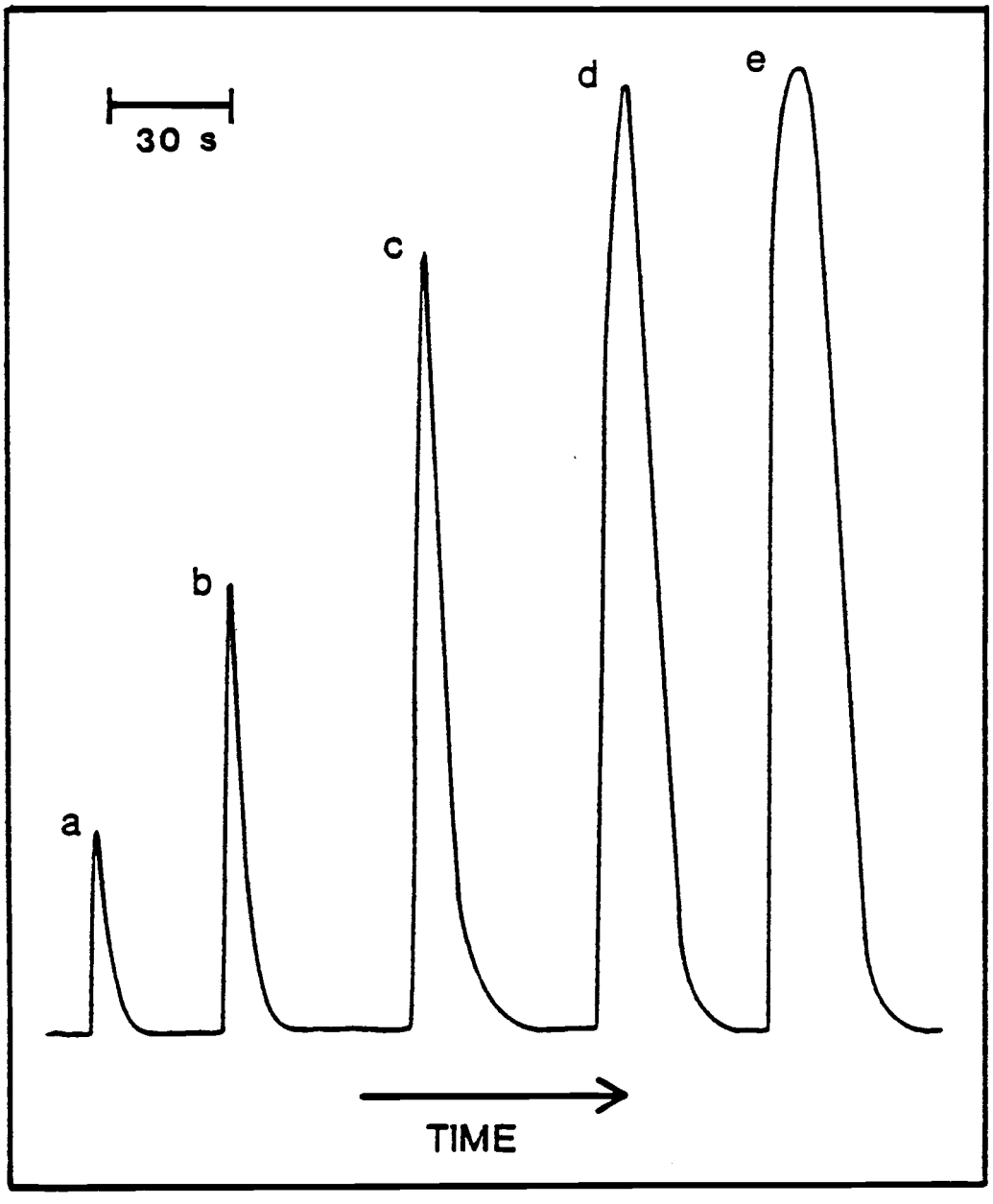

Figure 21. Effect of sample loop volume on peak shape. a) 29 µL, b) 78 µL, c) 180 µL, d) 400 µL, e) 550 µL. All injections were made using 12 µM NADH via the sample injection valve. H_2O in the reagent loop. Both pumps were set to 2.0 mL/min. Chart rate = 2 in/min, RC time constant = 0.1 s.

dilution at the center of the plug. The width of the undiluted region in the center of the plug increases with increasing loop volume.

Dispersion of the injected plugs upon arrival at the flow cell affects both stopped-flow and continuous-flow methods. As noted in Figure 21, the peak profiles for large volume loops are more bell-shaped as compared to the sharp peaks observed for small volume loops. Besides the obvious effect on signal levels, dispersion will also affect the run to run precision of both stopped-flow and continuous-flow measurements. For stopped-flow measurements there is always some deviation from run to run in the exact position on the plug within the flow cell. When stopping at the center of a large volume plug, this deviation in position has much less effect on the final concentrations of the sample and reagent in the cell. In contrast a small volume plug will be more sensitive to deviations in the stopping point since dispersion has made the concentration profile of the plug much sharper. This means that for small volume plugs (less than 180 µL) a small change in position along the axis of the plug, even near the center, will cause a significant change in the observed concentration of the injected solution. This difference between large volume and small volume plugs of 12 µM NADH can be seen in the example shown below:

Sample Loop Volume (µL)	RSD of Repetitive Stopped-Flow Measurements (12 runs)
78	3.1 %
550	0.84%

The precision of repetitive runs using a continuous-flow method will also be affected by the volume of the injected plug. For the continuous-flow methods used with this FIA system, measurements were

made by integrating a portion of the area of the peak generated by the passage of the plugs through the flow cell. The integration period normally used was 8 s which was centered around the peak maximum. The effect of different injection loop volumes on the RSD of repetitive, continuous-flow measurements is shown in the following example.

Sample Loop Volume (μL)	RSD of Repetitive Stopped-Flow Measurements (12 runs)
78	0.65%
180	1.1 %
550	0.33%

For small volumes (less than 78 μL) the run to run precision is good because nearly all of the plug passes through the flow cell during the measurement period. A small portion of the extended tail of the plug is the only part of the peak outside of the integration region. Since nearly all of the plug is measured, any variations in diffusion from run to run are averaged out over the measurement period. With the 180 μL sample loop, the run to run precision is worse because now a significant portion of the plug passes through the flow cell outside of the integration period. The volume of the loop is still small enough that significant dispersion occurs at the center portion of the plug where the measurement is made. Variations in the dispersion from run to run will therefore cause noticeable deviations in the value of the integration. Large volume loops (greater than 500 μL) show much lower run to run RSDs since the integration period is contained within the larger center region of the plug which is much less affected by dispersion.

The optimum loop volume and tubing diameter for the injectors was chosen to be 550 to 600 μL with an internal diameter of 1.5 mm. This loop proved to be unaffected by changes in viscosity of the sample or reagent therefore no errors would occur due to changes in the withdrawal flow rate for viscous solutions. The choice of this loop size was a compromise between minimal dispersion and minimal solution consumption. For both stopped-flow and continuous-flow measurements the 550 μL loop gave the greatest run to run precision.

Optimization of the Carrier Stream

After injection, the plugs of sample and reagent are merged and are carried on to the flow cell. During this interval, factors such as flow rate and the dimensions of the tubing can affect the results obtained from both stopped-flow and continuous-flow methods. Both the length and the internal diameter of the tubing between the tee and the flow cell should be minimized in order to minimize dispersion. This section of tubing contains a 4-turn mixing coil, approximately 2 cm in diameter, which maximizes mixing and the equilibration of temperatures while minimizing dispersion (79). The length of this section of tubing (including the mixing coil) must be at least 60 cm in order for the mixing coil to be completely submerged in the water bath while connected to the tee and the flow cell.

Since tubing diameter will effect the dispersion of injected plugs, a comparison was made between the use of 0.5 and 0.3 mm i.d. tubing (the smallest diameters available) between the tee and the flow cell. Figure 22 shows the profiles of peaks obtained from injections

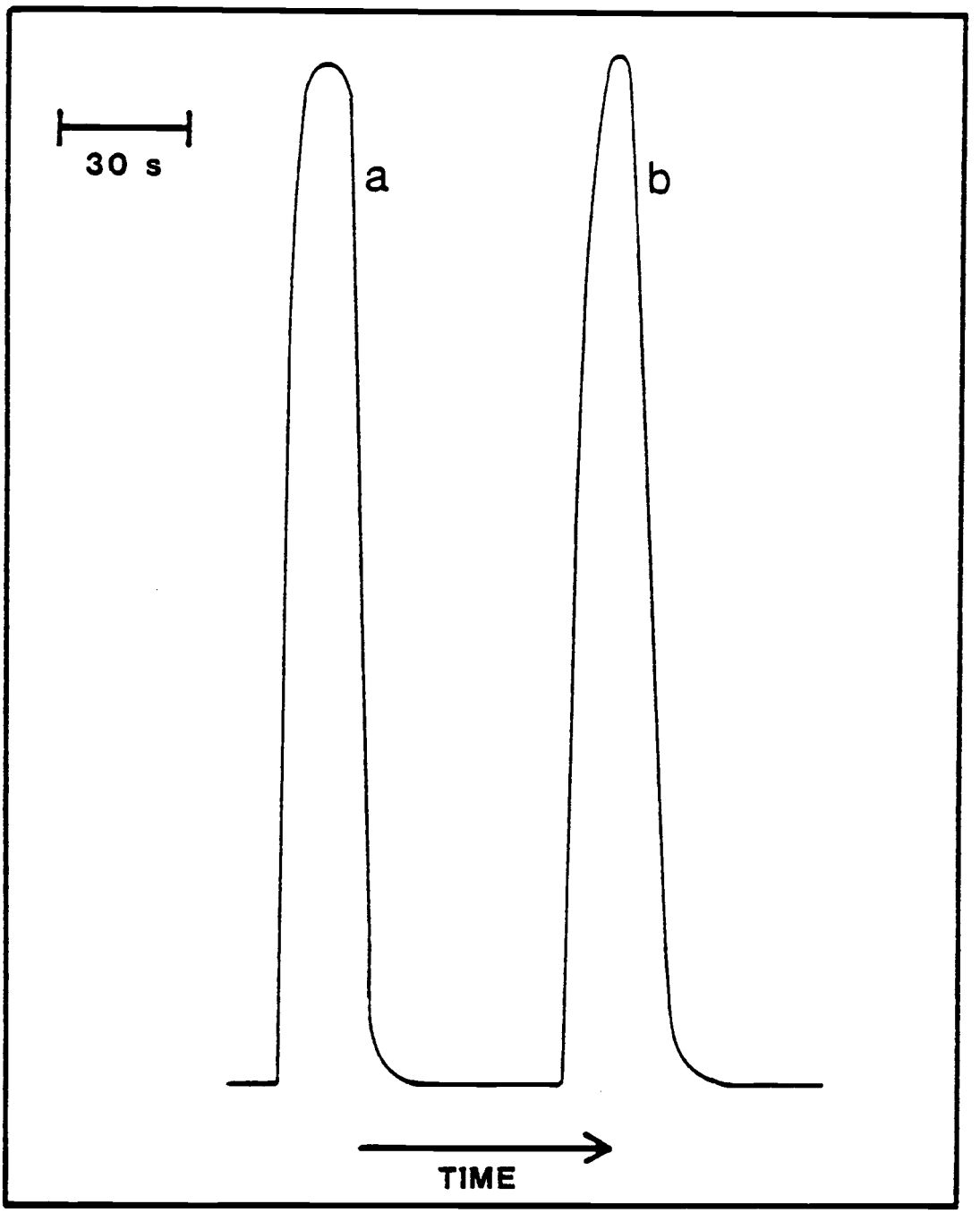

Figure 22. Effect of tubing i.d. between the injectors and the flow cell on dispersion and peak shape. a) 0.3 mm i.d. tubing b) 0.5 mm i.d. tubing. Both were injections of 12 µM NADH using a 550 µL sample loop, H_2O in reagent loop. Both pumps were set to 2.0 mL/min, chart rate = 2 in/min.

of 550 µL of NADH solution. It appears that less dispersion has occurred at the center of the plug when using 0.3 mm i.d. tubing but note that the width of the baseline of the two peaks are nearly equal. The dispersion caused by the poor rinsing efficiency of the flow cell (due to square sample cavity) must be the controlling factor effecting the baseline width of the peaks. For this reason no improvement in throughput would be seen if 0.3 mm i.d. tubing were used rather than 0.5 mm i.d. tubing.

Any improvement observed in the dispersion of the center portions of the injected plugs when using 0.3 mm i.d. tubing is offset by the increase in back pressure. The increased back pressure causes problems when conducting stopped-flow measurements by stopping the pumps. With 0.3 mm i.d. tubing nearly 12 s are required after the pumps have stopped before flow has completely stabilized as compared to less than 6 s when using 0.5 mm i.d. tubing.

Since the advantages of using 0.3 mm i.d. tubing did not outweigh the disadvantages, it was decided to use 0.5 mm i.d. tubing for the connection between the flow cell and the injection valves. An additional advantage of 0.5 mm i.d tubing was that if proved easier for constructing connections and the connections proved more reliable than those for the 0.3 mm i.d. tubing.

Flow Rate Optimization

The selection of the optimum flow rate for this system depends on several factors. It was decided that the mixing ratio of the sample and reagent plugs should be 1 to 2, therefore the flow rates of the two

pumps had to be equal. Since both pumps had been factory calibrated, no further adjustment was necessary except to select the same flow rate for both.

For both stopped-flow and continuous-flow methods the dispersion of the merged plug should be minimized. The effects of different flow rates on the observed dispersion of injected plugs of NADH were studied. For flow rates between 0.4 and 1.6 mL/min per pump (combined flow rates of 0.8 and 3.2 mL/min), no significant change was seen in the observed dispersion. Dispersion was judged by measuring the baseline of peaks. If dispersion is constant for a range of different flow rates the peak baseline widths will be inversely proportional to the flow rate (faster flow rate = shorter residence time = shorter baseline). Above 1.6 mL/min per pump the baseline width was no longer decreasing proportionally with increases in flow rate. It was concluded that for this system, dispersion was independent of flow rate from 0.8 to 2.0 mL/min per pump. Reference 78 reports that for systems such as this one that dispersion is a function of $F^{-0.64}$ where F is the flow rate in mL/min. Theoretically the observed dispersion should change by a factor of 1.8 between 0.8 and 2.0 mL/min. Since this was not observed, it was concluded that other factors such as the rinsing efficiency of the flow cell or dispersion caused by the various connections in the system were dominant over the effects of changing flow rate on dispersion.

Another factor in the operation of this system that is affected by flow rate is the rinse-out time of the flow cell following the end of the measurement period. The time required for the signal level to return to the baseline after the measurement was studied using a

stopped-flow method. Stopped-flow measurements were made on injections of 550 μL of 12 μM NADH solution stopped at the center of the plug. For a 0.8 mL/min flow rate (per pump) the time required between re-starting the flow and the return to baseline was 30 s. At 3.6 mL/min per pump, the time to return to baseline took 14 s. Since the rinse-out time was not directly proportional to the flow rate (i.e. residence time of the remainder of the plug in the flow cell) it was concluded that the rinsing efficiency of the flow cell was significantly affecting the rinse-out time.

For stopped-flow methods the time required for the plug to stabilize in the flow cell after pumps have stopped depends on the flow rate. Movement of the plug in the cell after pumps are halted can be observed on the chart recording. At 0.8 mL/min per pump, flow within the cell has completely stopped 4 s after pumps are halted, while at 3.6 mL/min, complete stoppage is not achieved until 11 s after the pumps halt. The higher back pressures generated at faster flow rates require longer delays in order to reach equilibrium.

Delay periods less than 2 s are adequate to allow the signal levels to stabilize when using the bypass loop to stop flow.

For stopped-flow methods using pump stoppage to halt flow, a 2.0 mL/min flow rate per pump was selected as optimum. This flow rate provides reasonably fast delivery of the merged plug to the flow cell (6 s) while allowing quick stopping times (less than 6 s) and a 16 s rinse period for the return to baseline after flow is restarted. Dispersion is also minimal at 2.0 mL/min per pump. When the bypass loop is used to stop flow, the only major change is with the flow stopping time, which is reduced to less than 2 s. The optimum flow

rate for both types of stopped-flow methods was also selected to be 2.0 mL/min per pump.

For continuous-flow methods the flow rate can effect the values generated from integrations of the peak area. For example, at 1.0 mL/min per pump, the total peak area of an injected plug of NADH will be nearly twice that obtained from the same plug when using a flow rate of 2.0 mL/min per pump. This is due to the reduced residence time of the plug in the flow cell at faster flow rates. For large volume loops (greater than 500 µL) and fairly short integration times (8 s or less) the effect of flow rate on the integration value is not so dramatic. For flow rates of 2.0 mL/min or less, an 8 s integration period measures only the center segment of the peak. The area of this center portion is not as sensitive to changes in residence time as is the area of the whole peak.

Since many of the factors that effect stopped-flow methods also effect continuous-flow techniques, the optimum flow rates should be nearly the same for both methods. A 2.0 mL/min flow rate proved to be optimum for continuous-flow measurements as well as for stopped-flow, since it provides minimal dispersion with minimal rinse-out times. For a 2.0 mL/min flow rate per pump the area measured by an 8 s integration time centered around the peak maximum was 65% of the total peak area. Faster flow rates would increase the percentage of total area measured by the 8 s integration time but would decrease the value obtained from the integration since the residence time of the plug will be reduced. A more detailed discussion of optimum integration times will be given later in this section.

A study was done to show the effect of different flow rates on the run-to-run RSD of both stopped-flow and continuous-flow measurements. Delay times and integration periods were adjusted so that equal signal levels were obtained for all flow rates tested. The results showed that no major difference was seen in the RSD for either measurement mode for flow rates between 0.8 and 3.6 mL/min per pump. It was concluded that the flow rate from run to run does not significantly affect the run to run precision of measurements made with this system. This is a reasonable assumption since the positive displacement pumps used in this system are precise to less than 0.1% in terms of flow rate, according to the manufacturer (99).

Measurement Methods

Upon arrival at the flow cell several options are available for measuring the injected plugs. Two methods for conducting kinetic measurements were described in the Experimental section (stopped-flow and dual peak methods). The following section will discuss the optimization of parameters which directly affect measurements made using the stopped-flow or dual peak methods.

The kinetic measurements made using the stopped-flow method are nearly identical to measurement times used for the cuvette, 8 or 16 s are also optimum for the flow cell. A parameter unique to stopped-flow measurements is the position on the peak where measurement is to be made. A study was made of the run-to-run precision of stopped-flow measurements at a variety of different positions on a 550 µL plug of an NADH solution. A peak profile of the 550 µL plug can be seen in Figure

21. As was expected, the precision of stopped-flow measurements was best when stopping flow at the center of the plug. The RSD increased when stopping flow on the ascending and descending sides of the peak where the concentration will change sharply with position along the axis of the plug. Besides improved precision, the maximum signal levels for kinetic measurements are obtained at the center of the plug where analyte and reagent concentrations are maximum.

Another factor that can affect the run to run precision of stopped-flow measurements is the method used to stop flow. Two methods of stopping flow were studied to compare their run to run reproducibility. In the first method, flow was stopped by halting both pumps while in the second method a bypass loop was installed on the flow cell which when switched, would divert flow around the cell thus isolating it from the carrier stream. The bypass loop method of stopping flow showed significantly better precision than the pump stoppage method. As was stated previously, flow is observed to continue for a short time after the pumps have halted. Such flow through the cell is not possible when the bypass loop is switched since the cell is isolated from the back pressure of the carrier stream. Using the bypass loop there is much less variability in which section of the plug is finally stopped in the flow cell.

Studies were made to find the optimum integration time for the measurement of peaks for the dual peak method. The start of the integration period was always adjusted so that it was centered around the peak, thereby providing maximum signal levels. Studies were made of using a range of different time intervals for the integration period. Repetitive measurements using integration times between 2 and

20 s were made using 550 µL plugs of 12 µM NADH passing through the cell at a flow rate of 4.0 mL/min (optimum conditions for dual peak measurements). The highest net signal to blank noise ratio was seen at an 8 s integration time. At longer integration times the amount of blank signal measured will increase faster than the amount of net NADH fluorescence so therefore the S/N ratio beings to decrease.

After optimum conditions had been established, a study was made to compare the run to run precision of the stopped-flow and the continuous-flow method. Steady state measurements were made with both methods using 12 repetitive injections of 550 µL of NADH. With an 8 s integration time, the dual peak method gave an RSD of 0.33% while the stopped-flow method, using the bypass loop to stop flow, showed an RSD of 0.45%. Although the difference is not significant, the dual peak method appears to be more precise for repetitive, steady-state measurements. Perhaps the fact that a much larger portion (65%) of each plug is measured with the dual peak method helps to average out deviations from run to run. In contrast the stopped-flow method measures less than 2% of the entire plug. A more complete comparison of these two methods will be presented in the discussion of the ethanol assay studies which were done using the FIA fluorometer.

Optimization and Performance of the Flow Cell

Optimization

The most important part of the FIA system, in terms of using fluorescence monitoring, was the flow cell. The spectral performance

of the flow cell was optimized by mounting excitation and emission slits on the flow cell housing. Both the signal to noise (S/N) ratio and the net NADH fluorescence to blank signal ratio were measured using a variety of slit sizes. The optimum combination was a 1.4 mm by 10 mm excitation slit and a 5 mm by 10 mm emission slit which produced the highest S/N and fluorophore to blank signal ratios. The resulting viewed volume was 70 µL which is significantly larger than the 10 µL volume (1 mm x 1 mm x 10 mm) of the sample cavity contained within this viewed volume. The mirror mounted on the inner wall of the flow cell opposite the emission slit is probably responsible for the optimum emission slit being wider than the sample cavity. The wider emission slit increases the collection efficiency of fluorescent light reflected from the mirror. Taller excitation and emission slits would increase the volume of sample viewed but it was found that the background fluorescence signal increased sharply when taller slits were used. The sharp increase in background fluorescence was produced by the teflon tubing used at the inlet and outlet of the quartz sample cavity.

The mirrors mounted on the inner walls of the flow cell housing opposite the excitation and emission slits were studied in terms of their effect on the S/N. Measurements were made while masking one or both mirrors and these results were compared to measurements made with neither mirror masked. The signal levels obtained with both mirrors uncovered were a factor of 4 greater than when both mirrors were masked. The S/N ratio for NADH solutions near the detection limit increased by a factor of 2. This improvement in the S/N is due to the fact that the blank signal is shot noise limited when neither mirror is used and therefore increasing the signal level will increase the S/N.

Performance

Using the conditions for the highest S/N ratio, the performance of the flow cell was studied by measuring the detection limit and upper limit of linearity for fluorescence measurements of NADH. In addition, studies were made of the measurement of NADH in a serum matrix. The results of these studies were compared to the values obtained when using a standard 3 mL quartz cuvette under equivalent experimental conditions. These results are shown in Table XXIII.

The viewed volume of solution in the cuvette was 150 µL compared to 10 µL for the flow cell. Due to this difference it would be expected that the slope of the NADH calibration curve would be 15 times less for the flow cell but the effect of the two mirrors enhances the flow cell signals by a factor of 4. This reduces the difference in the values of the slopes to only a factor of 3. The higher background fluorescence of the flow cell, due to a significant amount of cell wall within the viewed volume, causes the noise level of the buffer blank to be higher for the flow cell than for the cuvette. The higher noise level and lower value for the slope the NADH calibration curve results in a higher theoretical detection limit for the flow cell.

In a serum matrix the blank signal levels for both the cuvette and the flow cell increase significantly due to fluorescence from serum proteins and scattering from particulates. The detection limits for NADH are affected by the increased noise levels from serum solutions for both the flow cell and the cuvette. Somewhat higher SD's are observed with measurements of serum solutions when using the flow cell as compared to equivalent measurements made with the cuvette. This may

Table XXIII

Comparison of the Flow Cell and the Cuvette

Parameter	Flow Cell[a]	Cuvette[b]
Fluorescence Signal from Tris Buffer (counts)	65,400	10,150
SD of Buffer Signal (counts)	188	97
Slope of NADH Calibration Curve (counts/μM, in-cell)	1×10^4	4×10^4
Theoretical Detection Limit for NADH in Buffer (μM,in-cell)	4×10^{-2}	5×10^{-3}
Upper Limit of Linearity for NADH Fluorescence, -5% deviation (μM, in-cell)	95	20
Total Signal Level of a 1 to 40 Dilution (in-cell) of Q-PAK Serum II (counts)	206,800	309,302
SD of Signal from a 1 to 40 Dilution of Q-PAK Serum II (counts)	2108	1873
Theoretical Detection Limit for NADH in 1 to 40 Q-PAK Serum II (μM, in-cell)	0.1	0.04
Minimum Dilution (in-cell) of Q-PAK Serum II to Eliminate Absorption Interference	1 to 40	1 to 180

[a]All data were collected using a single injection valve equipped with a 1000 μL loop. Stopped-flow method used. Flow cell equipped with 1.4 x 10 mm slit on excitation window, 5 x 10 mm slit on emission window, 8 s M.T.

[b]Cuvette viewed volume defined by slits on the cell holder. 8 s measurement time.

be due to the effect of drifts caused by photodecomposition over the course of consecutive measurement periods when measuring a serum blank with the flow cell.

The average path lengths through solution for excitation and emission photons are both 1 mm for the flow cell compared to 5 mm for the cuvette. Note that with the cuvette, the excitation and emission beams pass through solution which is not within the viewed volume. In contrast, no portion of the emission or excitation beam can pass through solution outside the viewed volume of the flow cell. As a result of the decreased path length of the excitation beam and the containment of all solution within the viewed volume, the upper limit of linearity for NADH fluorescence is nearly a factor of 5 greater for the flow cell. This same effect is seen when pre- and post-filter effects are significant such as when measuring NADH in a serum matrix. The absorbance at 366 nm caused by serum proteins and the absorbance at 468 nm due to bilirubin produce pre- and post-filter effects for fluorescence measurements of NADH. Because of the shorter path lengths of the excitation and emission beams, dilutions of serum must be nearly 5 times greater with the cuvette as compared to the flow cell in order to eliminate the pre- and post-filter effects. Table XXIII shows the dilutions needed to reduce the attenuation to -3% when measuring NADH fluorescence in a solution made from a serum standard.

Drifts

A problem was encountered with the flow cell that had not been observed with the cuvette. This problem appeared as a negative drift

in the fluorescence signals from the flow cell during the measurement period. The magnitude of the drift depended on what type of solution was stopped in the flow cell and the concentration of that solution. Figure 23 shows the drifts of three different solutions as recorded by a strip chart recorder.

The characteristics of these negative drifts were studied in order to determine the cause of the decreasing signal levels. As the concentrations of the species under study is decreased, the absolute magnitude of the drift also decreases but the relative drift (ratio of the drift to the initial signal level) remains fairly constant. The second test was to block the excitation beam irradiating the flow cell and observe the effect on the drift. Both the NAD^+ and Serum II solutions showed almost no drift during the time the excitation beam was blocked (see Figure 23). It was therefore concluded that the drift was due either to photodecomposition of the fluorescing species or a heating effect caused by the absorption of the excitation beam. Higher temperatures reduce the fluorescence of most species and therefore if a solution in the cell were heating up, its net fluorescence would decrease. The effect of temperature on the fluorescence of the three species being studied (NAD^+, NADH and dilutions of Serum II) shows that the fluorescent signal from each of these species will decrease 1 to 2 % for every 1°C increase in temperature. The magnitude of the drift was much greater than could be explained by any heating effects. For the 1 to 10 dilution of Serum II the fluorescence signal decreased 20% during the first minute of the drift which would correspond to an increase in temperature of nearly 20°C.

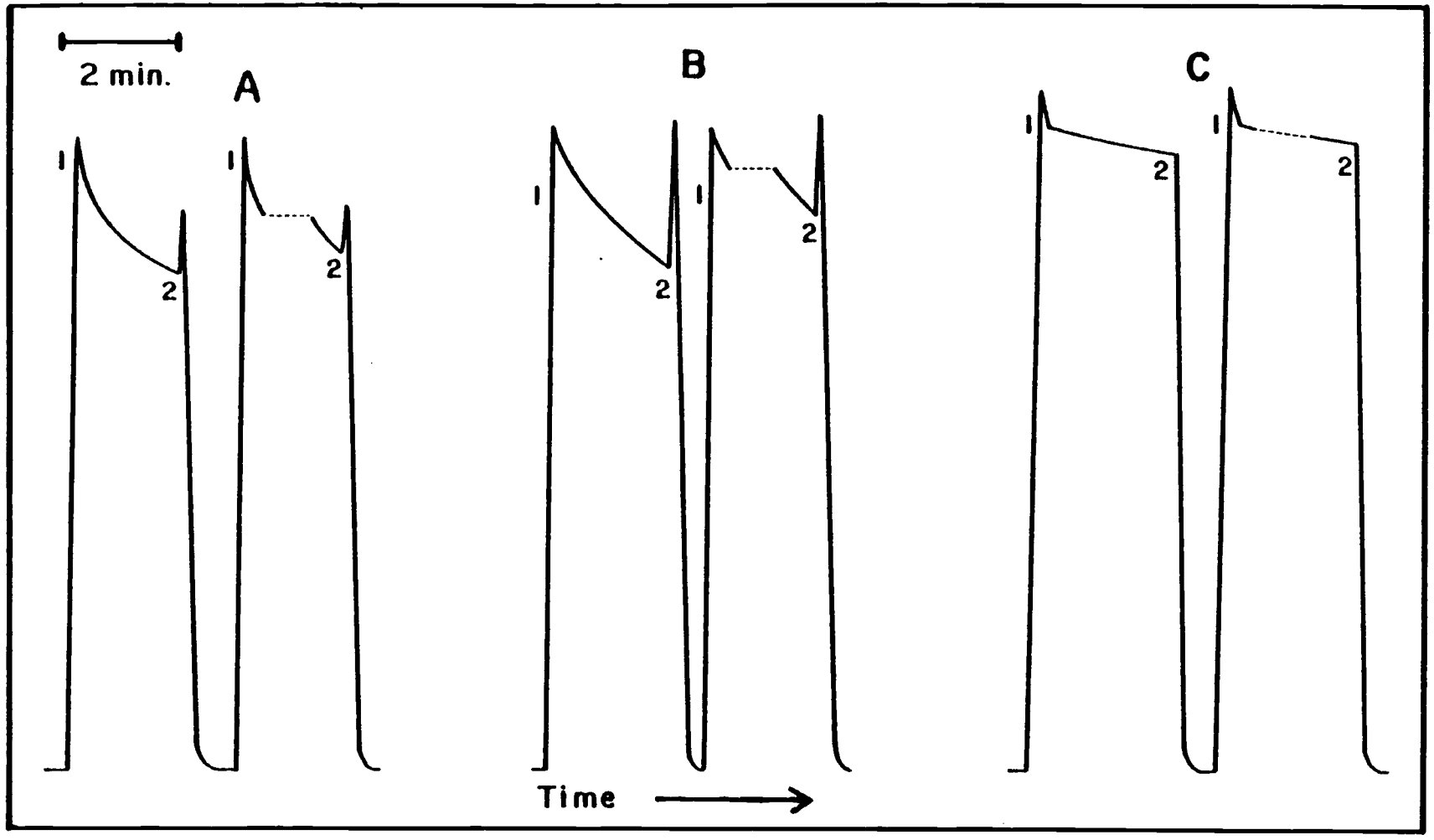

Figure 23. Observed drifts during stopped-flow measurements. A) 1 to 10 dilution of Q-PAK Serum II, in-vial, B) 19 mM NAD^+, in-vial, C) 12 μM NADH, in-vial. 1 = pumps stopped, 2 = pumps restarted. Excitation slit width = 2 mm. Dashed lines indicate period during which ex. beam blocked.

The major source of the negative drift must be photodecomposition. This assumption is substantiated by a report in the literature (41) which states that certain proteins found in serum are photosensitive. The magnitude of the drift depends on the specific protein and its concentration. For this reason the relative drift changes from one serum sample to the next since the concentration and the ratios of certain proteins vary from sample to sample.

Both NAD^+ and NADH show negative drifts when solutions of them are stopped in the flow cell. Both species are photosensitive as can be witnessed by the reduced drift seen when the excitation beam is blocked. It was not discovered as to why NAD^+ shows a higher relative drift than NADH.

Reducing the intensity of the excitation beam should decrease the rate of photodecomposition and thereby reduce the magnitude of the drifts. The most convenient method of reducing the excitation beam intensity for this system was to reduce the width of the slit on the excitation monochromator. For a 1 to 10 dilution of Serum II, reducing the slit width from 1.0 mm to 0.5 mm decreased the relative drift from 1.0% to 0.6%, for a 16 s measurement period. While the drift was reduced, the run to run RSD of rate measurements on the 1 to 10 dilution of Serum II did not change significantly.

In order for the drift to be negligible the relative drift should be less than the run to run RSD. For 16 s rate measurements of Serum II dilutions, the RSD is about 0.3%. It appears that from the previous data that by reducing the slit width to 0.25 mm the relative drift should be less than 0.3% and thus be insignificant relative to the run to run RSD for 16 s measurements (less than 0.3%).

For a 19 mM solution of NAD^+ (see Figure 23) the relative drift was 0.82% when using a 16 s measurement time with a slit width of 1.0 mm. A 19 mM NAD^+ concentration is much higher than would normally be used in a kinetic assay but at this level the drift was much easier to study. At a typical concentration of 4 mM NAD^+, the relative drift is reduced to 0.4% of the total signal level since at 4 mM much more of the total signal is due to background fluorescence which does not drift. Reducing the slit width to 0.5 mm would decrease the relative drift to less than 0.3%, thus making it insignificant relative to the precision of repetitive measurements.

The relative drifts of NADH solutions in the flow cell are much smaller than the relative drifts of Serum II or NAD^+. For a 16 s measurement period, the relative drift is about 0.4 % for 12 M NADH when using a 2.0 mm slit width. This value is nearly equal to the run to run standard deviation of 0.3% for 16 s rate measurements of solutions of 12 μM NADH. A slit width of 1.0 mm will reduce the drift to a point where it is insignificant (less than 0.3%).

Other methods rather than changing the slit width might be used to prevent these drifts from causing errors in rate measurements. Reducing the excitation beam intensity with a neutral density filter would decrease the rate of photodecomposition. Certainly another option is to use a kinetic method where the sample and reagent are not stopped within the flow cell. In the dual peak method, the time any one part of the total sample and reagent plug is within the viewed volume is very short compared to the total measurement time. Photodecomposition would therefore have no effect irregardless of the intensity of the excitation beam.

FIA Measurements of the Ethanol-ADH system

Introduction

In order to test the use of the FIA system for fluorescence kinetic methods, a simple, first-order reaction was required. The ethanol-ADH system was selected for these initial studies since it had been studied extensively by the discrete analysis method using the 3 mL cuvette. Many of the experimental conditions which were optimum for the cuvette studies are also optimum for the FIA method since the same fluorometer was used in both cases. Both dual peak and stopped-flow methods were used with the ethanol system and a comparison was made of the characteristics of both methods.

Optimizations of ADH and NAD^+

ADH and NAD^+ concentrations were optimized, using the stopped-flow method, to confirm that the optimum levels of these reagents for the cuvette assay were also optimum for measurements in the flow cell. The concentration of the reagents and sample in the flow cell are one half that for the unmixed solutions before injection since the sample and reagent plugs are merged with a ratio of 1 to 2 (both pumps operated at 2.0 mL/min) and the effect of dispersion is minimal since flow is stopped at the center of the large volume plugs.

Figure 24 shows the results of the ADH optimization studies. These results are equivalent to those from the cuvette studies where the observed reaction rate reaches a maximum and then declines as the

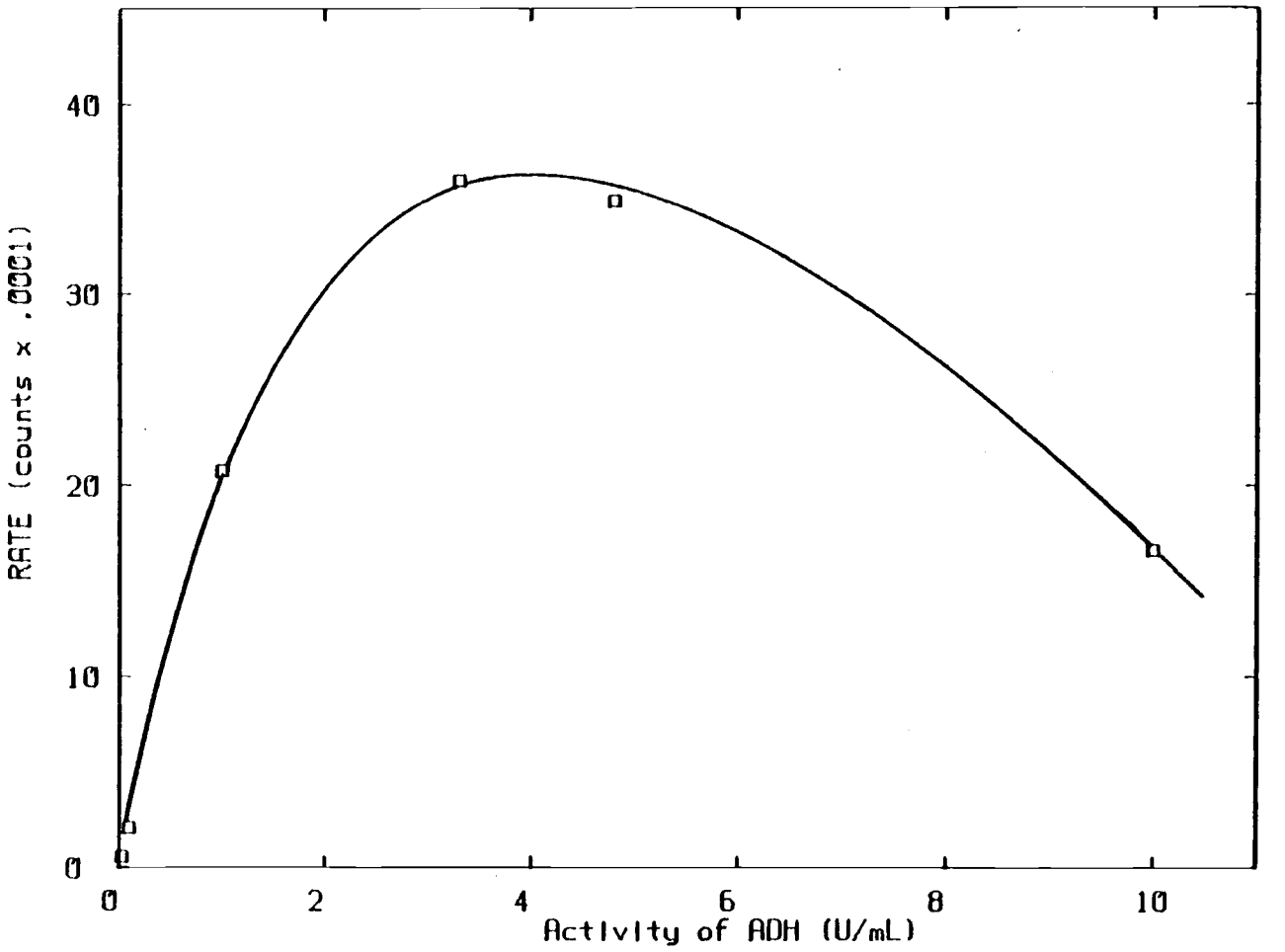

Figure 24. ADH optimization for FIA studies. The ADH levels reported here are the resulting in-cell activities. Other concentrations = 2 mM NAD^+ (in-cell) and 0.17 mM EtOH (in-vial). Data collected using the stopped-flow method.

ADH activity in the cell is increased above 7 U/mL. At ADH levels above 7 U/mL a significant amount of the reaction takes place prior to the measurement such that the initial ethanol concentration is no longer being measured.

With the dual peak method, the same type of curve would be generated except that the maximum would occur at a higher ADH activity. This is due to the fact that with the dual peak method, the signals obtained for a kinetic measurement correspond to the reaction taking place between the mixing time and the arrival of the plugs at the flow cell. With this system, one will measure the initial ethanol concentration no matter what the ADH level is. The plot of rate vs ADH activity will still reach a maximum since product inhibition and levels of NADH beyond the linear limit will cause the observed rates to level out.

For the studies conducted using the ethanol-ADH system with the FIA fluorometer, no blank reaction was observed. The particular batch of ADH used for these studies was evidently very low in ethanol. The ADH concentration therefore had very little effect on the blank signal and blank noise levels. The optimum ADH level was selected to be 7 U/mL since it was near the maximum shown on Figure 24. This concentration was used for both the stopped-flow and the dual peak method.

Figure 25 shows the effect of changing the NAD^+ concentration on the observed rate for an ethanol standard. The reaction rate levels off and becomes independent of the NAD^+ concentration at concentrations greater than 3 mM (6 mM in the reagent solution). However, as previously shown with cuvette studies, increased NAD^+ concentrations in the reagent produce greater noise in the measurement

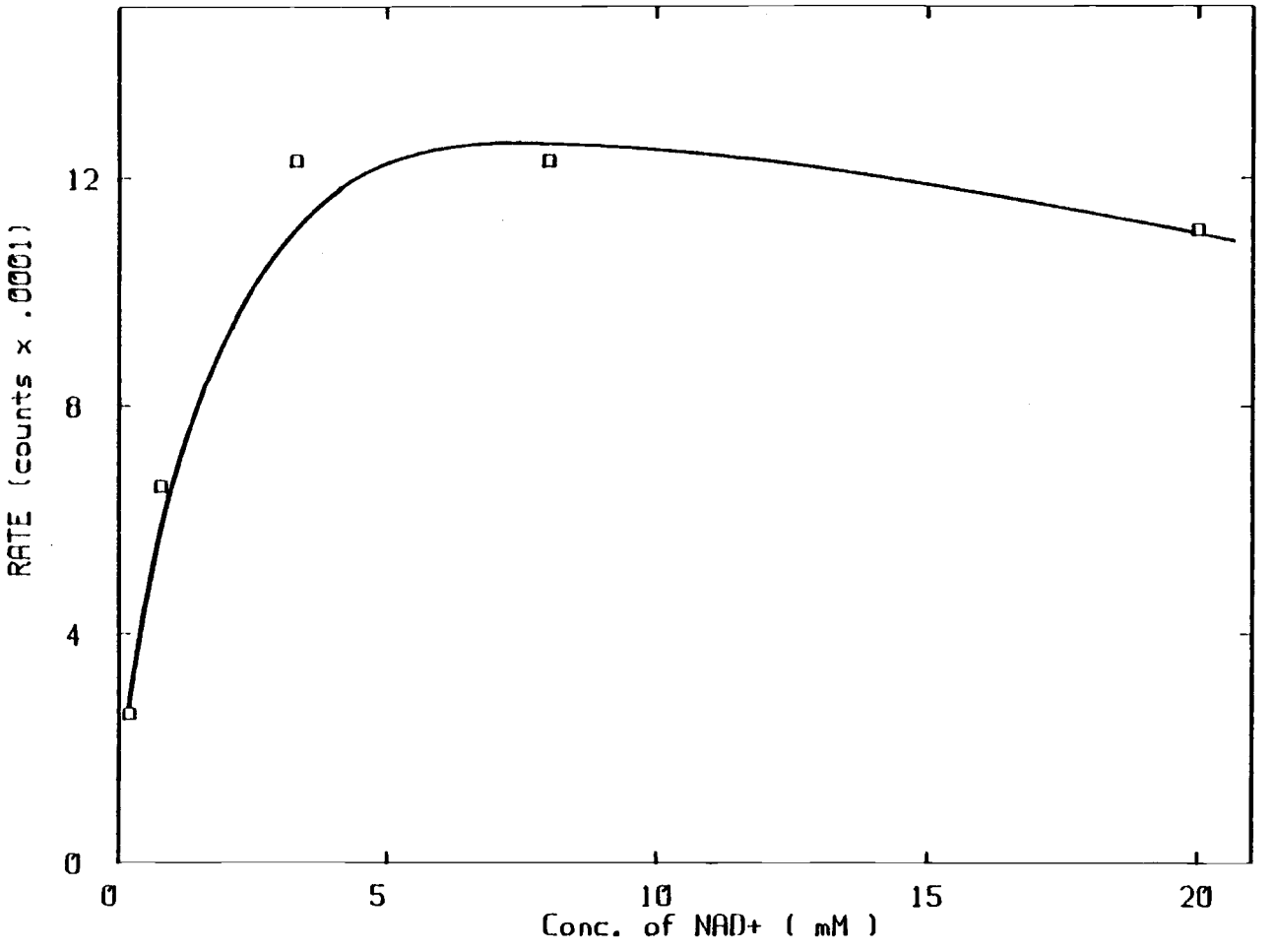

Figure 25. NAD^+ optimization for FIA studies. The NAD^+ levels reported here are the resulting in-cell concentrations. The rate measurements made for NAD^+ levels above 3 mM were corrected for the negative drift of photodecomposition. Other concentrations = 7 U/mL ADH (in-cell) and 0.17 mM EtOH (in-vial).

of the blank due to NAD^+ fluorescence and thus increase the detection limit. The optimum NAD^+ concentration for both the stopped-flow and the dual peak method can be found by maximizing the ratio of the observed reaction rate vs the blank noise level. Using a 16 s measurement time with the stopped-flow method the maximum of this ratio was at 2 mM (same as for the cuvette studies). This concentration is high enough to insure that the NAD^+ concentration will not change significantly even at the fastest reaction rates. Product inhibition becomes limiting before the NAD^+ concentration can drop low enough to affect the reaction rates. The negative drifts caused by photodecomposition when the reagent is stopped in the flow cell must also be considered when optimizing the NAD^+ concentration. Calculations have shown that the drift observed over a 16 s measurement period is no greater than the run to run noise level of blank for NAD^+ concentrations near 2 mM. The drift should therefore not have a major effect on an analysis using a 16 s measurement time.

Comparison of the Dual Peak and Stopped-flow Methods

Figure 26 shows a theoretical comparison of how rate values are calculated by the stopped-flow and the dual peak method. Both methods involve integrations and the difference between two integrations generates a rate value. With the stopped-flow method the reaction rate is measured while the reaction itself is proceeding within the flow cell. In the dual peak method, the measurement is made on the reaction that took place prior to the combined plugs reaching the cell. Figure 26 shows that if the reaction times are equal for both methods (i.e.

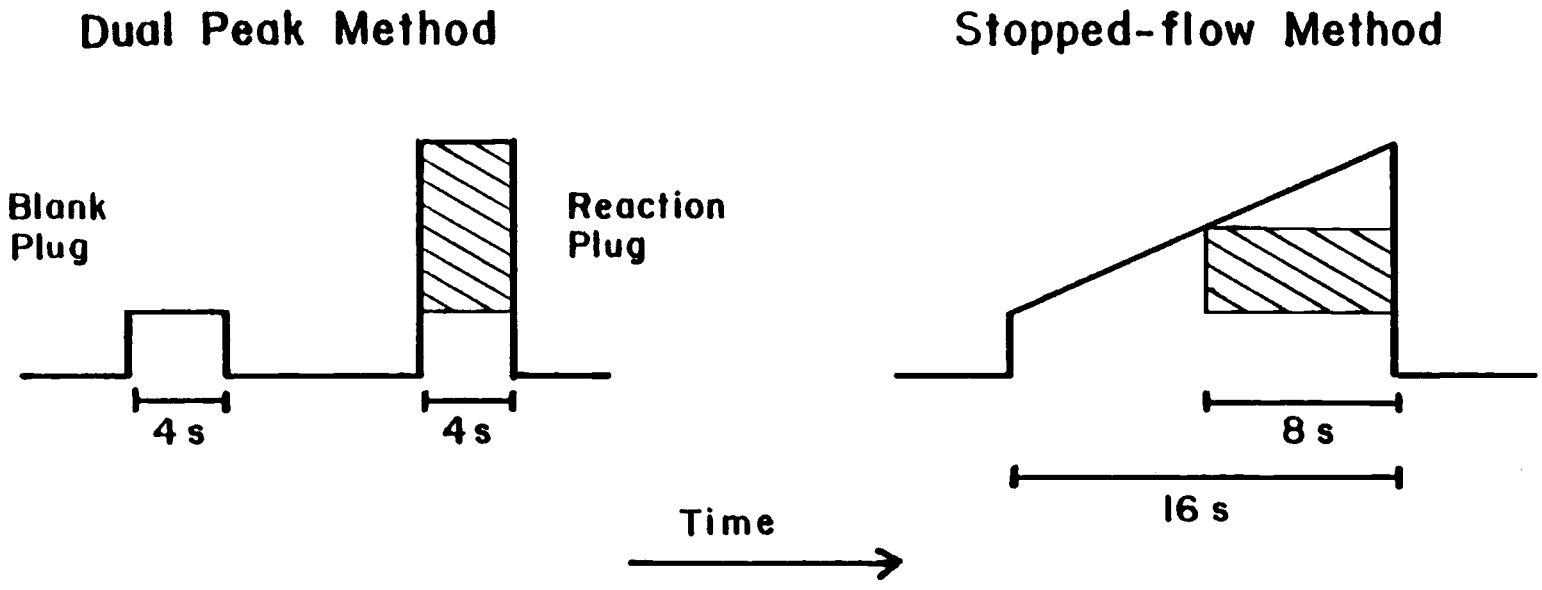

Figure 26. Theoretical comparison of rate measurement made using the stopped-flow and the dual peak methods. In this example, the rate values (shaded areas) are equal for the two methods. This is valid only if the measurements were made on identical reactions and if the time from merging the two plugs until arrival at the flow cell (dual peak reaction time) is equal to the stopped-flow integration time (16 s).

the time from mixing until the plug reaches the flow cell is equal to the stopped-flow measurement period), an integration period for each peak of the dual peak method must be 4 times shorter than the stopped-flow integration period, if equal rate values are desired. This assumes that measurements of the peaks are made in the center of the combined plugs where diffusion is minimal and thus the reagent and analyte concentrations are constant during the integration period for both methods. Two calibration curves for ethanol were made using both the stopped-flow and dual peak methods. The results are shown in Figure 27 and are summarized in Table XXIV. With the experimental conditions used for these FIA studies, the time from merging of the sample and reagent plugs until the combined plug reaches the flow cell (the approximate reaction time for the dual peak method) is about 6 s. When both pumps are operated at 2.0 mL/min a 16 s measurement period was found to be optimum for stopped-flow measurements. In order to obtain equal rate values for an identical reaction, the integration period for the dual peak method must be increased to a little over 10 s. For our system it was more optimal to make 8 s integrations so the measured rate values for equivalent reactions are therefore lower for the dual peak method than for the stopped-flow method (see slopes in Table XXIV) Even though the rate measurement values are not exactly equal, the values are close enough that the other characteristics of the two methods, such as detection limits or upper limits of linearity can be compared.

The stopped-flow method has a lower detection limit for ethanol than does the dual peak method. This is due to the fact that stopped-flow rate measurements of blanks where no reaction is proceeding are,

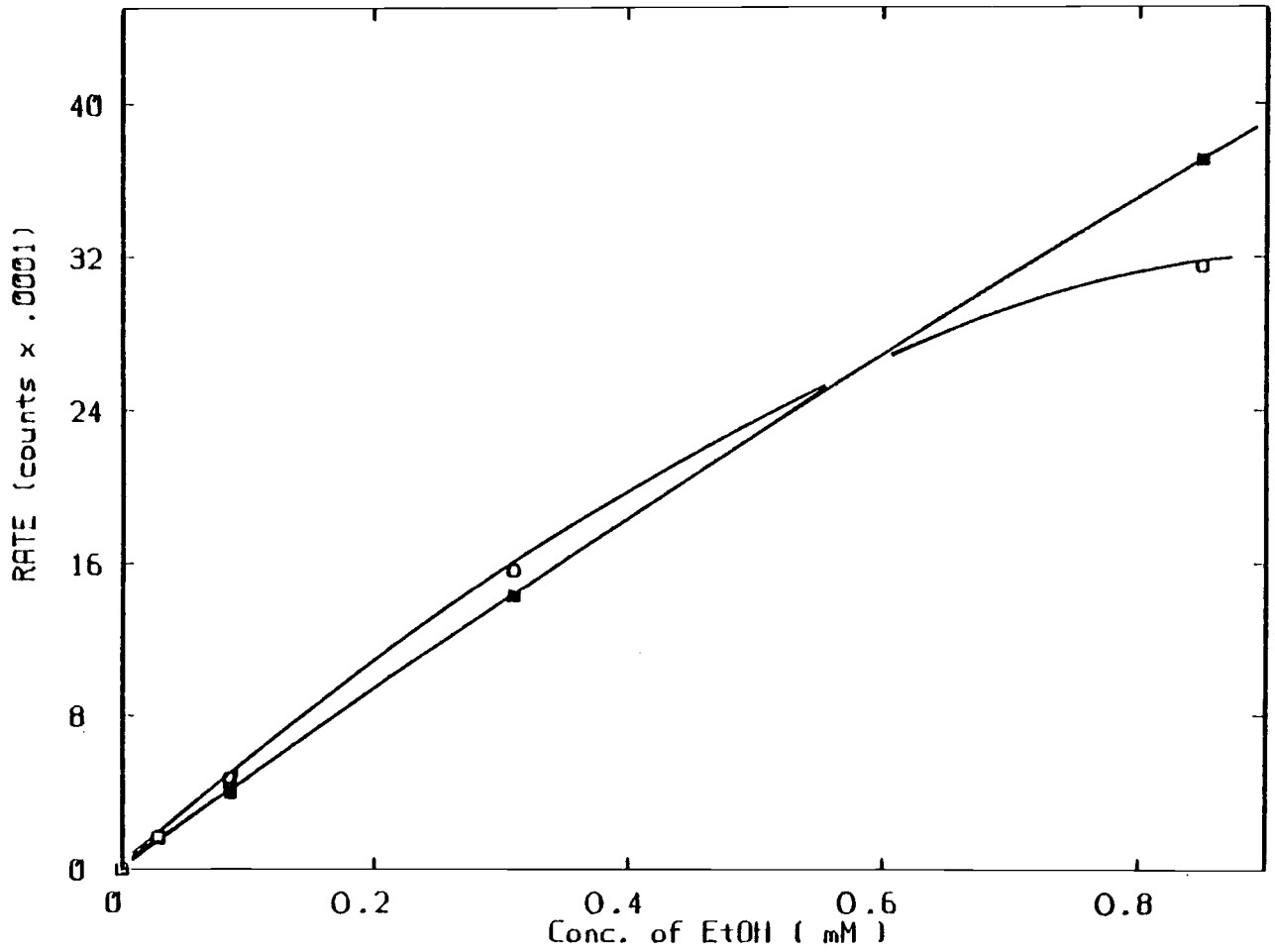

Figure 27. Calibration curves made using the dual peak method(■) and the stopped-flow method(o). The ethanol concentrations reported here are the in-vial concentrations. Other concentrations = 2 mM NAD^+ and 7 U/mL ADH, in-cell.

Table XXIV

Results of the Ethanol Assay using
Both the Stopped-flow and the Dual Peak Method[a]

Parameter Measured	Stopped-flow[b] Method	Dual Peak[c] Method
Slope of Calibration Curve (counts per M EtOH , in-vial)	5.6×10^8	4.6×10^8
SD of Blank Measurements (counts)	222	414
Theoretical Detection Limit (μM EtOH, in-vial)	0.8	2
Upper Limit of Linearity (mM EtOH, in-vial)	0.25	0.75

[a]7 U/mL ADH, 4mM NAD^+ in the reagent solution (prior to injection) for both methods.

[b]16 s measurement time, 8 s delay time.

[c]8 s integration time per peak.

for the most part, unaffected by small changes in the steady-state signal level from run to run. In contrast, the dual peak method requires the measurement of two individual plugs in order to make a single kinetic measurement. Variations in the delivery of a blank plug to the flow cell can change the signal level of either 8 s integration, therefore the precision of blank measurements made with the dual peak method is directly dependent on the reproducibility of delivering the blank plug to the flow cell. The values for the SD's of blank measurements using both methods are shown in Table XXIV. The variations in the delivery of the blank solutions to the flow cell result in a factor of two increase in the SD for the dual peak method. The difference in the SD's of the blank measurements for the two methods accounts for the higher detection limit for the dual peak method.

Calculations were made to determine the change in the NADH concentration at the detection limit of ethanol for the stopped-flow method. From data obtained from the chart recordings of the reactions of ethanol standards, the change in concentration of NADH which would be measured at the detection limit was 0.01 μM. This value is very close to the detection limit for NADH fluorescence using steady-state 8 s measurements. It can therefore be assumed that the stopped flow detection limit for ethanol is limited by the detectability of NADH using a fluorescence method. Making equivalent calculations for the dual peak method shows that a signal equivalent to 0.02 μM NADH is generated at the detection limit for ethanol.

Calculations were made to find what was responsible for the non-linearity in the calibration curves at high ethanol concentrations. The total NADH produced by the middle of the measurement period for the

stopped-flow method during the reaction taking place at the upper limit of linearity (0.25 mM ethanol) was calculated to be 9.4 μM. For the dual peak method, at the upper limit of linearity (0.75 mM ethanol), the NADH concentration present is 12 μM. Both of these values are well below the NADH concentration where fluorescence is no longer proportional to concentration, which was shown to be 95 μM for the flow cell.

Figure 27 shows the obvious difference in the limit of linearity between the two methods. For both methods product inhibition is a major contributor to the non-linearity as was the case for the ethanol assays made in the cuvette. The lower value for the upper limit of linearity for the stopped-flow method is due to the fact that much more reaction takes place prior to the measurement period. The average reaction times for both methods are shown below:

Stopped Flow:	6 s (travel time from tee to flow cell)	+	2 s (time for flow to completely stabilize)	+	8 s (½ the actual measurement time of 16 s.)	= Total 17 s	= 4% of the total rxn
Dual Peak:	6 s (travel time from tee to flow cell)	=			Total 6 s	=	1.2% of the total rxn

For equal sample and reagent concentrations, a factor of nearly 3 times as much product is present by the middle of the stopped-flow measurement as compared to that measured by the dual peak method.

As was shown in the discussion of the ethanol assay conducted in the cuvette, the Michaelis-Menton equation would predict the upper limit of linearity for this system to be at about 0.7 mM. This is

equivalent to the upper limit of linearity observed for the dual peak method, therefore it may be assumed that no higher limit is possible.

Analysis in a Serum Matrix

A comparison was made of the results of making two separate calibration plots using ethanol standards made up in buffer and equivalent standards made up in a 1 to 20 dilution of Versatol-A, a commercial serum standard (see Table XXV). The values obtained for the stopped-flow rate measurement of standards in serum were adjusted in order to compensate for the negative drift observed during the blank measurement. Both methods show a decrease in slope of about 7% for calibration curves produced with standards containing serum. The major cause of this decrease is pre- and post-filter effects of the serum matrix. The approximate dilution of versatol A in the flow cell during measurement is 1 to 40. At this concentration, this particular serum standard would cause a 4% decrease in the transmittance of the excitation radiation and a 6% decrease in the transmittance of fluorescence through the sample cavity. This should result in an approximate attenuation of 10% for fluorescence signals from NADH. This more than explains the reduction in the observed reaction rate when measuring ethanol in this particular serum matrix. A greater dilution of the serum matrix should eliminate this problem.

The precision in the run to run measurement of the serum blank compared to the buffer blank shows the effect of the greater steady-state signals caused by serum fluorescence. The fluorescence signal of the blank when using a 1 to 20 dilution of versatol A is a factor of 2

Table XXV

Analysis of Ethanol Standards in
Both a Buffer and Serum Matrix

Parameter Measured	Pyrophosphate Buffer	1 to 20 Dilution[a] of Versatol A
Dual Peak Method[b]:		
Slope of Calibration Curve (counts/M EtOH in-vial)	9.8×10^8	9.2×10^8
SD of the Blank (counts)	414	862
Theoretical Detection Limit (μM EtOH, in-vial)	0.9	2
Run-to-Run RSD (0.17 mM EtOH, in-vial)	2.9%	4.2%
Stopped-flow Method[c]:		
Slope of Calibration Curve (counts/M EtOH in-vial)	5.1×10^8	4.7×10^8
SD of the Blank (counts)	222	499
Theoretical Detection Limit (μM EtOH, in-vial)	0.9	2
Run-to-Run RSD (0.17 mM EtOH, in-vial)	1.6%	1.7%

[a] in-vial dilution (1 to 40 in-cell), sample spiked with EtOH.

[b] 10 U/mL ADH, 4 mM NAD^+ in reagent solution, 8 s integration time per peak.

[c] 6 U/mL ADH, 4 mM NAD^+ in reagent solution, 16 s meas. time.

greater than the fluorescence signal of the blank when no serum is present. This larger signal causes greater noise in the blank signal and amplifies the imprecision caused by variations in delivery of the solutions to the flow cell. Both the dual peak and the stopped-flow method show a proportional increase in detection limits when measuring ethanol in a 1 to 20 dilution of versatol due to this increased blank signal level.

Comparing the run to run SD's for rate measurements using 0.17 mM ethanol standards shows that the stopped-flow method is more precise. Even though earlier studies done with injections of NADH showed that the run to run SD's were nearly equal, there is an obvious difference when making actual rate measurements. The higher SD of the dual peak method would indicate that variations in the reaction taking place between the tee and the flow cell are significant. Perhaps there are significant differences from run to run in the mixing times or in the temperature of the tubing between the water bath and the flow cell, both of which could effect the rate measured by the dual peak method.

Throughput

The throughput or analysis rate per hour for typical FIA rate measurements are shown in Table XXVI. The throughput of the stopped-flow system could be improved if the sampling time of the injection loops were started during the 10 s delay period for rinsing the flow cell. Part of the time after injection may be used as part of the rinse-out time since approximately 6 s elapse after injection before the front of the combined plug reaches the flow cell. The minimum

Table XXVI

Throughput of FIA Methods

Stopped-flow Method[a]:

Time required to rinse 3 volumes of sample or reagent into the injection loops (∿ 600 µL).	=	12 s
Time from injection till the end of the 16 s measurement period, including a 2 s delay to insure flow has completely stopped.	=	26 s
Time for extra delay to insure sufficient rinsing between runs.	=	10 s
total time per run	=	48 s
throughput (runs/hr.)	=	75

Dual Peak Method[b]:

Time required to rinse 3 volumes of sample or reagent into the injection loops (∿ 600 µL)	=	12 s
Time from injection till the end of the 8 s integration period.	=	16 s
Time for an extra delay to insure sufficient rinsing between runs.	=	10 s
total time per peak	=	38 s
total time per rate measurement	=	76 s
throughput (runs/hr.)	=	47

[a]Bypass loop used to stop flow, pumps continuously running at 2.0 mL/min per pump.

[b]Pumps continuously running at 2.0 mL/min.

rinse time between the end of the stopped-flow period and the entrance of the next plug into the flow cell depends on the carry-over that can be tolerated. Under the conditions of this study, 16 s of flow are required to rinse out the flow cell until less than 0.2% of the net stopped-flow signal from 8.5 μM NADH is measured in the cell. This may be better rinsing than is required for all applications. The time per run can be reduced to a minimum of 16 s for rinsing and 20 s for the measurement, resulting in a total time of 36 s per run. The throughput for the dual peak method can also be increased. The time per run can be reduced to 30 s even if baseline resolution of the peaks is maintained. The width of the baseline is rather independent of the reaction rate of the combined plugs passing through the cell. The baseline width measured for a combined plug containing an ethanol concentration even greater than the upper limit of linearity was only 30% wider than the baseline for the blank.

The throughput of both methods could be improved if a flow cell with better rinse-out properties was used. The square bore of the sample cavity complicates rinse-outs since it is difficult to wash out the corners of the cavity. Higher throughput could also be achieved with faster flow rates during the period when the flow cell is being rinsed. The upper limit of linearity for the stopped-flow measurement of ethanol will increase at faster flow rates since less product is produced prior to the actual measurement period. Less product produced between mixing of the plugs and arrival at the flow cell means that at faster flow rates the detection limit for the dual peak method will increase. For the dual peak method, a compromise must be made between detection limits and throughput.

Comparison of the Two Methods

An overall comparison of these two methods of making kinetic measurements shows that the stopped-flow method in general, has more advantages. The stopped-flow method offers better precision, lower detection limits and faster throughput than a dual peak method operated under the same conditions. The dual peak method may be more advantageous in situations where photodecomposition is more critical or where product concentrations prior to measurement must be minimal.

CK Assay Using the FIA-Fluorometer System

A study was made of the application of the NADH-monitored CK assay to the FIA fluorometer system. The results of using fluorescence monitoring of NADH for measurements of CK activity in a cuvette were reported earlier. It was hoped that the fact that serum interference is less with the flow cell than it is with the cuvette would allow a smaller serum dilution to be used and thus would improve the effective detection limit for CK in serum.

Since the results from the ethanol assay using the FIA system had shown the stopped-flow method to be optimum for that type of assay, it was used for the studies of the CK assay. The initial studies showed that a 24 s delay was needed for the observed rate to reach a maximum. Such a long delay period would require a flow rate significantly less than 2.0 mL/min per pump in order for dual peak measurements to match the values obtained from the stopped-flow method. A slower flow rate would be less than optimum by lengthening the rinse-out period and

increasing the total measurement time. For these reasons the stopped-flow method, using a 2.0 mL/min flow rate per pump, was selected as optimum for this assay.

For stopped-flow measurements there is an advantage to the 24 s delay period. During the 24 s that flow is stopped in the cell, the drifts observed with stopped-flow measurements will have diminished significantly. For example, stopped-flow measurements of a 1 to 10 dilution of Q-PAK Serum II show a 1.5% negative drift during the 16 s measurement following an 8 s delay. Increasing the delay time from 8 to 24 s reduces the drift to less than 0.6% for the 16 s measurement. For the CK assay a 24 s delay allows for the maximum rate to be measured while minimizing the effects of drifts due to photodecomposition.

The difference between the reagents used for the FIA studies and those done with the cuvette was primarily the factor of 4 increase in the ADP concentration for the FIA studies. Although the same type of ADP was used for both systems (A-4286, Sigma Chem. Co.), a fresh batch of ADP was obtained for the FIA studies. The ATP level in the fresh batch of ADP was lower by a factor of 5 (0.02% mol/mol) than that observed for the ADP used in the cuvette studies (0.10% mol/mol). The lower level of ATP contamination allowed the optimum concentration of ADP to be increased to 1.2 mM in-cell.

Two separate calibration curves were obtained, one using CK standards made up with rabbit-muscle enzyme and another using 4 different serum standards, each diluted 1 to 50 in-cell (i.e. a 1 to 25 dilution of each standard was made prior to injection). The results of these assays are shown in Table XXVII.

Table XXVII

CK Calibration Curves using FIA-Fluorometer

Parameter Measured	Rabbit-Muscle Standards	Serum[a] Standards
Slope of Calibration Curve (counts per U/mL, in-cell)	2.9×10^7	1.1×10^7
SD of Blank Measurements (counts)	423	1083
Theoretical Detection Limit (mU/mL, in-cell)	0.03	0.2
Upper Limit of Linearity (mU/mL, in-cell)	55	~150
Run-to-Run RSD	1.2% (4.4 mU/mL)	1.9% (8.3 mU/mL)

[a] 1 to 50 dilutions (in-cell) of Q-PAK Serum I and II, Qualify I and II. The in-cell CK activities were calculated from the reported values on the package inserts.

The increased slopes of both calibration curves, compared to the results of the cuvette study, are due to several factors. The increased ADP concentration helped to raise the observed activity of the CK present in the flow cell. The level of phosphocreatine was also increased by nearly a factor of 2 (to 20 mM) since it was reported in reference 118 that concentrations near 20 mM were optimum. Another factor that increased the slopes was an increase in the net signal levels of NADH due to a realignment of the flow cell within the fluorometer. The stir bar motor and housing were replaced prior to the start of the CK assay studies with the FIA fluorometer. Replacement of the stir-bar motor housing required realignment of the cell holder within the excitation and emission beams. The alignment was adjusted so that nearly a factor of 4 increase was seen in the net signal levels of NADH compared to the previous alignment which evidently had not been optimum for use with the flow cell. The buffer blank signal levels increased by less than a factor of 2 so no significant change was seen in the blank noise level.

Calculations were made using the chart recordings to determine the actual activities of the CK standards used for the calibration curves. According to the Michaelis-Menton equation the observed activity should be 0.6 times the maximum CK activity when the ADP concentration is at 1.2 mM. The observed activities calculated for the rabbit-muscle CK standards are a factor of 4 greater than would be predicted, while the observed activities for the serum standards are nearly equal to the activity predicted by the Michaelis-Menton equation. These findings are consistent with the calculations of actual activity made for the cuvette study. Again it was assumed that the serum standards represent

a better match to the activities of CK which would be found in fresh samples.

The detection limit for the measurement of CK in serum is affected by the high fluorescence signals from the serum blank. The detection limit for CK in undiluted serum is significantly better for the FIA studies than it was for the cuvette because of the lower spectral interferences by serum in the flow cell and the increased slope of the calibration curve. A final dilution of 1 to 50 in cell (1 to 25 prior to injection) is sufficient to eliminate the pre- and post-filter effects of the 4 serum standards used in this study. Using the in-cell detection limit of 0.19 mU/mL, the theoretical detection limit for CK in undiluted serum was calculated to be 9.5 mU/mL. This value is below 12 mU/mL which is the lower boundary for the normal range of CK activities in serum (15).

At the upper limit of linearity for the rabbit-muscle standards, 55 mU/mL, the NADH concentration present by the middle of the measurement period was calculated to be 40 μM. This corresponds to a 3% decrease in the ADP concentration and at 40 μM the fluorescence signal from NADH would be 2 to 3% below its linear value. At the upper limit of linearity for the curvette studies 10 μM NADH was present by the middle of the measurement period. Both the higher ADP level and the greater upper limit for NADH fluorescence with the flow cell are responsible for the higher upper limit of linearity.

The upper limit of linearity could not be tested for the serum standards since no standard had a high enough CK activity. The upper limit was therefore estimated to be near 150 mU/mL since a serum

standard of this activity should produce 40 μM NADH by the middle of the measurement period.

The resulting linear range of CK in serum for this system is from 0.19 to 150 mU/mL. With a 1 to 50 dilution, in-cell, the normal range of CK activity in serum will be within the linear range and even CK activities over 100 times the normal range can be analyzed without further dilutions.

3-Loop FIA System

The last study conducted with the FIA fluorometer system was to investigate the use of a 3rd injection valve in conjunction with the sample and reagent injection valves. Three injection loops allow the sample plug to be merged with two individual reagent plugs. Many applications can be made of this system that were not possible or practical with the 2-loop system. This arrangement would simplify studies of optimum reagent concentrations since the concentration of one component of the reagent, injected via the 3rd loop, could be changed from run to run without remaking the complete reagent solution. Another use for the 3-loop system would be for an assay in which two components of the reagent were not stable or compatible when mixed for extended periods of time. With the 3-loop FIA system, the two parts of the reagent could be merged immediately before measurement.

Only a brief study was made of the operation of the 3-loop system such that not all the operating parameters of this system were systematically optimized. The optimum of certain parameters such as the initial delay and sampling time, etc. are identical for both the 3-loop

and the 2-loop system. Other parameters, such as flow rate, were not specifically optimized for the 3-loop system but optimum values were estimated from the results of optimization studies of the 2-loop system.

Since the optimum flow rate per pump for the 2-loop system, 2.0 mL/min, produces a flow rate of 4.0 mL/min in the combined stream, it was assumed that for the 3-loop system the combined flow rate should also be 4.0 mL/min. All 3 pumps were therefore set to 1.4 mL/min., resulting in a combined flow rate of 4.2 mL/min which is as close to 4.0 mL/min as can be obtained with this system. With all three pumps operating at the same flow rate the mixing ratio for each loop was 1 to 3 in the combined carrier stream.

Initial studies with 550 µL injections of NADH showed that much broader peaks were produced with the 3-loop system. This is due to the increased length of an injected plug in the carrier stream when the mixing ratio is 1 to 3 rather than 1 to 2. Since the flow rate of the carrier stream and the tubing diameters are equal for the 3-loop and 2-loop systems, dispersion should not be significantly different for the two systems. The longer length, in time, of the merged plug would therefore mean that the nondispersed region in the center of the plug would also be longer. The plugs injected in the 3-loop system are therefore less affected by dispersion than were equal volume plugs injected in the 2-loop system, thus the optimum loop volume is probably less than 500 µL for the 3-loop system.

Repetitive stopped-flow measurements were made with injections of 550 µL of NADH using each loop individually. The RSD values of 10 runs for each loop were 0.54%, 0.66% and 0.52% for the sample valve, reagent

valve and the 3rd valve, respectively. These values match the run-to-run precision observed for similar studies done with the 2-loop system.

In order to conduct actual kinetic measurements, the ethanol assay was adapted to the 3-loop system. Separate solutions of NAD^+ and ADH were made up to inject via the 3rd loop and reagent loop, respectively. The concentrations of both solutions were made up 1.5 times greater than were optimum for the 2-loop system since the in-cell concentrations will be diluted 2 to 3 relative to the 2-loop system. A series of ethanol standards made up in buffer were analyzed to produce a calibration curve. The results of this study are summarized below:

Slope of the Calibration Curve (counts/M ethanol in vial)	=	1.8×10^9
SD of Blank Measurements (counts)	=	389
Theoretical Detection Limit (μM ethanol in vial)	=	0.43
RSD of Repetitive Runs (at 21 μM ethanol in vial)	=	1.1%

The higher value for the slope is due to the increased net signal levels of NADH after realignment of the cell holder. Taking that into account, the results are otherwise equivalent to those obtained for the 2-loop system. The RSD values of repetitive rate measurements of an ethanol standard are also equivalent for the two systems, therefore it does not appear that the use of a 3rd injection value adds any imprecision to the system operations.

Another capability of the 3-loop system is that certain blank measurements can be made which are not possible or practical with the 2-loop system. For example, blank measurements can be made of NAD^+

and a serum sample in the absence of ADH in order to measure the drift caused by photodecomposition. This same measurement could be made using the 2-loop system but a separate solution containing only NAD^+ would have to be prepared. Measurements of NAD^+ and a serum sample spiked with ethanol (21 μM, in vial) were made using the 3-loop system. To exaggerate the effects of the photodecomposition, the NAD^+ solution was made up to be 12 mM in-cell which is 6 times the optimum concentration and the serum standard was made up to an in-cell dilution of 1 to 51 (1 to 17 prior to injection). The results of this study are shown below:

Observed 16 s Rate Measurement (NAD^+, ADH and the Serum Standard)	=	38,630 counts
Expected 16 s Rate Measurement (calculated from the slope of the calibration curve)	=	42,630 counts
Blank Rate Measurement (Drift due to NAD^+ and serum in cell)	=	- 3,841
Corrected 16 s Rate Measurement (Observed rate + Blank Rate)	=	42,471

In this exaggerated example, the measurement of the blank allowed the observed rate to be corrected to prevent errors due to photodecomposition. If the rate measurement had not been corrected, the reported concentration of ethanol in the sample would have been low by 9%.

CONCLUSIONS

Fluorescence kinetic methods were proven to be effective for monitoring enzymatic serum assays as shown by the results of the ethanol and glucose studies. The ability to discriminate against steady state background fluorescence by kinetic measurements is necessary for fluorometric monitoring in serum since there is significant variation in the background fluorescence from sample to sample. The use of NADH as the fluorophore gave good results for the ethanol and glucose systems even though the sensitivity of the fluorescence method was compromised by both the high background fluorescence and high dilutions necessary to eliminate absorption interference by serum components. It was shown that the detection limit for NADH in a buffer solution using fluorescence monitoring was 30 times lower than the detection limit for NADH using absorbance monitoring. In a typical 1 to 200 dilution of serum, the fluorescence detection limit for NADH, in-cell, is only about a factor of 4 better than that for the absorbance method.

Studies using the LDH system showed that monitoring the decrease in fluorescence is less optimum than measuring the increase in fluorophore concentration for enzymatic fluorescence kinetic methods. For maximum linear range a high level of fluorophore must be present, therefore the sensitivity of fluorometric measurements is significantly reduced by the high noise levels due to the high blank fluorescence signals. The noise level of 2.8 μM NADH, the optimum

concentration for the LDH assay was nearly 3 times higher than that for a 1 to 150 dilution of Q-PAK Serum II. This clearly illustrates the magnitude of noise in the blank even without contributions from the serum sample itself.

Application of the fluorescence kinetic method to CK analysis showed the limitations of fluorometric measurements of NADH in a serum matrix. The need for large dilutions to minimize absorption interference and the high background fluorescence from serum resulted in detection limits above the normal levels of CK in serum. To obtain detection limits for CK below normal serum levels and also below the detection limit for absorbance methods, an increase in the measurement time from 16 s to 3 minutes is necessary. The advantage of faster analysis times must be sacrificed for sensitivity in this example.

The use of an alternate fluorophore, such as resorufin, eliminated much of the interference effects and also showed 50 times greater sensitivity than NADH. The use of an alternate fluorophore is a more efficient way to eliminate interference than are sample clean-up procedures. This would be especially true for enzyme assays, where serum proteins would have to be removed without effecting the activity of the analyte enzyme. Sample clean-up procedures often add significantly to the time and expense of each assay.

The results of these studies showed that the detection limits of the fluorescence kinetic methods were often limited by the purity of

the reagents as was the case for the CK assay where ADP purity limited the sensitivity. Reagent clean-up procedures were not investigated in this research but perhaps some simple procedures could be used to at least reduce the level of contamination in reagents. In the CK assay for example, it may be possible to reduce the relative concentration of ATP in an ADP solution by adding an enzyme and proper cofactors to convert ATP to ADP prior to the start of the reaction. If the activity of this "clean-up" enzyme were kept low it would not cause significant interference in the rate measurement of CK. Such a procedure would improve the sensitivity of this assay and eliminate variations in the level of contamination of ADP solutions from batch to batch.

From these studies of enzymatic fluorescence kinetic methods, a procedure was established for optimizing this type of assay. First, studies of the fluorophore itself must be conducted to determine the range of linearity, minimum serum dilutions to eliminate interference and the optimum measurement period. Secondly, the reagent concentrations must be adjusted to obtain the maximum of the reaction rate vs. blank noise ratio. Unlike absorbance methods where reagent concentrations generally have little effect on blank noise levels, fluorometric methods are affected by the blank signal and subsequent noise level contributed by reagent fluorescence. For optimum conditions, a compromise is often necessary between the fastest reaction rate and the lowest blank noise level.

The computer-controlled FIA system has significantly enhanced the ease of operation and versatility of the microcomputer-based kinetic spectrofluorometer. One of the main advantages of using the FIA system for automation was its relative simplicity which allowed easy adaptation to computer control. Computer control greatly simplifies optimizations of operating parameters such as flow rate, since changes can be made with software rather than adjustments of the hardware. Another important feature of computer control is that it is very effective for timing and synchronization of operations of each component, which is critical for the optimum performance of the system.

The single most critical component of the FIA-fluorometer system is the fluorescence flow cell, since it can affect the performance of both the fluorometer and the FIA system. The spectral properties of the flow cell used for these studies showed significantly less interference than did the cuvette. Less dilution of serum was required, thus the detection limits in terms of the undiluted sample were improved by nearly a factor of 3. The main weakness of the flow cell was its poor rinse-out efficiency which contributed significantly to the observed dispersion and baseline width of injected plugs of solution. A simple way to improve the performance of the flow cell would be to reduce the cross sectional area of the sample cavity and subsequently the width of the excitation and emission slits on the cell housing. This would improve the rinse-out efficiency and also

lower the pre-and post-filter effects of serum components, thereby compensating for the loss in sensitivity.

The performance of enzymatic fluorescence kinetic serum assays with the FIA fluorometer proved that this type of assay could be automated using an FIA system. The versatility of the FIA ratemeter allows the use of several different modes of kinetic measurement. The most effective method for enzymatic serum assays was shown to be the stopped-flow method. The main problem encountered with stopped-flow measurements was from drifts caused by photodecomposition. It appeared that the photodecomposition did not effect the actual reaction rates of the assays studied in this research. It may be possible to prevent photodecomposition during the measurement period by irradiating the samples prior to analysis.

The FIA system provides greater throughput than was obtained for manual operation of the fluorometer since the FIA system reduces the time of solution delivery and cell rinse-out per run by nearly 10 s. Improved precision in solution delivery is also apparent by comparing the run to run precision of steady state measurements of NADH. For the cuvette studies, the RSD of measurements of 1 μM NADH was about 1.5 to 2%, where with stopped-flow FIA measurements the run-to-run RSD was 0.45%.

The addition of a third injection loop to the FIA system certainly expanded the versatility and capabilities of the FIA ratemeter. The operation of the third loop did not sacrifice any performance or precision of the 2-loop system. The most useful

application of the 3-loop system may be for optimization studies since changes in the reagent composition can be easily made without remaking the entire reagent for each run. The third loop could serve to inject a standard for the operation of a standard addition technique.

Future studies of the FIA fluorometer should include the application of gradients for kinetic assays. The use of gradients of individual components of the reagent could simplify the optimization of each component to single run operations. If a gradient of one or more components is merged with a stream containing a steady state concentration of all other components including the analyte, an optimization curve would be generated by the detector response. Many other novel kinetic measurement modes may be possible using gradients of either the sample or the reagent.

Bibliography

1. H. L. Pardue, A Comprehensive Classification of Kinetic Methods of Analysis used in Clinical Chemistry, Clin. Chem. 23, 2189-2201 (1977).

2. R. L. Wilson, Design, Development and Optimization of a Fluorometric Reaction Rate Instrument and Method of Analysis for Metal Ions, Oregon State University, (1976).

3. H. V. Malmstadt, C. J. Delaney, and E. A. Cordos, Instruments for Rate Determinations, Anal. Chem. 44, 79A-89A (1972).

4. H. B. Mark, Jr., L. J. Papa, and C. N. Reilley, Reaction Rate Methods, Adv. Anal. Chem. Instrum. 2, 255-385 (1963).

5. H. B. Mark, Jr., Reaction Rate Methods in Analysis, Talanta 19, 717-746 (1972).

6. H. B. Mark, Jr. and G. A. Rechnitz, Kinetics in Analytical Chemistry, Wiley-Interscience, New York (1968).

7. K. B. Yatsimerskii, Kinetic Methods of Analysis, Pergamon press, Oxford, (1966).

8. H. L. Pardue in: Advances in Analytical Chemistry and Instrumentation, (C.N. Reilley and F.W. McLafferty, eds.), Vol. 7, pp. 141-207, Wiley-Interscience, New York, (1968).

9. W. J. Blaedel and G. P. Hicks in: Anvances in Analytical Chemistry and Instrumentation, (C. N. Reilley and F.W. McLafferty, eds.) Vol. 3, pp. 126-140, Wiley-Interscience, New York, (1964).

10. J. D. Ingle and Mary A. Ryan in: Modern Fluorescence Spectroscopy Vol. III, (E.L. Wehry, ed.) Plenum Press, New York, (1980).

11. G. G. Guilbault, Handbook of Enzymatic Methods of Analysis, Marcel Dekker Inc., New York, (1976).

12. H. U. Bergmeyer, ed., Methods of Enzymatic Analysis, Academic Press Inc., New York, (1963).

13. O. H. Lowry, J. V. Passonneau, A Flexible System of Enzymatic Analysis, Academic Press Inc., New York (1972).

14. G. G. Guilbault, Use of Enzymes in Analytical Chemistry, Anal. Chem. 40, 459R-471R (1968).

15. N. Tietz, Fundamentals of Clinical Chemistry, W.B. Saunders Co., Philadelphia, (1976).

16. W. Roberts, On the Estimation of the Amylolytic and Proteolytic Activity of Pancreatic Extracts, Proc. Roy. Soc. London 32, 154-161 (1881).

17. L. B. Rogers, Analytical Chemistry: The Journal and the Science, the 1950's, Anal. Chem. 50, 1298A-1301A (1978).

18. S. R. Crouch, F. J. Holler, P. K. Notz, and P. M. Beckwith, Automated Stopped-Flow Systems for Fast Reaction-Rate Methods, Appl. Spec. Rev. 13(2), 165-259 (1977).

19. T. O. Tiffany in: Modern Fluorescence Spectroscopy (E. L. Wehry, Ed.) Vol. 2, pp. 1-48, Plenum Press, New York (1976).

20. R. L. Wilson and J. D. Ingle, Jr., Evaluation of Ratemeters: Application To An Improved Fixed-Time Instrument, Anal. Chim. Acta, 83, 203-214 (1976).

21. R. A. Parker and Harry L. Pardue, Miniature On-Line Digital Computer for Multipurpose Applications, Applications to Kinetic Analyses, Anal. Chem. 44, 1622-1628 (1972).

22. E. S. Irack and H. V. Malmstadt, Ratemeter Interface for a Minicomputer-controlled Reaction-Rate Instrument, Anal. Chem. 45, 1766-1770 (1973).

23. R. L. Wilson and J. D. Ingle, Jr., Design and Operation of a Fluorometric Reaction Rate Instrument, Anal. Chem. 49, 1060-1065 (1977).

24. J. D. Ingle, Jr. and S. R. Crouch, Theoretical and Experimental Factors Influencing the Accuracy of Analytical Rate Measurements, Anal. Chem. 43, 697-701 (1971).

25. J. D. Ingle, Jr., and S. R. Crouch, Signal to Noise Ratio Theory of Fixed-Time Spectrophotometric Reaction Rate Measurements, Anal. Chem. 45, 333-338 (1973).

26. T. C. O'Haver, The Development of Luminescence Spectrometry as an Analytical Tool, J. Chem. Ed. 55, 423-428 (1978).

27. A History of Analytical Chemistry (H. A. Laitenen and G. W. Ewing, ed.), Division of Analytical Chemistry of the American Chemical Society (1977).

28. S. Udenfriend, Fluorescence Assay in Biology and Medicine, Academic Press, New York, (1962).

29. H. Theorell and A. Nygaard, Kinetics and Equilibria in Flavoprotein Systems, 1. A Fluorescence Recorder and its Application to a Study of the Dissociation of the Old Yellow Enzyme and its Resynthesis from Riboflavinphosphate and Protein, Acta. Chem. Scand. 8, 877-888 (1954).

30. O. H. Lowry, N. R. Roberts, and J. I. Kapphahn, The Fluorometric Measurement of Pyridine Nucleotides, J. Biol. Chem. 224, 1047-1064 (1957).

31. R. L. Wilson and J. D. Ingle, Jr., A Kinetic Fluorometric Determination of Aluminum. Anal. Chim. Acta, 92, 417-421 (1977).

32. E. A. Bozhevol'nov, S. U. Kreingol'd, and L. I. Sosenkova, Comparative Study of Three Reagents for the Kinetic Determination of Copper Traces, Khim. Veshchesty. No. 30, 176-185 (1967), in Russian, C.A. 69: 73657d.

33. G. G. Guilbault and G. J. Lubrano, A Fluorometric Kinetic Method for the Determination of Organophosphorus and Organocarbonyl Compounds, Anal. Chim. Acta. 43, 253-261 (1968).

34. D. N. Kramer, Design of Fluorometric Analytical Methods, Pure Appl. Chem. 48, 65-67 (1976).

35. H. Steinhart, Determination of Tryptophan in Foods and Feedstuff with a Kinetic Method, Anal. Chem. 51, 1012-1016 (1979).

36. H. C. Clarke, A Photodecomposition Fluorometric Method for the Determination of Riboflavin in Whole Blood, Intern. Z. Vitaminforsch. 39, 182-191 (1969).

37. J. J. Aaron, J. E. Villafranca, V. R. White, and J. M. Fitzgerald, A Quantitative Photo-Chemical-Fluorimetric Method for Measurement of Nonfluorescent Vitamin K, Appl. Spec. 30, 159-162 (1976).

38. O. Warburg, Wassenstoffubertragende Fermente, Verlag-Springer, Berlin (1948).

39. N. Kaplan, S. Colowick and C. Barnes, Effect of Alkali on Diphosphopyridine Nucleotide, J. of Biol. Chem. 191, 461-472 (1951).

40. G. G. Guilbault, Practical Fluorescence. Theory, Methods and Techniques, Marcel Dekker Inc., New York (1973).

41. F. R. Chen, Photoinactivation of L-Glutamate Dehydrogenase in a Spectrofluorometer, Biochem. and Biophysical Res. Comm. 17, 141-145 (1964).

42. R. Bonnichsen and H. Theorell, An Enzymatic Method for the Microdetermination of Ethanol., Scand. J. of Clin. Lab. Invest. 3, 58-62 (1951).

43. F. W. Ellis and J. B. Hill, An Automated Fluorometric Procedure for the Enzymatic Determination of Ethanol in Fingertip Blood, Clin. Chem. 15, 91-101 (1969).

44. H. V. Malmstadt and T. P. Hadjiioannou, Specific Enzymatic Determination of Alcohol in Blood by an Automatic Spectrophotometric Reaction Rate Method. Anal. Chem. 34, 455-458 (1962).

45. T. P. Hadjiioannou, S. I. Hadjiioannou, J. Avery, H.V. Malmstadt, Automated Anzymatic Determination of Ethanol in Blood, Serum, and Urine with a Miniature Centrifugal Analyzer., Clinical Chemistry 22, 802-805 (1976).

46. J. C. W. Kuan, S. S. Kuan and G. G. Guilbault, The Immobilized-Enzyme Stirrer Part 2. Fluorimetric Determination of Ethanol with the Use of Immobilized Alcohol Dehydrogenase., Analytica Chimica Acta 100, 229-233 (1978).

47. J. I. Peterson and D. S. Young, Evaluation of the Hexokinase/Glucose-6-PO_4 Dehydrogenase Method of Determination of Glucose in Urine, Analytical Biochemistry 23, 301-316 (1968).

48. S. Kaufman, Studies on the Mechanisms of the Reaction Catalyzed by the Phosphorylating Enzyme, J. of Biol. Chem. 216, 153-158 (1955).

49. M. W. Slein, in Methods of Enzymatic Analysis (H. U. Bergmeyer, ed.), Academic Press Inc., New York (1963).

50. B. Scherstein and G. Tibbling, Semiautomated Assay of Normal Concentrations of Urinary Glucose by an Enzymatic Fluorometric Technic, Clin. Chem. 14, 243-252 (1968).

51. B. Lloyd, J. Burrin, P. Smythe and K. G. M. M. Alberti, Enzymatic Fluorometric Continuous-Flow Assays for Blood Glucose, Lactate, Pyruvate, Alanine, Glycerol and 3-Hydroxybutyrate., Clin. Chem. 34, 1724-1729 (1978).

52. T. O. Tiffany, J. M. Jansen, C. A. Burtis, J. B. Overton and C. D. Scott, Enzymatic Kinetic Rate and End-point Analyses of Substrate, by Use of a GeMSAEC Fast Analyzer, Clin. Chem. 18, 829-835 (1972).

53. H. V. Malmstadt and S. I. Hadjioannou, A New Automatic Rate Method for Selective Determination of Glucose in Serum, Plasma, or Blood, Anal. Chem. 34, 452-455 (1962).

54. G. G. Guilbanlt, M. H. Sadar and K. Peres, Fluorometric Determination of Carbohydrates, Anal. Biochem. 31, 91-101 (1969).

55. G. G. Guilbault, P. J. Brignac and M. Zimmer, Homovanillic Acid as a Fluorometric Substrate for Oxidative Enzymes, Anal. Chem. 40, 190-196 (1968).

56. W. E. C. Wacker, D. D. Ulmer and B. L. Vallee, Metalloenzymes and Myocardial Infarction. II. Malic and Lactic Dehydrogenase Activities and Zinc Concentrations in Serum, New Eng. J. of Med. 255, 449-460 (1956).

57. L. Brocks and H. G. Olken, An Automated Fluorometric Method for the Det. of LDH in Serum, Clin. Chem. 11, 748-762 (1965).

58. G. G. Guilbault and R. Zimmerman, A Semi-Solid Surface Fluorescence Method for the Det. of LDH, Anal. Clin. Acta 58, 75-80 (1972).

59. I. T. Oliver, A Spectroscopic Method for the Determination of CK and Myokinase, Biochem. J. 61, 116-122 (1955).

60. S. M. Sax and J. J. Moore, Fluorometric Measurement of Creatine Kinase Activity, Clin. Chem. II, 951-958 (1965).

61. A. L. Sherwin, G. R. Siber and M. M. Elhilali, Fluorescence Technique to Demonstrate Creatine Phosphokinase Isoenzymes, Clin. Chim. Acta 17, 245-249 (1967).

62. M. S. Denton, W. D. Bastick, S. R. Dinsmore and J. E. Mrochek, Chromatographic Separation and Continuously Referenced, On-line Monitoring of CK Isoenzymes by Use of an Immobilized - Enzyme Microreactor., Clin. Chem. 24, 1408-1413 (1978).

63. H. K. Y. Lau and G. G. Guilbault, A "Reagentless" Fluorometric Method for Creatine Kinase Activity in Serum., Clin. Chem. 19, 1045-1048 (1973).

64. A. L. Siegel and P.S. Cohen, An Automated Determination of Creatine Phosphokinase, "Automation in Analytical Chemistry, Technicon Symposia 1966," (E. Kawerau, et al., Eds.), White Plains, NY (1967).

65. G. A. Fleisher, Automated Method for the Determination of Serum CK Activity, Clin. Chem. 13, 233-240 (1967).

66. J. A. S. Rokos, S. B. Rosalki and D. Tarlow, Automated Fluorometric Procedure of Measurement of Creatine Phosphokinase Activity, Clin. Chem. 18, 193-201 (1969).

67. J. B. Armstrong, J. A. Lowden and A. L. Sherwin, Automated Fluorometric CK Assay. Measurement of 100-Fold Normal Activity without Serum Dilution, Clin. Chem. 20, 560-565 (1974).

68. G. G. Guilbault and D. N. Kramer, Fluorometric Procedure for Measuring the Activity of Dehydrogenases, Anal. Chem. 37, 1219-1221 (1965).

69. M. Rhodes and L. Wooltorton, A New Fluorometric Method for the Determination of Pyridine Nucleotides in Plant Material, Phytochemistry 7, 337-353 (1968).

70. C. C. Gilhuus-Moe and G. Gogstad, Methodological Studies on a Direct Enzymatic Fluorometric Quantitation of Total Bile Acids in Serum, Fresenius Z. Anal. Chem. 290, 181-182 (1978).

71. F. Mashige, K. Imai and T. Osuga, A Simple and Sensitive Assay of Total Serum Bile Acids, Clin. Chim. Acta 70, 79-86 (1976).

72. W. B. Furman, Continuous-Flow Analysis. Theory and Practice. Marcel Dekker Inc., New York (1976).

73. L.T. Skeggs, An Automated Method for Colorimetric Analysis, Am. J. of Clin. Path. 28, 311-322 (1957).

74. C. B. Ranger, Flow Injections Analysis; Principles, Techniques, Applications and Design, Anal. Chem. 53, 20A-30A (1981).

75. B. Rocks and C. Riley, Flow Injection Analysis: A New Approach to Quantitative Measurements in Clinical Chemistry., Clin. Chem. 28, 409-421 (1982).

76. J. Ruzicka and E.H. Hansen, Flow Injection Analysis. Principles, Applications and Trends, Anal. Chim. Acta 114, 19-44 (1980).

77. K. K. Stewart, Flow Injection Analysis: A Review of It's Early History, Talanta 28, 11-18 (1981).

79. R. Tijssen, Axial Dispersion and Flow Phenomena in Helically Coiled Tubular Reactors for Flow Analysis and Chromatography., Anal. Chim. Acta 114, 71-89 (1980).

80. K. K. Stewart, Depulsing System for Positive Displacement Pumps, Anal. Chem. 49, 2125-2126 (1977).

81. B. W. Renoe, K. K. Stewart, G. R. Beecher, M. R. Wills and J. Savory, Automated Multiple FIA in Clinical Chemistry. Determination of Albumin with Bromocresol Green, Clin. Chem. 26, 331-334 (1980).

82. H. Bergamin, E. A. G. Zaggato, F. J. Krug and B. F. Reis, Merging Zones in Flow Injection Analysis, Anal. Chim. Acta 101, 17-23 (1978).

83. M. F. Ginè, H. Bergamin, E. A. G. Zaggato and B.F. Reis, Simultaneous Detection of Nitrate and Nitrite by FIA, Anal. Chim. Acta 114, 191-197 (1980).

84. K. K. Stewart, J.F. Brown, and B.M. Golden, A Microprocessor Control System for Automated Multiple Flow Injection Analysis, Anal. Chim. Acta 114, 119-127 (1980).

85. B. Karlberg and S. Thelander, Extraction Based on the Flow Injection Principle. Part 3: Fluorometric Determination of Vitamin B_1 (Thiamine) by the Thiochrome Method, Anal. Chim. Acta 114, 129-136 (1980).

86. T. Imasaka, T. Harada and N. Ishibashi, Fluorimetric Determination of Gallium with Lumogallion by FIA Based on Solvent Extraction, Anal. Chim. Acta 129, 195-203 (1981).

87. J. I. Braithwaite and J. W. Miller, FIA with a Fluorimetric Detector for Determinations of Glycine and Albumin, Anal. Chim. Acta 106, 395-399 (1979).

88. J. H. Dahl, D. Espersen and A. Jensen, Differential Kinetic Analysis and FIA (Part 1). CDTA Complexes of Mg and Sr, Anal. Chim. Acta 105, 327-333 (1979).

89. J. Růžička and E. H. Hansen, Stopped-flow and Merging Zones, A New Approach to Enzymatic Assays by FIA., Anal. Chim. Acta 106, 207-224 (1979).

90. P. J. Worsfold, J. Ruzicka and E. H. Hansen, Rapid Automated Enzymatic Method for the Determination of Alcohol in Blood and Beverages using FIA, Analyst 106, 1309-1317 (1981).

91. M. A. Ryan, Design and Development of an Instensified Diode Array System and Its Application to New Fluormetric Reaction Rate Methods of Analysis, Oregon State University (1981).

92. M. A. Ryan and J. D. Ingle, Jr., Construction of a Microcomputer-Based Reaction-Rate Ratemeter, Talanta 28, 539-542 (1981).

93. A. S. Ambrose, unpublished work, Oregon State University (1978).

94. Sea-16 Users Manual, Seawell Marketing Inc., 315 NW 85th St., Seattle, WA (1979).

95. Little Buffered Motherboard Manual, Seawell Marketing Inc., 315 N.W. 85th St., Seattle, WA (1979).

96. L. R. Dewald, unpublished work, Oregon State University (1978).

97. G. L. Campi, A Reaction Rate Determination of Aluminum with a Microcomputer-Based Spectrofluorometer, Oregon State University (1982).

98. KIM-1 Microcomputer Module; Publications 6500-15B, 6500-10A, 6500-50A, MOS Technology, 950 Rittenhouse Rd., Morristown, PA (1976).

99. IVEK Pump Manual, IVEK Corp., 4 Plain Hill Rd, Springfield, VT (1980).

100. Operation Manual for the Tecnicon Autoanalyzer; Technicon Publication No. TA1-0201-00, Technicon Instruments Corp., Tarrytown, NY (1971).

101. D. F. Marino, unpublished work, Oregon State University (1980).

102. C. Boisvert, A Couple of 6522 Applications, Interactive Newsletter 1, p. 9, Rockwell International, P.O. Box 3669 RC 55, Anaheim, CA (1980).

103. L. G. Morin, Creatine Kinase, Re-examination of Optimum Reaction Conditions, Clin. Chem. 23, 1569-1575 (1977).

104. E. J. Cohn, F. R. N. Gurd, D. M. Surgenor, B. A. Barnes, R. K. Brown and G. Derouaux, Separation of Protein Components of Human Plasma, J.A.C.S. 72, 465-474 (1950).

105. J. L. Oncley, F. R. N. Gurd and M. Melin, Preparation and Properties of Serum and Plasma Proteins XXV. Composition and Properties of Human Serum Beta-Lipoproteins., J.A.C.S. 72, 458-464 (1950).

106. J. G. Atwood and H. W. Marshall, Factors in Serum that Limit Speed and Precision of Ultramicro Enzyme Rate Measurements, Lab. Med. Newsletter 5, 6-8 (1973).

107. G. J. Proksch and D. P. Bonderman, Preparation of Optically Clear Lyophilized Human Serum for Use in Preparing Control Material, Clin. Chem. 22, 456-460 (1976).

108. M. L. Mertens and J. H. R. Kagi, A Graphical Correction Procedure for Inner Filter Effect in Fluorescence Quenching Titrations, Anal. Biochem. 96, 448-455 (1979).

109. C. C. Wratten and W. W. Cleland, Product Inhibition Studies on Yeast and Liver Alcohol Dehydrogenase, Biochemistry 2, 935-941 (1963).

110. J. G. Atwood and J. L. DiCesare, Making Enzymatic Methods Optimum for Measuring Compounds with a Kinetic Analyzer, Clin. Chem. 21, 1263-1269 (1975).

111. J. E. Davis and J. Pevnick, Optimization of the Coupled Enzymatic Measurement of Substrate, Anal. Chem. 51, 529-533 (1979).

112. N. C. Melchior and J. B. Melchoir, The Role of Complex Metal Ions in the Yeast Hexokinase Reaction, J. of Biol. Chem. 231, 609-623 (1957).

113. L. Glaser and D. H. Brown, Purification and Properties of d-Glucose-6-PO_4 Dehydrogenase, J. of Biol. Chem. 216, 67-79 (1955).

114. R. J. L. Bondar and D. C. Mead, Evaluation of Glucose-6-PO_4 Dehydrogenase from Leuconostoc Mesenteroides in the Hexokinase Method for Determining Glucose in Serum, Clin. Chem. 20, 586-590 (1974).

115. A. L. Lehninger, Biochemistry, 2nd edition, p. 204, Worth Publishers Inc., NY (1975).

116. S. Passen and W. Gehnaro, An Automated System for the Fluorometric Determination of Serum Lactate Dehydrogenase, Am. J. of Clin. Path. 46, 69-81 (1966).

117. S. N. Buhl, K. Y. Jackson and B. Graffunder, Optimal Reaction Conditions for Assaying Human Lactate Dehydrogenase Pyruvate-to-Lactate at 25, 30 and 37°C., Clin. Chem. 24, 261-266 (1978).

118. G. Szasz, W. Gruber and E. Bernt, Cratine Kinase in Serum 1. Determination of Optimum Reaction Conditions, Clin. Chem. 22, 650-656 (1976).

119. L. G. Morin, Creatine Kinase - Re-examination of Optimum Reaction Conditions, Clin. Chem. 23, 1569-1575 (1977).

120. M. M. Nachlas, S. I. Margulies, J.D. Goldberg and A.M. Seligman, The Determination of Lactic Dehydrogenase with a Tetrazolium Salt, Anal. Biochem. 1, 317-326 (1960).

121. C. Green, J.L. Oncley and M.L. Karnovsky, Lipid Composition of Lipoproteins of Normal Human Plasma, J. of Biol. Chem. 235, 2884-2885 (1960).

Appendices

Appendix I

Program Listings for the FIA-Ratemeter System

Main Program (BASIC)

```
5 CM = Ø
6 DIM PR(4),T(4)
7 PRINT"DO YOU WANT CONTINOUS RUN MODE ?"
8 INPUT" ";CN
9 INPUT"# OF RUNS (ADD VALUE OF CM)";CO
10 IF CN = 1 GOTO 125
11 PRINT"DO YOU WANT TO CHANGE MEAS. CONDITIONS?"
20 INPUT " ";IN
25 IF IN = Ø THEN 125
28 PRINT" INPUT MEASUREMENT TIME (IN SEC.)"
30 INPUT " MEASNO = ";MEASNO
33 PRINT" INPUT Ø.25 SEC. TIME INTERVALS PER MEMORY DATA POINT"
35 INPUT" TIME =";TIME
36 MEASNO = MEASNO * (1/(TIME*.25))
37 HLDT = TIME
38 PRINT"INPUT DELAY (IN SEC.)"
39 DELAY = DELAY * 4
40 INPUT " DELAY TIME =";DELAY
41 C3 = MEASNO/2
43 RCAL = Ø
45 OFFSET = Ø
50 PRINT"DVM MODE - INPUT 4, RATE MODE - INPUT 1"
53 PRINT "INPUT MODE OF CALCULATION"
55 INPUT "MODE OF CALCULATION";MODE
58 PRINT "INPUT # OF PAGES FOR DATA STORAGE"
60 INPUT " PAGES = ";PAGE
63 PAGE = PAGE + 6 :REM CORRECT FOR PLACEMENT INTO "TOP"
65 GT = 126/(MEASNO) :REM RECALCULATION OF FULL PAGE VALUE
70 QT = INT(GT)
80 FALL = QT * MEASNO * 2
85 PRINT "VALUES PER PAGE OF DATA",QT
90 POKE 992,MEASNO
95 POKE 993,TIME
100 POKE 994 ,DELAY
105 POKE 995,OFFSET
110 POKE 996,MODE
115 POKE 997,PAGE
120 POKE 849,FALL
125 GOTO 600
153 POKE 11,09
155 POKE 12,03
160 X = USR(Y)
170 OVRFLO = PEEK(231)
175 RATSYN = PEEK(230)
180 DATFUL = PEEK(229)
```

```
185 IF OVRFLO = 170 THEN 215  :REM FOR OVERFLOW
190 IF DATFUL = 187 THEN 205  :REM DATA SPACE FULL
195 IF RATSYN = 99 THEN 245 : REM SIGNALS NEG. RATE
198 IF RATSYN = 11 THEN 225 :REM SIGNALS POS, RATE
200 IF RATSYN = 0 THEN 235 : REM SIGNALS DVM MODE
205 PRINT " DATA STORAGE IS FULL !"
210 GOTO 400
215 PRINT "THERE IS AN OVERFLOW"
220 STOP
225 B$ = "POS. RATE ="
230 GOTO 246
235 B$ = "DVM VALUE ="
240 GOTO 246
245 B$ ="NEG. RATE ="
246 CF = PEEK(1037) :REM THIS LOC SIGNALS FLOW RATE CHANGE
247 LASTI = PEEK(1034) :REM THIS SIGNALS IF LAST INT HAS OCCURED
248 IF LASTI > 1 THEN POKE 32782,127 :REM DISABLES ALL 6522 INT.S
250 X = PEEK(1005)
255 Y = PEEK(1006)
260 Z = PEEK(1007)
265 Z = Z * 65536.0
270 Y = Y * 256.0
275 SUM = X + Y + Z
276 IF RATSYN <> 99 THEN 278
277 SUM = 16777215 - SUM :REM TO CONVERT NEG. RATE TO POS. VALUE
278 POKE 11,15 :POKE 12,05 :X = USR(Y) :REM TO PROTECT PRINT FROM INT.
279 IF CF <> 207 GOTO 281
280 PRINT"FINAL F.R." :POKE 1037 ,00
281 PRINT B$,SUM
282 POKE 11,17 :POKE 12,05 :X = USR(Y) :REM RE-ENABLES INTERRUPTS
283 IF RCAL = 1 THEN 350
285 IF RATSYN = 0 THEN 305 :REM FOR RETURN TO DVM MODE
290 POKE 11,184 :REM FOR RETURN TO RATE MODE
295 POKE 12,03
300 X = USR(Y)
302 GOTO 170
305 POKE 11,202 :REM RETURN TO DVM
310 POKE 12,03
315 X = USR(Y)
320 GOTO 170
325 POKE 11,14 : REM FOR 1ST RECALCULATION
326 POKE 229,0 :REM REZERO FULL PAGE SIGNAL
330 POKE 12,01
335 X = USR(Y)
340 GOTO 170
350 IF RATSYN = 0 THEN 375
355 POKE 11,41
360 POKE 12,01
365 X = USR(Y)
370 GOTO 170
375 POKE 11,65 : REM RECAL. OF DVM MODE
```

```
380 POKE 12,01
385 X = USR(Y)
390 GOTO 170
395 STOP
400 PRINT"RECALCULATE DATA ?"
401 IF CN = 1 THEN RCAL = 0
402 IF CM = CO GOTO 7
403 IF CN = 1 GOTO 10
405 INPUT"-";RCAL
410 IF RCAL = 1 THEN 435
415 PRINT "START NEW RUN ?"
420 INPUT "-";R2
425 IF R2 = 1 THEN 7
430 STOP
435 PRINT "CHANGE CONDITIONS FOR RECALCULATION ?"
440 INPUT"-";CRC
445 IF CRC = 1 THEN 455
450 GOTO 325
455 PRINT" INPUT NEW MEASUREMENT TIME (IN SEC.)"
460 INPUT "MEASNO =";MEASNO
465 MEASNO = MEASNO * (1/(HLDT * .25))
467 C3 = MEASNO/2
470 AT = 126/(MEASNO) :REM RECAL. FULL PAGE VALUE
475 AT = INT(AT)
480 F2 = AT * MEASNO * 2
485 IF F2 < FALL GOTO 495
490 POKE 1020,FALL :REM LOAD THE SMALLER OF THE TWO
492 GOTO 500
495 POKE 1020,F2 :REM FULL PAGE VALUES INTO $YINDEX
500 POKE 992,MEASNO
505 PRINT" INPUT OFFSET IN SEC. (LAST VALUE PER PAGE MAY BE WRONG)"
510 INPUT"OFFSET =";OFFSET
515 OFFSET = OFFSET * 4
520 POKE 995,OFFSET
525 F3 = PEEK(1020)
530 LVP = F3/(MEASNO * 2)
535 PRINT " # OF VALUES PER PAGE (RECAL.)", LVP
540 PRINT " INPUT NEW MODE (4 OR 1)"
545 INPUT "MODE =";MODE
550 POKE 996,MODE
555 GOTO 325
560 STOP
600 IF CN = 1 GOTO 692
601 PRINT"DO YOU WANT TO CHANGE LOOPS,PUMPS,SAMPLER TIMES?"
605 INPUT "-";C8
610 IF C8 = 0 GOTO 692
611 D6 = 0
615 PRINT "INPUT DELAY FOR INITIAL RINSE (IN SEC.)"
620 INPUT "-"; D1 : D1 = D1 * 4
625 PRINT "INPUT DELAY FOR SAMPLING (IN SEC.)"
630 INPUT "-";D2 : D2 = D2 * 4
635 PRINT "INPUT DELAY BETWEEN REAGENT AND SAMPLE"
```

```
640 INPUT "-"; D3 : D3 = D3 * 4
645 PRINT"INPUT DELAY FOR RINSING BOTH LOOPS (SEC.) (SAMPLE INJECTED)"
650 INPUT "-";D4 : D4 = D4/.1309
665 POKE 233,D1 : REM RINSE, BYPASS 1, BYPASS 2
670 POKE 234,D2 : REM SAMPLE , BYPASS 1, BYPASS 2
675 POKE 235,D3 : REM RINSE, SAMPLE 1, BYPASS 2
685 PRINT"INPUT DELAY BETWEEN SAMPLE INJ. AND CHANGE OF FLOW RATE"
690 INPUT "-"; D5 : D5 = D5/0.1309
692 IF D6 = 1 GOTO 705 :REM D6 SIGNALS RE-RUN SET-UPP FOR D5<D4
693 IF D6 = 2 GOTO 725 :REM D6 SIGNALS RE-RUN SET-UP FOR D4<D5
695 IF D4<D5 GOTO 720 :D4 = D4 - D5 :D6 = 1
696 D4 = D4 - D5
697 D6 = D6 + 1
700 IF D4 < 1 THEN D4 = 1
705 POKE 1152,D5 :REM LOADS 1ST T2 DELAY INTO INT. SUBROUTINE
710 POKE 1258,D4 :REM LOADS 2ND T2 DELAY INTO CHANGE FLOW SERV ROUTINE
715 POKE 6142,208 :REM LOADS INT. VECTOR (LO BYTE) WITH 1ST SERVICE ROU
716 POKE 1195,125 :REM PREVENTS UNWANTED INTS. BEFORE DISABLING
718 GOTO 740
720 D5 = D5 - D4 : IF D5 < 1 THEN D5 = 1
721 D6 = 2
725 POKE 1152,D4 :REM LOADS APPROP. T2 DELAYS FOR D4<D5
726 POKE 1195,D5
727 POKE 1258,125 :REM PREVENTS UNWANTED INTS. BEFORE DISABLING
730 POKE 6142,160 :REM LOADS  INT. VECTOR WITH 1ST SERIVEC ROUTINE
735 REM THE 1ST SERVICE ROUTINE DEPENDS ON WHETHER D5 >D4 ,D4>D5
740 IF CN = 1 GOTO 850
741 PRINT"DO YOU WANT TO CHANGE FLOW RATES?"
742 INPUT" ";D9 :IF D9 = 0 GOTO 850
745 PRINT"FLOW RATES MUST BE 0.0 TO 4.4 ML/MIN IN MULTIPLES OF 0.2"
750 PRINT"INPUT INITIAL AND FINAL FLOW RATES FOR SAMPLE PUMP(PA7-PAA3)"
755 INPUT "INITIAL";PR(1) :INPUT "FINAL";PR(2)
760 PRINT"INPUT INITIAL AND FINAL FLOW RATES FOR REAGENT PUMP(PB4-PB0)"
765 INPUT"INITIAL";PR(3) : INPUT"FINAL";PR(4)
770 FOR I = 1 TO 4 :REM THIS LOOP CONVERTS PR VALUES TO PROPER FORM
775 QR = INT(PR(I)) :TR = PR(I) - QR :TR = TR/2 * 10
780 IF QR = 4 GOTO 800
785 QR = QR * 8 : GOTO 805
800 QR = 28 : TR = TR + 1
805 T(I) = QR + TR :
810 NEXT I
815 FOR J = 1 TO 2 :REM GETS T(1) AND T(2) INTO FORM FOR PA7 - PA3
820 T(J) = T(J) *8
825 NEXT J
830 POKE 1035,T(2) :REM 1035 = $40B FINAL FLOW PA7 - PA3
832 T(4) = T(4) + 32 :REM THIS SWITCHES FLOW CELL BYPASS VIA PB5
835 POKE 1036,T(4) :REM 1036 = NXTFB  ($40C) FINAL FLOW PB4-PB0
840 POKE 1038,T(1) :REM 1038 = FLOPA  INIT.FLOW PORT A (PA7-PA3)
845 POKE 1039,T(3) :REM 1039 =FLOPB  INITIAL FLOW PORT B(PB4-PB0)
850 PX =PEEK(32776) :REM CLEARS INTERRUPT FLAG OF T2 BY READING LO BYTE
```

```
855 POKE 1037,00 :REM CLEARS LOCATION USED TO SIGNAL CHANGED FLOW RATE
860 POKE 1034,00 :REM CLEARS LOCATION USED TO COUNT # OF INTERRUPTS
862 CM = CM + 1
863 PRINT"THIS IS RUN NUMBER  ";CM
865 PRINT" FIA SUBROUTINE IS RUNNING  !"
870 POKE 11,16 :POKE 12,04 : X = USR(Y) :REM TO FIA SUBROUTINE
875 PRINT" BACK FROM FIA SUBROUTINE"
880 GOTO 153 :REM GO TO DATA COLLECTION PORTION OF PROGRAM
885 STOP
```

Ratemeter Subroutine

```
LINE # LOC     CODE       LINE

0002  0000               PAD    =$1700
0003  0000               PADD=$1701
0004  0000               PBDD=$1703;DIRECTION
0005  0000               PBD=$1702;INPUT NMI
0006  0000               STPCLK =$1707;READ&STOP
0007  0000               CLKSET =$170F;CLOCK CO1600;VERSATILE PORT
0008  0000               VECTIN =$17FA          ; VECTORS HERE
0009  0000               MEASNO =$03E0
0010  0000               TIME   =$03E1
0011  0000               DELAY  =$03E2
0012  0000               SELECT =$03E4;DVM 4,FIXED 1
0013  0000               OFFSET =$03E3
0014  0000               TOP    =$03E5
0015  0000               MEAS2  =$03E7
0016  0000               TIMER  =$00E4
0017  0000               OVRFLO =$03E8
0018  0000               YINDEX =$03FC
0019  0000               NEG    =$03E9
0020  0000               RATE1  =$03EA
0021  0000               SER1   =$03ED
0022  0000               SER2   =$03EE
0023  0000               SER3   =$03EF
0024  0000               PORT   =$03F5
0025  0000               CNTR   =$03F6
0026  0000               SPOT   =$03F7
0027  0000               RESET  =$1C22
0028  0000               ZERO   =$03F0
0029  0000               STORE1 =$00E0
0030  0000               DELAY2 =$03F1
0031  0000               DUMMY  =$03F2
0032  0000               DRUG   =$03FD
0033  0000               ALLFUL =$00E5
0034  0000               NEGRAT =$00E6
0035  0000               ERROFL =$00E7
0036  0000               YHOLD  = $016A
0037  0000                      *=$0300
0038  0300  A9 06              LDA #06
0039  0302  85 E1              STA $00E1
0040  0304  85 E3              STA $00E3
0041  0306  A9 00              LDA #00
0042  0308  85 E0              STA $00E0
0043  030A  A9 01              LDA #01
0044  030C  85 E2              STA $00E2
0045  030E  A9 11              LDA #<ROUTIN
0046  0310  20 00 02           JSR INIT;INITIALIZE
0047  0313  A9 02              LDA #>ROUTIN
0048  0315  A9 3C              LDA #%11100
0049  0317  8D 02 17           STA PBD;INJECTOR
0050  031A  AD E2 03           LDA DELAY;ONCE PRER PROG START
0051  031D  8D F1 03           STA DELAY2;INITIAL DELAY
0052  0320  A9 00              LDA #0
0053  0322  8D 02 17           STA PBD          ;INJECTOR PULSE
0054  0325  8D 01 17           STA PADD         ;INPUT
0055  0328  A0 00              LDY #0
0056  032A  CE F1 03    DELOOP DEC DELAY2
```

```
LINE # LOC     CODE       LINE

0057  0336  30 0D             BMI RECOL
0058  0338  A9 F4             LDA #244        ;.25SEC
0059  033A  8D 07 17           STA STPCLK;NONINTERUPT
0060  033D  2C 07 17    CKLOOP BIT STPCLK;CLK DONE?
0061  0340  10 FB             BPL CKLOOP
0062  0342  4C 33 03           JMP DELOOP
0063  0345  20 DA 02    RECOL  JSR RTMEAS
0064  0348  CE E7 03           DEC MEAS2
0065  034B  AD E1 03    COLECT LDA TIME
0066  034E  85 E4               STA TIMER;INIT TIMER
0067  0350  C0 FE               CPY #254; MUST BE EVEN #
0068  0352  B0 94               BCS NXPG
0069  0354  4C 58 03           JMP TOWAIT
0070  0357  60          TFINAL RTS
0071  0358  A9 00       TOWAIT LDA #0
0072  035A  91 E0               STA (STORE1),Y
0073  035C  91 E2               STA (STORE1+2),Y
0074  035E  8D E8 03           STA OVRFLO      ;INITIALIZE
0075  0361  A9 04               LDA #%100
0076  0363  8D 02 17           STA PBD; CLEAR COUTNERS
0077  0366  0E 02 17           ASL PBD; OPEN GATE
0078  0369  C6 E4       RETIME DEC TIMER;TIME UP?
0079  036B  30 35               BMI TPOINT;STORE POINT
0080  036D  A9 F4               LDA #244;LOAD CLOCK
0081  036F  8D 07 17           STA STPCLK
0082  0372  2C 07 17    CLKOOP BIT STPCLK;.25S UP?
0083  0375  30 F2               BMI RETIME
0084  0377  AD 00 17    CHANGE LDA PAD
0085  037A  10 F6               BPL CLKOOP      ;MSB IS LO
0086  037C  AD 00 17    CHECK  LDA PAD
0087  037F  10 11               BPL RESTOR:ONE COUNT
0088  0381  2C 07 17           BIT STPCLK;TIME UP?
0089  0384  10 F6               BPL CHECK       ;WAIT FOR LO AT MSB
0090  0386  C6 E4               DEC TIMER       ;TIME UP?
0091  0388  30 10               BMI TPOINT      ;STORE POINT
0092  038A  A9 F4               LDA #244        ;RESTART 0.25S
0093  038C  8D 07 17           STA STPCLK
0094  038F  4C 7C 03           JMP CHECK
0095  0392  EE FD 03    RESTOR INC DRUG
0096  0395  AD FD 03           LDA DRUG
0097  0398  91 E2               STA (STORE1+2),Y
0098  039A  D0 D6               BNE CLKOOP
0099  039C  EE E8 03           INC OVRFLO      ;>32K
0100  039F  4C 72 03           JMP CLKOOP
0101  03A2  20 13 02    TPOINT JSR POINT;STORE DATA
0102  03A5  CE E7 03    ANOTHR DEC MEAS2
0103  03A8  10 A1               BPL COLECT
0104  03AA  A9 01               LDA #1;1 IS FIXEDT
0105  03AC  2C E4 03           BIT SELECT
0106  03AF  F0 0B               BEQ NEXT
0107  03B1  20 CD 02           JSR XRIGHT
0108  03B4  20 3D 02           JSR FIXEDT
0109  03B7  EA                 NOP; FOR BASIC
0110  03B8  AD FC 03           LDA YINDEX
0111  03BB  A8                 TAY             ; RESTORE3 Y
```

```
LINE # LOC     CODE       LINE

0112  03BC  A9 04       NEXT   LDA #4
0113  03BE  2C E4 03            BIT SELECT;4 IS DVM
0114  03C1  F0 82               BEQ RECOL        ;COLECT MORE PTS.
0115  03C3  20 CD 02            JSR XRIGHT
0116  03C6  20 8B 02            JSR DVM
0117  03C9  EA                  NOP: FOR BASIC
0118  03CA  AD FC 03            LDA YINDEX
0119  03CD  A8                  TAY: RESTORES Y
0120  03CE  4C 45 03            JMP RECOL;MORE DATA
0121  03D1  4C 22 1C     FINAL  JMP RESET        ;TO STOP
0122  03D4                      *=$0200
0123  0200  A9 00        INIT   LDA #0
0124  0202  8D ED 03            STA SER1         ;CLEARING
0125  0205  8D EE 03            STA SER2
0126  0208  8D EF 03            STA SER3
0127  020B  A9 7F               LDA #%01111111   ;PORTS OUT
0128  020D  8D 03 17            STA PBDD         ;1=OUTPUT
0129  0210  60                  RTS
0130  0211  C6 E4        ROUTIN DEC TIMER;NO. OF .25S
0131  0213  A9 00        POINT  LDA #0
0132  0215  8D FD 03            STA DRUG
0133  0218  85 E5               STA ALLFUL
0134  021A  85 E7               STA ERROFL
0135  021C  0E 02 17            ASL PBD          ; CLOSE GATE
0136  021F  AD 00 17            LDA PAD
0137  0222  91 E0               STA (STORE1),Y; LOWER BYTE
0138  0224  AD E8 03            LDA OVRFLO
0139  0227  F0 11               BEQ LATER        ;NO OVERFLOW
0140  0229  A9 AA               LDA #170         ;SIGNAL OVERFLOW
0141  022B  85 E7               STA ERROFL
0142  022D  AD E8 03            LDA OVRFLO
0143  0230  8D EF 03            STA SER3         ; PRINT AMT OVERFLOW
0144  0233  A9 00               LDA #0           ; SIGNALS NO RATE
0145  0235  85 E6               STA NEGRAT       ; WAS CALCULATED
0146  0237  20 5A 01            JSR BCD
0147  023A  C8           LATER  INY
0148  023B  C8                  INY
0149  023C  60                  RTS
0150  023D  20 7D 02     FIXEDT JSR TOCLR        ;SUBROUTINE CALCS RATE
0151  0240  4E E7 03            LSR MEAS2;DIVIDE BY 2
0152  0243  20 99 02            JSR ADDER        ;THIS ADDS!
0153  0246  A9 03               LDA #3           ;3 HIGHER LOC
0154  0248  8D F2 03            STA DUMMY;FOR ADD1
0155  024B  20 DA 02            JSR RTMEAS;FOR ADDER
0156  024E  4E E7 03            LSR MEAS2;DIVIDE BY 2
0157  0251  20 99 02            JSR ADDER;ADD 2ND GROUP
0158  0254  20 BF 02            JSR SUB1;LO BYTE
0159  0257  20 C2 02            JSR SUB2;MIDDLE BYTE
0160  025A  20 C2 02            JSR SUB2;TOP BYTE
0161  025D  B0 17               BCS NOMINS
0162  025F  4C 6F 02            JMP YESMIN       ; LET BASIC CALC. NEG RATE
0163  0262  EA                  NOP
0164  0263  EA                  NOP
0165  0264  A9 00               LDA #0           ;GET PLUS VALUE
0166  0266  20 BF 02            JSR SUB1
```

```
LINE # LOC     CODE       LINE

0167  0269  20 C2 02          JSR SUB2
0168  026C  20 C2 02          JSR SUB2
0169  026F  A9 63        YESMIN LDA #99          ; SIGNALS NEG  RATE
0170  0271  85 E6               STA NEGRAT
0171  0273  4C 7A 02          JMP STUMP
0172  0276  A9 0B        NOMINS LDA #11          ; SIGNALS POS RATE
0173  0278  85 E6               STA NEGRAT
0174  027A  20 4F 01    STUMP  JSR RATBCD
0175  027D  A2 05        TOCLR  LDX #5;SUBROUTINE
0176  027F  A9 00               LDA #0;CLEAR WORK SPACE
0177  0281  8D F2 03            STA DUMMY;FOR ADD1
0178  0284  9D EA 03    CLEAR  STA RATE1,X
0179  0287  CA                 DEX
0180  0288  10 FA               BPL CLEAR;TIL ALL CLEARED
0181  028A  60                 RTS
0182  028B  20 7D 02    DVM    JSR TOCLR;CLEARS WORK SPACE
0183  028E  20 99 02            JSR ADDER
0184  0291  A9 00               LDA #00          ; SIGNALS DVM MODE
0185  0293  85 E6               STA NEGRAT
0186  0295  20 4F 01            JSR RATBCD
0187  0298  60                 RTS
0188  0299  20 B0 02    ADDER  JSR ADD1; LO BYTE
0189  029C  20 B4 02            JSR ADD2;HI BYTE
0190  029F  A9 00               LDA #0;TO GET CARRY
0191  02A1  7D EA 03            ADC RATE1,X;X IS 2 OR 5
0192  02A4  9D EA 03            STA RATE1,X
0193  02A7  CE E7 03            DEC MEAS2;ONE PT.DONE
0194  02AA  F0 03               BEQ BOTTOM;ALL DONE?
0195  02AC  4C 99 02            JMP ADDER;NO-GET MORE
0196  02AF  60           BOTTOM RTS
0197  02B0  AE F2 03    ADD1   LDX DUMMY; FROM FIXEDT
0198  02B3  18                  CLC;READY TO ADD
0199  02B4  BD EA 03    ADD2   LDA RATE1.X;LO BYTE
0200  02B7  71 E0                ADC (STORE1),Y;LO BYTE
0201  02B9  9D EA 03            STA RATE1,X;ACCUM HERE
0202  02BC  E8                  INX;NEXT BYTE
0203  02BD  C8                  INY;NEXT BYTE
0204  02BE  60                  RTS
0205  02BF  A2 00        SUB1   LDX #0;LO FIRST
0206  02C1  38                  SEC;READY TO SUB
0207  02C2  BD ED 03    SUB2   LDA RATE1+3,X;LATER DATA
0208  02C5  FD EA 03    SUB3   SBC RATE1,X;EARLY DATA
0209  02C8  9D EA 03            STA RATE1.X;STORE IN EARLY
0210  02CB  E8                  INX; NEXT BYTE
0211  02CC  60                  RTS
0212  02CD  98           XRIGHT TYA              ; MOV Y BACK MEASNO
0213  02CE  8C FC 03            STY YINDEX; SAVE Y
0214  02D1  38                  SEC
0215  02D2  ED E0 03            SBC MEASNO
0216  02D5  38                  SEC
0217  02D6  ED E1 03            SBC MEASNO;2 BYTES
0218  02D9  A8                  TAY              ; REFILL Y
0219  02DA  AD E1 03    RTMEAS LDA MEASNO;REINIT MEAS2
0220  02DD  8D E7 03            STA MEAS2
0221  02E0  60                  RTS
```

```
LINE # LOC     CODE        LINE

0222  02E1                      *=$010E
0223  010E  A0 00               LDY #0
0224  0110  A9 06               LDA #06
0225  0112  85 E1               STA $00E1
0226  0114  85 E3               STA $00E3
0227  0116  20 00 02    NXRCL  JSR INIT
0228  0119  A9 01               LDA #1
0229  011B  2C E4 03           BIT SELECT;1 IS FIXEDT
0230  011E  F0 11               BEQ AROUND
0231  0120  AC E3 03           LDY OFFSET
0232  0123  20 DA 02    REPEAT JSR RTMEAS;LOAD MEAS2
0233  0126  20 3D 02           JSR FIXEDT
0234  0129  AC 6A 01           LDY YHOLD       ; RESTORE THE Y REGISTER
0235  012C  CC FC 03           CPY YINDEX; THRU NEW DATA
0236  012F  90 F2               BCC REPEAT
0237  0131  A9 04      AROUND LDA #4          ;4 IS DVM
0238  0133  2C E4 03           BIT SELECT
0239  0136  F0 11               BEQ LAST
0240  0138  AC E3 03           LDY OFFSET; SKIP Y POINTS
0241  013B  20 DA 02    TODVM  JSR RTMEAS;LOAD MEAS2
0242  013E  20 8B 02           JSR DVM
0243  0141  AC 6A 01           LDY YHOLD       ;  TO RESTORE Y REGISTER
0244  0144  CC FC 03           CPY YINDEX; THRU NEW DATA
0245  0147  90 F2               BCC TODVM
0246  0149  4C 30 01    LAST   JMP OMPG        ; NEXT PAGE , RECAL.
0247  014C  4C 22 1C           JMP RESET
0248  014F  A2 02      RATBCD LDX #2
0249  0151  BD EA 03    MOVE   LDA RATE1,X
0250  0154  9D ED 03           STA SER1,X; LOAD COUNT DOWN
0251  0157  CA                 DEX             ; FOR 3 BYTES
0252  0158  10 F7               BPL MOVE
0253  015A  68          BCD    PLA             ; FOR RETURN TO BASIC
0254  015B  68                 PLA
0255  015C  68                 PLA
0256  015D  68                 PLA
0257  015E  8C 6A 01           STY  YHOLD      ; SAVE THE Y REGISTER !
0258  0161  60                 RTS
0259  0162                     * =$02E8
0260  02E8  E6 E1       NXPG   INC $00E1; INCREASE PAGE #
0261  02EA  E6 E3               INC $00E3
0262  02EC  A9 00               LDA #0; INITIAILIZE Y INDEX
0263  02EE  A8                  TAY
0264  02EF  AD E5 03           LDA TOP
0265  02F2  C5 E1               CMP $00E1
0266  02F4  D0 42               BNE TOWAIT
0267  02F6  A9 3B               LDA #187        ; SIGNALS DATA IS FULL
0268  02F8  85 E5               STA ALLFUL
0269  02FA  4C 57 03           JMP TFINAL
0270  02FD                     *= $0180
0271  0180  E6 E1       OMPG   INC $00E1       ; INCREASE PAGE #
0272  0182  E6 E3               INC $00E3
0273  0184  A9 00               LDA #0          ; INITIALIZE Y INDEX
0274  0186  A8                  TAY
0275  0187  AD E5 03           LDA TOP
0276  018A  C5 E1               CMP $00E1
```

```
LINE # LOC    CODE      LINE

0277  018C  D0 88           BNE NXRCL
0278  018E  A9 BB           LDA #187
0279  0190  85 E5           STA ALLFUL
0280  0192  60              RTS             ; FOR RETURN TO BASIC
0281  0193                  .END            ; THATS ALL FOLKS !!!!!!

ERRORS = 0000 <0000>


SYMBOL   VALUE

ADD1     02B0   ADD2     02B4   ADDER    0299   ALLFUL   00E5
ANOTHR   03A5   AROUND   0131   BCD      015A   BOTTOM   02AF
CHANGE   0377   CHECK    037C   CKLOOP   033D   CLEAR    0284
CLKOOP   0372   CLKSET   170F   CNTR     03F6   COLECT   034B
DELAY    03E2   DELAY2   03F1   DELOOP   0333   DRUG     03FD
DUMMY    03F2   DVM      0298   ERROFL   00E7   FINAL    03D1
FIXEDT   023D   INIT     0200   LAST     0149   LATER    023A
MEAS2    03E7   MEASNO   03E0   MOVE     0151   NEG      03E9
NEGRAT   00E6   NEXT     03BC   NOMINS   0276   NXPG     02E8
NXRCL    0116   OFFSET   03E3   ONPG     0180   OVRFLO   03E8
PAD      1700   PADD     1701   PBD      1702   PBDD     1703
POINT    0213   PORT     03F5   RATBCD   014F   RATE1    03EA
RECOL    0345   REPEAT   0123   RESET    1C02   RESTOR   0392
RETIME   0369   ROUTIN   0211   RTMEAS   02DA   SELECT   03E4
SER1     03ED   SER2     03EE   SER3     03EF   SPOT     03F7
STORE1   00E0   STPCLK   1707   STUMP    027A   SUB1     028F
SUB2     02C2   SUB3     02C5   TFINAL   0357   TIME     03E1
TIMER    00E4   TOCLR    027D   TODVM    013B   TOP      03E5
TOWAIT   0358   TPOINT   03A2   VECTIN   17FA   XRIGHT   02CD
YESMIN   026F   YHOLD    016A   YINDEX   03FC   ZERO     03F0

END OF ASSEMBLY
<
```

FIA Subroutine

```
LINE # LOC     CODE       LINE

0002  0000                FLOPB  = $049F        ; CONTAINS FLOW RATE FOR PORT B
0003  0000                FLOPA  = $049E        ;FLOW RATE PORT A
0004  0000                NXTFA  = $040B        ;FINAL FLOW PORT A
0005  0000                NXTFB  = $040C        ;FINAL FLOW PORT B
0006  0000                DEL    = $00DF
0007  0000                       *=$0410
0008  0410  A9 E9              LDA #233         ; 233 = $00E9
0009  0412  85 DF              STA $00DF        ; PLACE FOR LOCATION OF DELAYS
0010  0414  A9 FF              LDA #255         ; I/O SET-UP FOR PORT A AND B
0011  0416  8D 03 80           STA $8003
0012  0419  A9 BF              LDA #191         ;LEAVES PB6 AS INPUT
0013  041B  8D 02 80           STA $8002
0014  041E  AD 9F 04           LDA FLOPB        ; LOAD INITIAL FLOW RATE INTO PORT B
0015  0421  8D 00 80           STA $8000        ; PORT B
0016  0424  AD 9E 04           LDA FLOPA        ; LOAD INITIAL FLOW RATE INTO PA
0017  0427  18                 CLC              ; CLEARS CARRY FOR ADDITION
0018  0428  69 06              ADC #06          ; SETS LOW BITS FOR AN INITIAL RINSE
0019  042A  8D 01 80           STA $8001        ; PORT A
0020  042D  A0 00              LDY #00
0021  042F  20 5A 04           JSR TIMER
0022  0432  C8                 INY
0023  0433  AD 01 80           LDA $8001        ;RETAINS VALUE IN $8001 (PORT A)
0024  0436  18                 CLC
0025  0437  69 01              ADC #01          ;ADDS 1 TO START SAMPLING
0026  0439  8D 01 80           STA $8001
0027  043C  20 5A 04           JSR TIMER
0028  043F  C8                 INY
0029  0440  AD 01 80           LDA $8001        ;RETAINS VALUE OF PORT A
0030  0443  38                 SEC              ;SETS CARRY BIT  FOR SUBTRACTION
0031  0444  E9 02              SBC #02          ;SUBTRACTS 2 TO PUT REAGENT LOOP ON L
0032  0446  8D 01 80           STA $8001
0033  0449  20 5A 04           JSR TIMER
0034  044C  C8                 INY
0035  044D  AD 01 80           LDA $8001        ;RETAINS VALUE OF PORT A
0036  0450  38                 SEC
0037  0451  E9 05              SBC #05          ;SUBTRACTS 5 TO PUT SAMPLE ON LINE,
0038  0453  8D 01 80           STA $8001        ;SAMPLER IN RINSE
0039  0456  20 6B 04           JSR LSTIME
0040  0459  60                 RTS
0041  045A  B1 DF        TIMER  LDA (DEL),Y
0042  045C  AA                 TAX
0043  045D  A9 F4              LDA #244
0044  045F  8D 07 17           STA $1707
0045  0462  2C 07 17           BIT $1707
0046  0465  10 FB              BPL *-3
0047  0467  CA                 DEX
0048  0468  D0 F5              BNE *-9
0049  046A  60                 RTS
0050  046B  A9 04        LSTIME LDA  #04         ;LOADS HI BYTE OF INT. SERVICE
0051  046D  8D FF 17           STA $17FF        ;ROUTINE INTO HI BYTE OF INT. VECTOR
0052  0470  A9 E8              LDA #224         ; TIMER1 = FREE RUN TIMER2 = COUNTER
0053  0472  8D 0B 80           STA $800B
0054  0475  A9 7F              LDA #127         ; DISABLES ALL DEVICES ON 6522
0055  0477  8D 0E 80           STA $800E
0056  047A  A9 A0              LDA #160         ; ENABLES ONLY TIMER2 INTERRUPT
```

```
LINE # LOC     CODE       LINE

0057  047C  8D 0E 80          STA $800E
0058  047F  A9 FF             LDA #255        ; LOADS FF INTO LO BYTE OF TIMER2
0059  0481  8D 08 80          STA $8008
0060  0484  A9 00             LDA #00         ; LOADS 00 INTO HI BYTE OF TIMER2
0061  0486  8D 09 80          STA $8009
0062  0489  A9 FF             LDA #255        ; LOADS FF INTO BOTH
0063  048B  8D 04 80          STA $8004       ; TIMER 1 COUNTERS
0064  048E  8D 05 80          STA $8005
0065  0491  58                CLI
0066  0492  60                RTS
0067  0493                    *=$04A0         ; INTERRUPT SERVICE ROUTINE
0068  04A0  A9 06             LDA #06         ; BACK TO RINSE FOR ALL DEVICES
0069  04A2  18                CLC             ;CLEARS CARRY BIT
0070  04A3  6D 01 80          ADC $8001       ;RETAINS FLOW RATE
0071  04A6  8D 01 80          STA $8001
0072  04A9  EA                NOP
0073  04AA  A9 64             LDA #100        ; LOADS LOW BYTE OF TIMER 2
0074  04AC  8D 08 80          STA $8008       ;
0075  04AF  A9 00             LDA #00         ; HI BYTE OF TIMER 2 =0
0076  04B1  8D 09 80          STA $8009
0077  04B4  A9 FF             LDA #255        ;LOADS FF INTO TIMER 1
0078  04B6  8D 04 80          STA $8004
0079  04B9  8D 05 80          STA $8005
0080  04BC  A9 D0             LDA #208        ;LOW BYTE (D0) OF INT. SERV. ROUTINE
0081  04BE  8D FE 17          STA $17FE
0082  04C1  A9 04             LDA #04         ; HI BYTE OF INT.SERVICE ROUTINE
0083  04C3  8D FF 17          STA $17FF
0084  04C6  EE 0A 04          INC $040A       ;INCREMENTS COUNTR FOR # OF INT.S
0085  04C9  AD 0E 80          LDA $800E       ;CLEARS T2 INT. FLAG AND RE-ENABLES
0086  04CC  8D 0E 80          STA $800E
0087  04CF  40                RTI
0088  04D0                    *=$04D0
0089  04D0  AD 01 80          LDA $8001       ;SAVES STATUS OF LOWER I/O PORTS
0090  04D3  38                SEC
0091  04D4  ED 0E 04          SBC FLOPA       ; SUB.S THE INITIAL FLOW RATE
0092  04D7  18                CLC
0093  04D8  6D 0B 04          ADC NXTFA       ;ADDS FINAL FLOW RATE VALUUE
0094  04DB  8D 01 80          STA $8001
0095  04DE  AD 0C 04          LDA NXTFB       ;LOADS FINAL PORT B FLOW RATE
0096  04E1  8D 00 80          STA $8000
0097  04E4  A9 CF             LDA #207        ; SIGNALS CHANGE IN FLOW RATE
0098  04E6  8D 0D 04          STA $040D
0099  04E9  A9 64             LDA #100        ;RESETS 6522 CLOCK
0100  04EB  8D 08 80          STA $8008
0101  04EE  A9 00             LDA #00
0102  04F0  8D 09 80          STA $8009
0103  04F3  A9 FF             LDA #255
0104  04F5  8D 04 80          STA $8004
0105  04F8  8D 05 80          STA $8005
0106  04FB  A9 A0             LDA #160        ;LOADS L0 BYTE OF NEXT INT ROUT.
0107  04FD  8D FE 17          STA $17FE
0108  0500  A9 04             LDA #04         ;HI BYTE OF INT.SERVICE ROUTINE
0109  0502  8D FF 17          STA $17FF
0110  0505  EE 0A 04          INC $040A       ;INCREMNTS COUNTER FOR # OF INTS.
0111  0508  AD 0E 80          LDA $800E       ;CLEARS T2 FLAG AND REENABLES
```

```
LINE # LOC     CODE       LINE

0112  050B  8D 0E 80          STA $800E
0113  050E  40               RTI
0114  050F  78               SEI            ;SUBROUTINE TO PREVENT AN INTERRUPT
0115  0510  60               RTS
0116  0511  58               CLI
0117  0512  60               RTS
0118  0513                   .END

ERRORS = 0000 <0000>



SYMBOL TABLE

SYMBOL    VALUE

DEL       00DF    FLOPA     040E    FLOPB     040F    LSTIME    046B
NXTFA     040B    NXTFB     040C    TIMER     045A
END OF ASSEMBLY
<
```

Appendix II

Design and Operation of the Dionex Sample Injection Valve

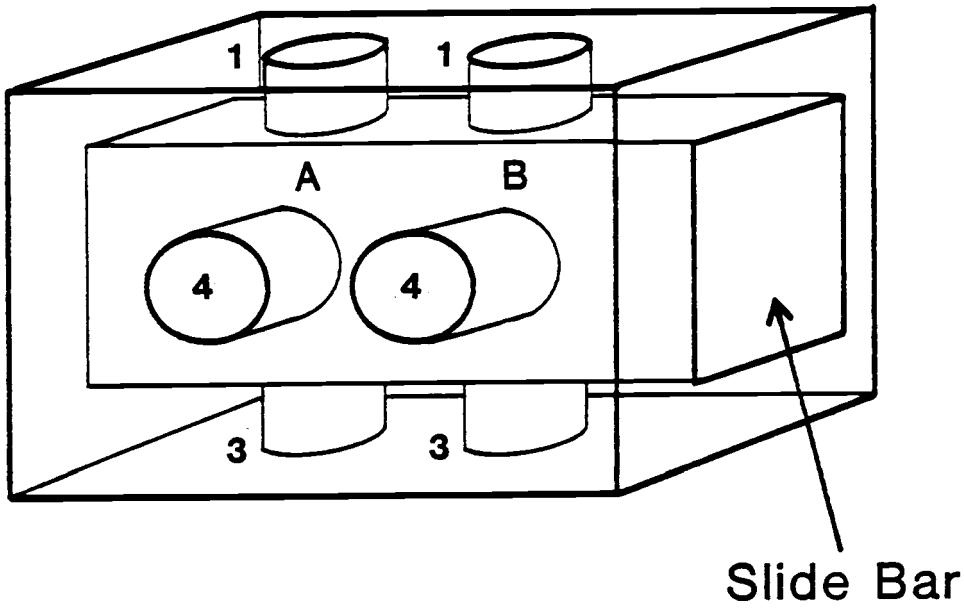

The figure shown above represents the orientation of the connections on a Dionex sample injection valve. The numbers and letters correspond to the numbers shown on the figure on the following page. The pneumatic actuators are not shown on this figure but are mounted on opposite ends of the valve housing.

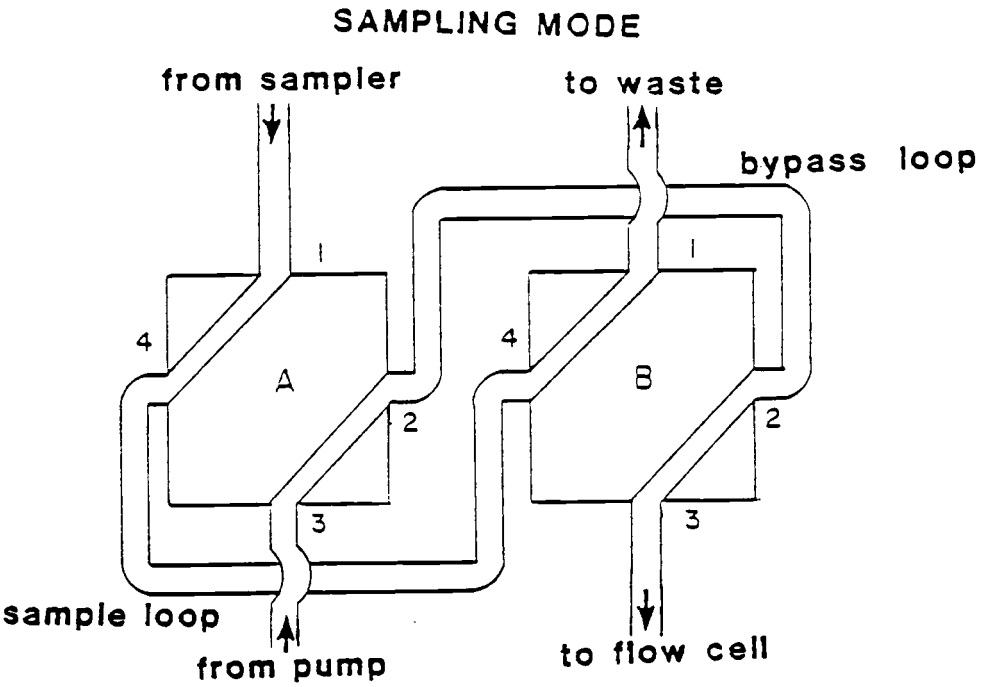

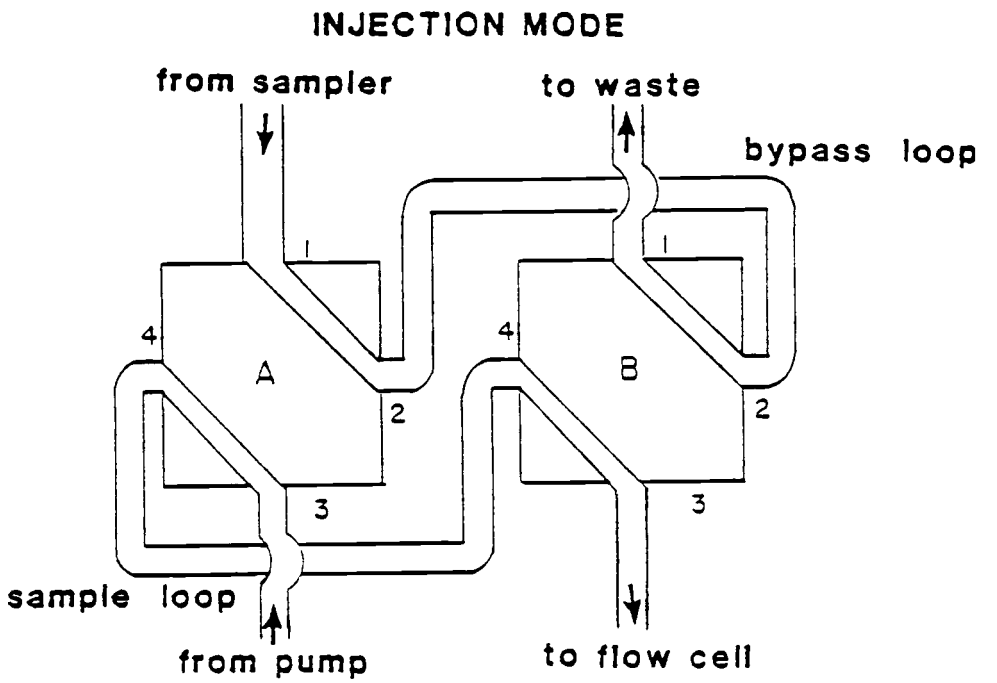

Operation of the Dionex Sample Injection Valve

Appendix III

Conversion of Flow Rate Values into 5 Bit Numbers for I/O Ports[a]

The steps of the conversion of a value in units of mL/min to the appropriate 5 bit binary number are listed below:

1. Split the value into 2 parts, an integer and a fraction.
2. Multiply the fractional value by 5.
3. Multiply the integer value by 8.
4. Add the results of steps 2 and 3.

This procedure is repeated for all 4 values, except that the two values for the reagent pump must be multiplied by 8 in order to shift the values to the upper 5 bits of I/O port A. The BASIC program then POKEs the 4 converted values into memory for storage until the FIA subroutine is executed.

As an example, the conversion of 2.2 mL/min for the reagent pump is shown below:

Step 1. Integer = 2 , Fraction = 0.2

Step 2. 5 x 0.2 = 1.0

Step 3. 8 x 2 = 16

Step 4. 16 + 1 = 17

For the reagent pump, the result of step 4 is multiplied by 8, thus 8 x 17 = 136.

When the decimal number 136 is finally loaded into I/O port

A, the resulting binary number will be 10001000_2. PA7 and PA3 are high, thus a flow rate of 2.2 mL/min (2.0 + 0.2) is selected.

[a]Refer to lines 770-825 in the FIA Ratemeter program (BASIC) in Appendix I.